

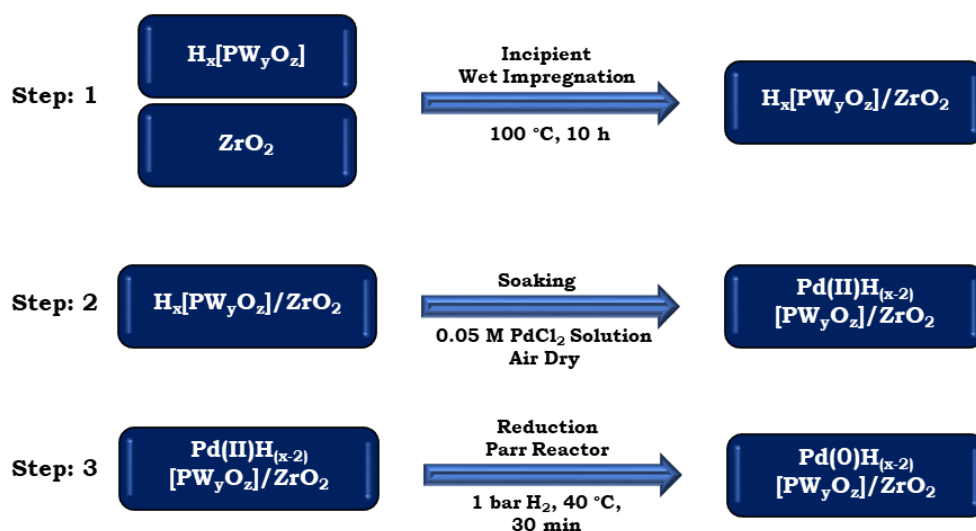
PART-A

Ion Exchange Method

Designing of catalyst by ion exchange method

Ion exchange method is consisting of three steps for the synthesis of PdNPs stabilized by zirconia supported TPA/LTPA. *Step-I*: TPA/LTPA is supported on zirconia by incipient wet impregnation method. *Step-II*: Exchange of available counter protons by Pd using soaking method. *Step-III*: Finally, this Pd exchanged zirconia supported TPA/LTPA is converted to stabilized PdNPs by reducing in Parr reactor. Synthetic scheme by ion exchange method is given in scheme 1, where, $H_x[PW_yO_z]$ = 12-tungstophosphoric acid, TPA ($H_3PW_{12}O_{40}$) or Mono lacunary tungstophosphoric acid, LTPA ($H_7PW_{11}O_{39}$).

PdNPs Stabilized by Zirconia Supported Heteropoly acids (Heterogeneous)



Scheme 1 Synthetic scheme for stabilized PdNPs via ion exchange method.

CHAPTER 1

PdNPs Stabilized by Zirconia
Supported TPA: Synthesis,
Characterization and
Applications to C-C coupling
and Hydrogenation



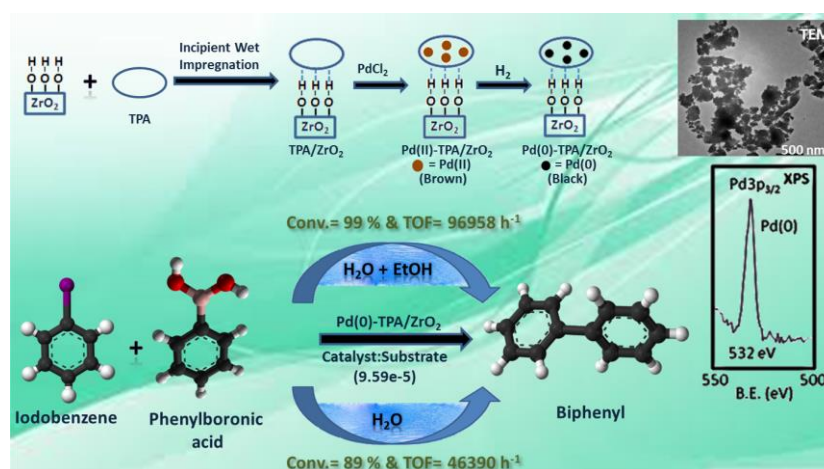
Stabilized Palladium Nanoparticles: Synthesis, Multi-spectroscopic Characterization and Application for Suzuki–Miyaura Reaction

Anish Patel¹ · Anjali Patel¹

Received: 25 July 2018 / Accepted: 15 September 2018 / Published online: 24 September 2018
 © Springer Science+Business Media, LLC, part of Springer Nature 2018

Abstract

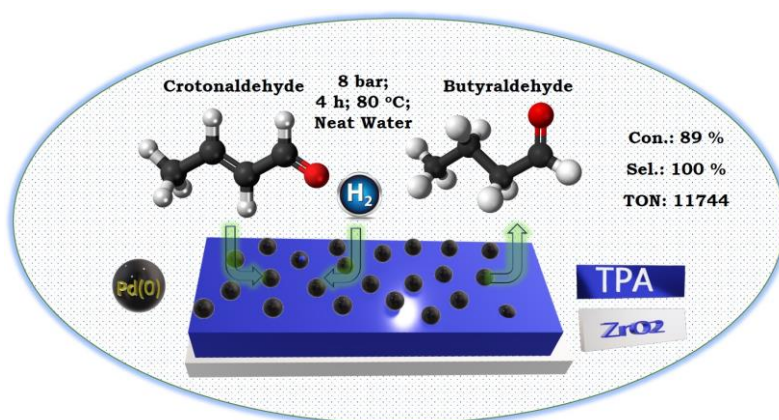
The present article demonstrates a simple method for synthesizing the highly stabilized Pd(0) nanoparticles by using supported 12-tungstophosphoric acid as a stabilizer as well as a carrier. The obtained material was characterized by different methods and the presence of nanoparticles on the surface of the carrier was confirmed, especially by TEM and XPS. As an application, the use of material was explored for the well-known fascinating organic transformation, Suzuki–Miyaura cross coupling reaction in aqueous medium as well as in neat H₂O. It was found that the material shows an outstanding activity as the heterogeneous catalyst (0.0096 mol% of Pd) for both aqueous medium (99% conversion, TOF 96958 h⁻¹) and in neat H₂O (89% conversion, TOF 46390 h⁻¹) towards biphenyl. The catalyst was recovered by filtration only, regenerated and reused without any significant loss in conversion. Study shows that the present catalyst is truly heterogeneous and sustainable for the said reaction, in either of the medium. The viability of the catalyst was learned toward different substrates and found to be excellent in almost all cases.



Anish Patel¹ · Anjali Patel¹

Abstract

Stabilized Pd(0) nanoparticles by supported 12-tungstophosphoric acid (Pd(0)-TPA/ZrO₂) was explored as a sustainable recyclable catalyst for selective C=C hydrogenation of cyclohexene and crotonaldehyde. The catalyst shows an outstanding performance [catalyst to substrate ratio (1:1.31 × 10⁴)] towards high conversion as well as 100% selectivity of the desired product with high turnover number (> 10,000) and turnover frequency (> 2600 h⁻¹) for both the systems. The use of neat water as a solvent and mild reaction conditions makes the present system environmentally benign and green. Moreover, the catalyst could be recovered and reused up to five cycles without any significant loss in their conversion as well as selectivity. The viability of the catalyst was evaluated towards different aromatic as well as aliphatic arenes and found to be excellent in all the cases. The obtained selectivity, especially butyraldehyde, was correlated with the nature of the catalyst as well as solvent and based on the study, a plausible mechanism for both the reactions was also proposed.



As discussed in general introduction, surpassing advantages of heterogeneous catalyst attract number of groups to design heteropoly acid stabilized nano catalysts for various applications. In this context, we found few reports on Pd nanoparticles stabilized by supported 12-tungstophosphoric acid (TPA).

In 2012, first time, Yamashita et al. synthesized stabilized Pd nanoparticles stabilized via silica supported cesium salt of 12-tungstophosphoric acid ($\text{Pd}/\text{Cs}_{2.5}\text{H}_{0.5}\text{PW}_{12}\text{O}_{40}/\text{SiO}_2$) by photo-assisted deposition method. It was found to be an active catalyst for the direct synthesis of hydrogen peroxide from molecular H_2 and O_2 [1].

In 2016, Zhang et al. developed facile and green one-pot method for 12-tungstophosphoric acid stabilized tri-component catalyst comprising of Pd nanoparticles on macroporous carbon ($\text{Pd}@\text{H}_3\text{PMo}_{12}\text{O}_{40}/\text{MPC}$). This synthesized material was applied to promote the development of new electrochemical sensors and electrode materials [2].

In 2017, Zhao et al. fabricated 12-tungstophosphoric acid stabilized palladium nanoparticles on reduced graphene oxide ($\text{Pd}/\text{H}_3\text{PW}_{12}\text{O}_{40}/\text{RGO}$) by a simple photoreduction one-pot method. Obtained material was utilized for effective electrooxidation of ethylene glycol and glycerol [3]. In the same year, Zhang et al. designed ex-situ decorated ordered mesoporous carbon with palladium nanoparticles via 12-tungstophosphoric acid ($\text{Pd}-\text{H}_3\text{PW}_{12}\text{O}_{40}\text{-OMC}$). Its efficiency was evaluated for sensitive detection of acetaminophen in pharmaceutical products [4].

In 2018, Leng and Dai anchored palladium nanoparticles on 12-tungstophosphoric acid attached melem porous hybrid ($\text{H}_3\text{PW}_{12}\text{O}_{40}/\text{melem}$, as stabilizing agent) by hybridization and post chemical reduction. The catalytic efficiency of the synthesized material was evaluated for boosting capacity of formic acid dehydrogenation efficiency [5].

Zhang et al. in the same year developed tricomponent stabilized nanohybride comprising of Pd, 12-tungstophosphoric acid and nitrogen doped hollow carbon spheres (Pd/H₃PW₁₂O₄₀/NHCS). The designed material was applied for selective electrochemical sensor for acetaminophen [6].

In this chapter, we are reporting the synthesis of Pd nanoparticles (PdNPs) stabilized via Zirconia supported 12-tungstophosphoric acid (TPA/ZrO₂) by exchange method. The synthesized nanocatalyst, Pd-TPA/ZrO₂, was characterized by elemental analysis EDX, TGA, FT-IR, XPS, TEM, HRTEM, STEM, BET and XRD. The efficiency of the catalyst was evaluated as a sustainable heterogeneous catalyst for SM coupling in aqueous as well as **neat water**, Heck coupling and hydrogenation of cyclohexene and crotonaldehyde hydrogenation in water. Influence of various parameters such as catalyst amount, temperature, pressure, time, base, solvent, solvent ratio was studied for respective reactions to obtain maximum conversion. The catalyst was regenerated, reused and the regenerated catalyst was characterized by EDX, XRD, BET and XPS to confirm the stability of the catalyst. Scope and limitation of synthesized catalyst was investigated towards different substrates. Activity of the catalyst for the said reactions was compared with the reported systems. Probable mechanism for crotonaldehyde hydrogenation was also proposed.

EXPERIMENTAL

Materials

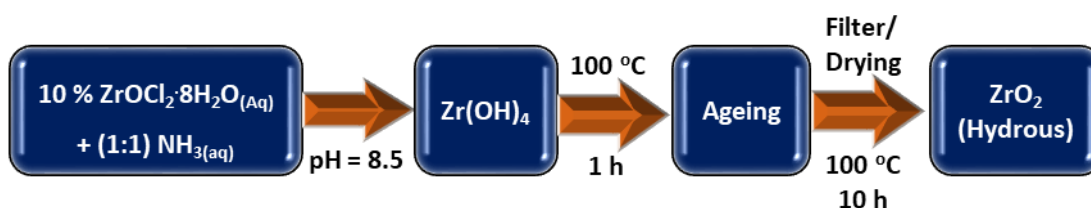
All chemicals used were of A. R. grade. 12-tungstophosphoric acid, zirconium oxychloride, 25 % (w/v) ammonia, palladium chloride, iodobenzene, phenylboronic acid, styrene, dimethyl formamide, potassium carbonate, cyclohexene, crotonaldehyde, petroleum ether, ethyl acetate and dichloromethane were obtained from Merck and used as received.

Catalyst Synthesis

Stabilized palladium nanoparticles by zirconia supported 12-tungstophosphoric acid (Pd-TPA/ZrO₂) was synthesized in three steps.

Step-1: Synthesis of Zirconia (ZrO₂)

ZrO₂ was synthesized following the same method reported by our group [7]. Aqueous ammonia solution (12 % w/v) was added to aqueous solution of ZrOCl₂·8H₂O (10 % w/v) up to pH 8.5. The precipitates were aged at 100 °C on the water bath for 1 h, filtered, washed with conductivity water until a chloride free filtrate was obtained and dried at 100 °C for 10 h. The obtained material was designated as ZrO₂ (Scheme 1).



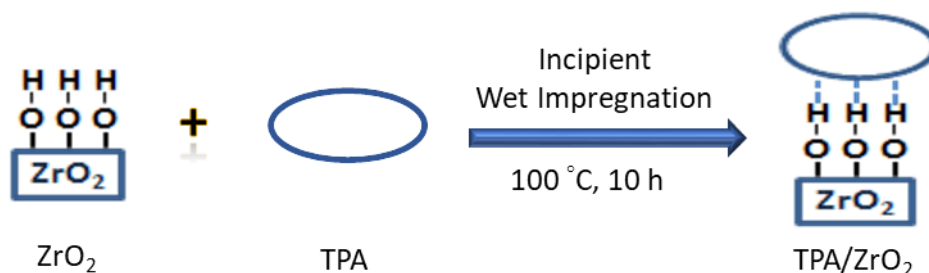
Scheme 1 synthesis of zirconia.

Step-2: Synthesis of zirconia supported 12-tungstophosphoric acid (TPA/ZrO₂)

TPA/ZrO₂ was synthesized by incipient wet impregnation method as reported by our group earlier [8]. 1 g of ZrO₂ was impregnated with aqueous solution of

TPA (0.3/30 g mL⁻¹ of double distilled water) and dried at 100 °C for 10 h (Scheme 2). The obtained material was designated as TPA/ZrO₂.

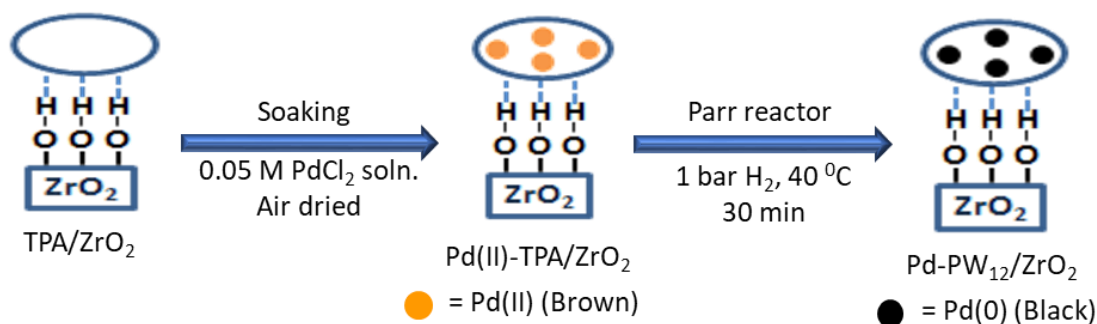
It should be noted that reports [8-16] from our group confirmed that 30 % TPA/ZrO₂ is best among whole series (10-40 % loading) and that is why it was directly taken for this work.



Scheme 2 Synthesis of TPA/ZrO₂.

Step-3: Synthesis of Pd-TPA/ZrO₂

Palladium(II) was deposited on supported 12-tungstophosphoric acid via exchanging the available protons of TPA [17]. 1 g of TPA/ZrO₂ was soaked with 25 mL 0.05 M aqueous solution of PdCl₂ for 24 h with stirring. The solution was filtered, washed with distilled water in order to remove the excess of palladium and dried in air at room temperature. The resulting catalyst (brown colored) was designated as Pd(II)-TPA/ZrO₂. Finally, synthesized catalyst was charged in a Parr reactor under 1 bar H₂ pressure, at 40 °C for 30 min to reduce Pd(II) to Pd(0). The catalyst was removed from reactor and kept in air to attain the room temperature. The obtained catalyst (black colored) was designated as Pd-TPA/ZrO₂ (Scheme 3). The same procedure was followed for the synthesis of Pd/ZrO₂.



Scheme 3 Synthesis of Pd-TPA/ZrO₂.

Catalytic Evaluation

C-C Coupling

SM coupling was carried out in a 50 mL glass batch reactor with a magnetic stirrer. The reactor was flushed with N₂. In an experiment, aryl halide (1.96 mmol), phenylboronic acid (2.94 mmol), K₂CO₃ (3.92 mmol), C₂H₅OH: H₂O (3:7 mL) and catalyst were charged into the glass batch reactor. Similarly, for Heck coupling, initially, the glass reactor was flushed using N₂ gas. In an experiment, aryl halide (0.98 mmol), styrene (1.47 mmol), K₂CO₃ (1.96 mmol), DMF: H₂O (3:2 mL) and catalyst were charged into the reactor.

In both the reactions, reactor was heated at desired temperature in an oil bath with stirring, under N₂ gas atmosphere. After completion of reaction, the mixture was cooled and the organic phase was extracted by dichloromethane as an extracting solvent. The organic phases were then dried with anhydrous magnesium sulfate and analyzed by GC. The obtained products were identified by comparison with the authentic samples and also purified by column chromatography on silica gel with a mixture of ethyl acetate and petroleum ether as an eluent and confirmed by ¹H & ¹³C NMR.

Hydrogenation

The catalytic hydrogenation was carried out using Parr reactor instrument having three major components: The batch type reactor of 100 mL capacity which is made up of SS-316, H₂ reservoir with electronic temperature and pressure controller. In typical reaction, 9.87 mmol of cyclohexene with 50 mL of water as solvent and catalyst were charged to the reactor vessel. The reactor was flushed thrice with H₂ gas to remove any air present. 10 bar H₂ pressure was applied for the reaction which was set at 80 °C with the stirring rate of 1700 rpm for 4 h. The continuous decrease in pressure inside the vessel was utilized for determination of the reaction progress. After completion, the reaction mixture was cooled to room temperature and then H₂ pressure was released from the vent valve. The organic layer was extracted using dichloromethane, whereas catalyst was collected from the junction of two phases and recovered by centrifugation. The organic phase was then dried with anhydrous magnesium sulfate and analyzed by GC. The obtained product was identified by comparison with the authentic sample and also purified by column chromatography on silica gel and confirmed by ¹H NMR.

For the optimization of parameters for maximum conversion, all the reactions were carried out twice. However, under optimized conditions, all the reactions were carried out thrice and the obtained results were reproducible with an error of ± 1 %.

Conversion and selectivity of each product was calculated as follows:

$$\text{Conversion} = \frac{(\text{initial mol\%}) - (\text{final mol\%})}{(\text{initial mol\%})} \times 100$$

$$\text{Selectivity} = \frac{\text{moles of product formed}}{\text{moles of substrate consumed}} \times 100$$

Further, Turnover Number (TON) and Turnover Frequency (TOF) was calculated using the equation:

$$TON = \frac{\text{moles of product}}{\text{moles of catalyst}}$$

$$TOF = \frac{TON}{\text{reaction time}}$$

Leaching Test

Leaching is a negative property for any catalyst. Any leaching of catalyst from the support would make the catalyst unattractive. So, it is necessary to study the stability of polyanion onto support in order to reuse the catalyst. When the HPA react with a mild reducing agent such as ascorbic acid [18], it develops blue coloration, which can be used for the quantitative characterization for the leaching of HPA from the support. In the current work, we have used this method for determining the leaching of TPA from ZrO₂ supports.

Standard samples amounting to 1-5% of TPA in water were prepared. To 10 mL of the above samples, 1 mL of 10% ascorbic acid was added. The mixture was diluted to 25 mL. The resultant solution was scanned at a λ_{max} of 785 nm for its absorbance values. A standard calibration curve was obtained by plotting values of absorbance with percentage solution. In a typical reaction, 1 g catalyst was refluxed for 4 h with 10 mL of conductivity water. 1 mL of the supernatant solution was then treated with 10% ascorbic acid. No development of blue color indicates absence of any leaching. The same procedure was repeated with water, methanol, glycerol and also with the filtrates of all the reaction mixtures after completion of the reaction. The above procedure was followed for all catalysts and no leaching was found. In the present case, the absence of blue color indicates no leaching of TPA from support into reaction medium. The study indicates the presence of chemical interaction between the HPA and support, as well as stability of the resultant catalysts under reaction conditions. Leaching of Pd in the reaction mixture was checked by using atomic adsorption spectrometer AAS GBC-902 instrument.

RESULTS AND DISCUSSION

Catalyst Characterization

The gravimetric analysis shows 0.4 wt% of Pd in Pd(II)-TPA/ZrO₂ [19]. EDX values of W (16.87 wt%) and Pd (0.47 wt%) are in good agreement with calculated one (16.91 wt% of W, 0.4 wt% of Pd). Very low % of Pd indicates that only the protons of TPA are exchanged [17]. EDX elemental mapping of the catalyst is shown in figure 1.

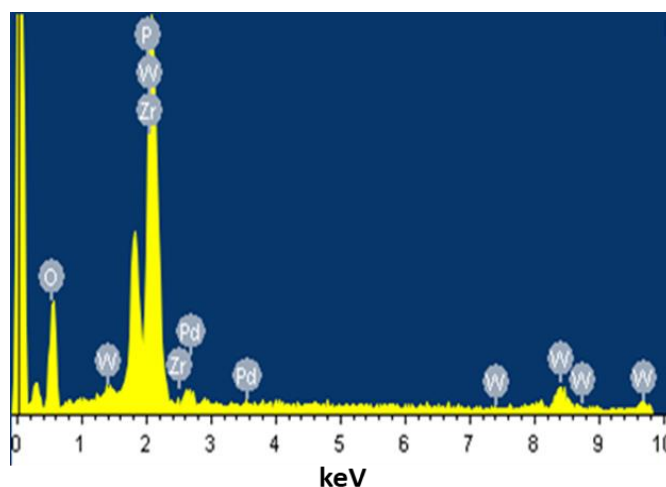


Figure 1 EDX mapping.

TGA curve (Figure 2) of TPA/ZrO₂ shows the 12.6% weight loss in the temperature range of 70-100 °C indicating the loss of adsorbed water molecules and then there is no weight loss observed up to 500 °C indicating the stability of the supported catalyst. TGA curve of Pd-TPA/ZrO₂ shows the 13% weight loss up to 150 °C due to the loss of adsorbed water molecules. No weight loss is observed up to 500 °C indicating the stability of the catalyst up to 500 °C.

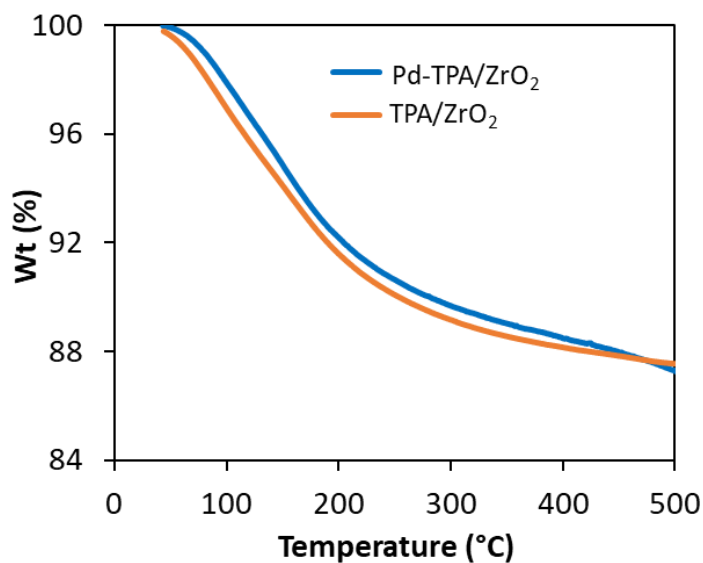


Figure 2 TGA curves.

FT-IR spectra of TPA, ZrO₂, TPA/ZrO₂ and Pd-TPA/ZrO₂ are shown in figure 3. TPA shows its characteristic bands at 800, 893, 987 and 1088 cm⁻¹ corresponding to W-O-W, W=O and P-O stretching, respectively. FT-IR spectrum of ZrO₂ indicates two bending vibrations at 1600 and 1370 cm⁻¹ for O-H-O and H-O-H vibrations and weak bending vibration of Zr-O-H at 600 cm⁻¹. The FT-IR spectrum of TPA/ZrO₂ shows characteristic stretching vibration bands of W-O-W, W=O and P-O at 812, 964 and 1070 cm⁻¹, respectively indicating the presence of TPA. Whereas, Pd-TPA/ZrO₂ shows the characteristic bands at 824, 945 and 1056 cm⁻¹ corresponding to stretching vibration for W-O-W, W=O and P-O but with significant shift may be due to the change in the environment. Here, additional band corresponding to Pd-O band is not observed, this may be due to the merging of band with Zr-O.

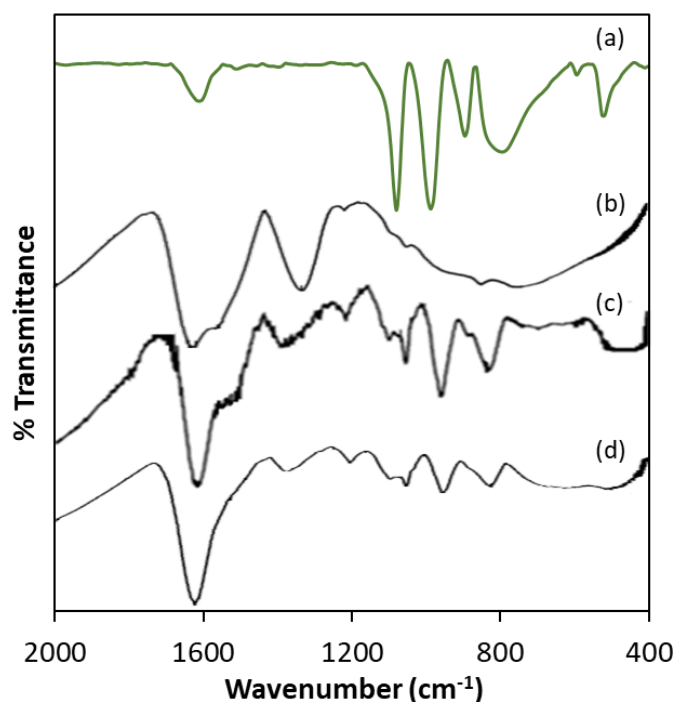


Figure 3 FT-IR spectra of (a) ZrO_2 , (b) TPA (c) TPA/ZrO_2 and (d) Pd-TPA/ZrO_2 .

To confirm the electronic state of the Pd, W and O high resolution XPS spectra of TPA/ZrO_2 and Pd-TPA/ZrO_2 were recorded (Figure 4). TPA/ZrO_2 shows (Figure 4a) a very intense peak at binding energy 532 eV corresponds to O1s as it contains number of O atoms of TPA and ZrO_2 support, whereas Pd-TPA/ZrO_2 shows (Figure 4d) the direct overlap peak between $\text{Pd}3p_{3/2}$ and O1s peaks at binding energy 532 eV, which is in good agreement with the reported one [20], and cannot be assigned to confirm the presence of $\text{Pd}(0)$. Hence, we have presented instrument generated full spectra (Figure 4a & 4d) images, supporting the presence of $\text{Pd}(0)$. This is further confirmed by recording the high resolution $\text{Pd}3d$ spectrum (Figure 4e) which shows a low intense spin orbit doublet peak at binding energy 335.6 eV and 340.2 eV correspond to $\text{Pd}3d_{5/2}$ and $\text{Pd}3d_{3/2}$, confirming the presence of $\text{Pd}(0)$ [5,21,22]. Two additional high intense peaks at binding energy 331 eV and 345 eV attributed to $\text{Zr}3p_{3/2}$ and $\text{Zr}3p_{1/2}$, respectively [23].

TPA/ZrO₂ shows (Figure 4c) a well resolved spin-orbit doublet of W4f_{7/2} and W4f_{5/2} at binding energy 35.6 and 37.6 eV (spin-orbit splitting, 2.0 eV), characteristic of W(VI), confirming the presence of W(VI). Pd-TPA/ZrO₂ also shows (Figure 4f) a single spin-orbit pair at binding energy 35.7 and 37.7 eV (spin-orbit splitting, 2.0 eV) confirming no reduction of W during the synthesis [21, 24].

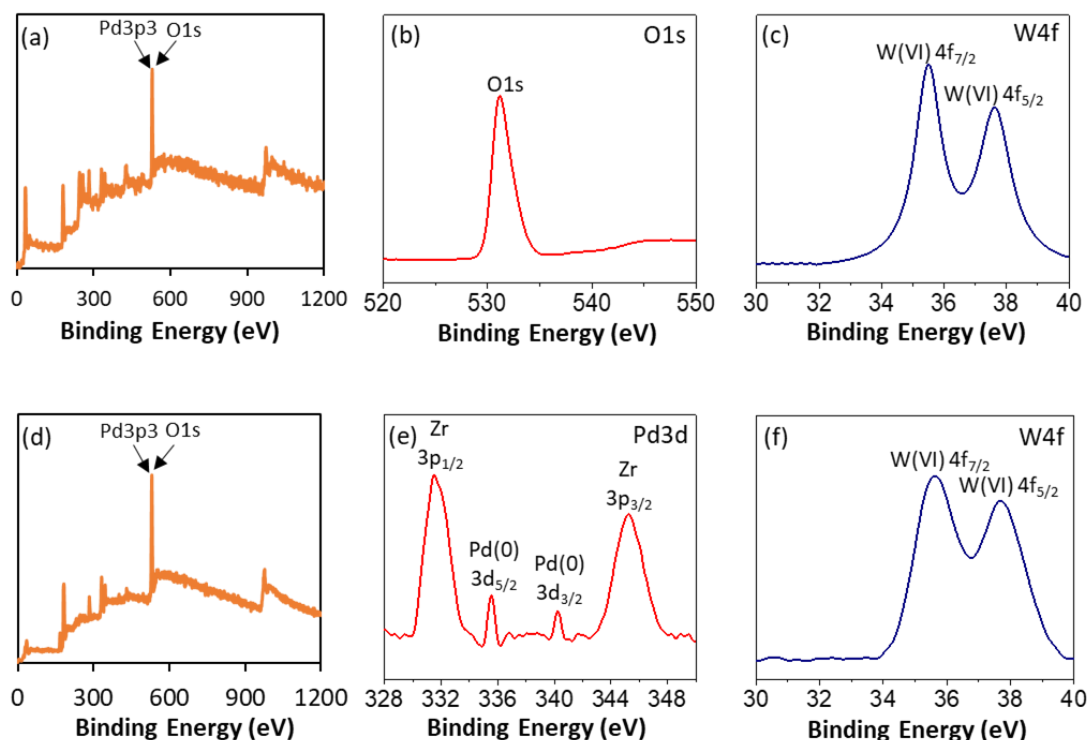


Figure 4 XPS spectra of PdTPA (a, b and c) and PdTPA/ZrO₂ (d, e and f).

TEM micrographs of the Pd-TPA/ZrO₂ are displayed in figure 5(a-c). SAED image 5a indicates the non-crystalline dispersion of PdNPs in the synthesized catalyst. Image 5(b-c) shows the dark uniform suspension in the amorphous nature of the catalyst indicating the high dispersion of PdNPs onto surface of support. To further confirm, HRTEM micrographs were also recorded as shown in figure 5(d-f), which clearly shows the uniform dispersion of PdNPs throughout the morphology, without aggregates formation, confirming the stabilization of PdNPs by TPA.

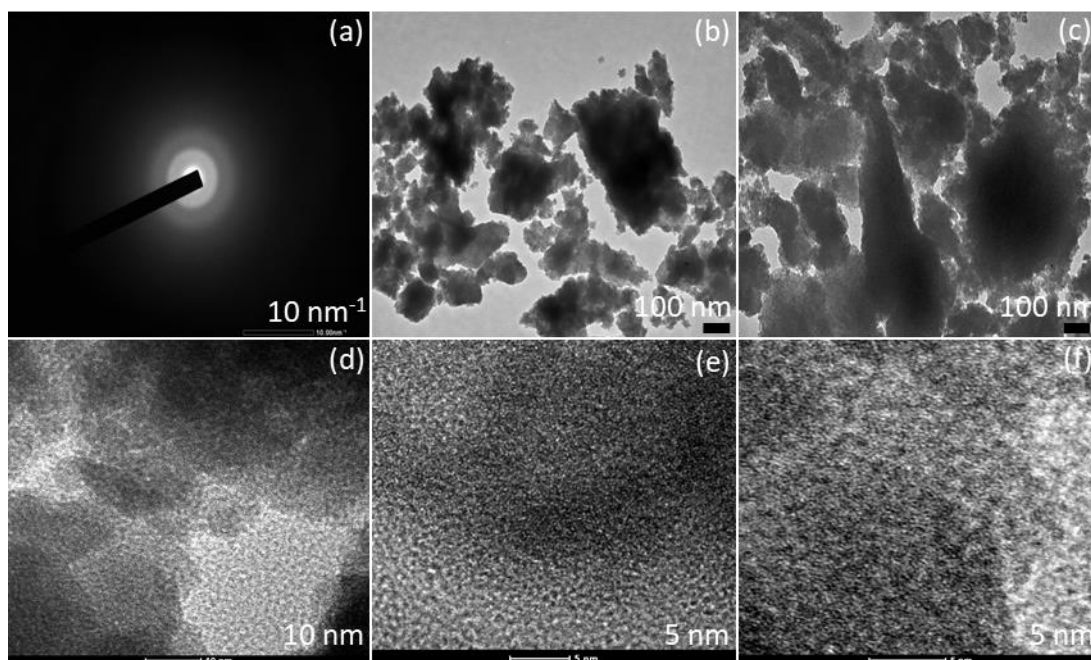


Figure 5 (a) SAED, (b-c) TEM and (d-f) HRTEM images of Pd-TPA/ZrO₂.

For more insight of PdNPs, an advance technique, STEM was utilized to probe the behavior of PdNPs. HAADF STEM image (Figure 6a) shows the highly dispersed PdNPs onto the surface. Whereas, elemental image of Pd (Figure 6b) as well as overlapping image (Figure 6f) clearly indicate the presence of isolated PdNPs homogeneously dispersed without any cross talks between them. The absence of Pd aggregates conclude that TPA/ZrO₂ is very much capable to decrease the high surface free energy of PdNPs, by providing combinedly the facility of high surface area for dispersion as well as stabilizing nature. Elemental images (Figure 6b-e) confirm the presence of all possible elements in the synthesized catalyst.

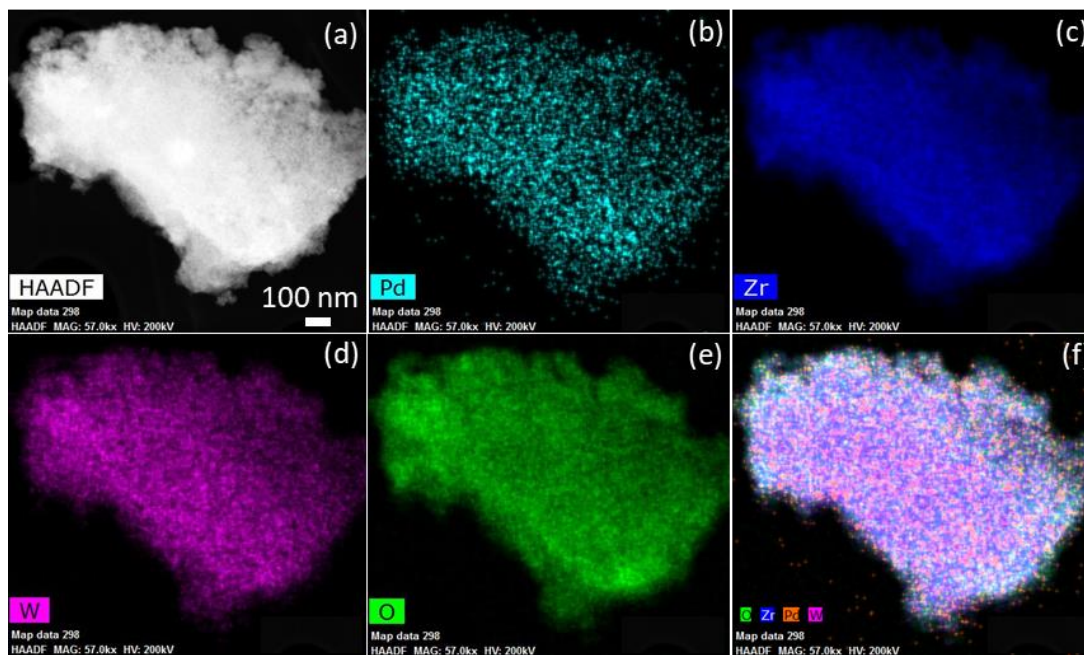


Figure 6 (a) HAADF STEM, (b-e) elemental and (f) overlapping images of Pd-TPA/ZrO₂.

The increase in surface area of the Pd(II)-TPA/ZrO₂ (169 m²/g) as compared to that of TPA/ZrO₂ (146 m²/g) indicates high uniform dispersion of the Pd on the surface of TPA/ZrO₂ [17]. The observed drastic increase in the value of surface area of Pd-TPA/ZrO₂ (203 m²/g) as compared to that of Pd(II)-TPA/ZrO₂ (169 m²/g), conforming the reduction of Pd(II) to Pd(0) and in good agreement with the known fact that nanoparticles have higher surface area than the parent one. It is very interesting to note down that in spite of different surface area, the nitrogen adsorption desorption isotherms (Figure 7) are almost similar for all systems confirming no change in the basic structure.

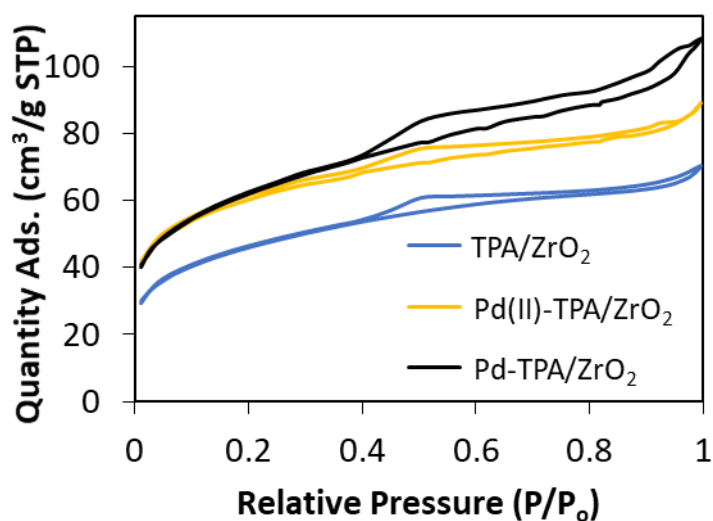


Figure 7 Nitrogen sorption isotherms.

The XRD patterns of TPA, ZrO₂, TPA/ZrO₂ and Pd-TPA/ZrO₂ are shown in figure 8. The XRD pattern of ZrO₂ shows the amorphous nature of the support. The XRD pattern of TPA/ZrO₂ does not show any characteristic diffraction line indicating a high dispersion of TPA in a non-crystalline form on the surface of TPA/ZrO₂. In XRD pattern of Pd-TPA/ZrO₂, absence of any crystalline peak corresponds to Pd(0), is due to the very low concentration of Pd(0) on the surface of the catalyst as well as high dispersion of PdNPs on the surface of TPA/ZrO₂.

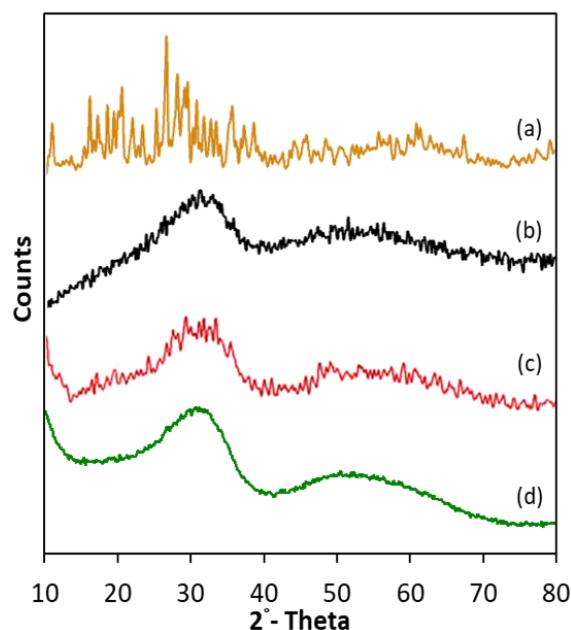


Figure 8 XRD patterns of (a) TPA, (b) ZrO₂ (c) TPA/ZrO₂ and (d) Pd-TPA/ZrO₂.

In summary, FT-IR data shows that TPA structure remains intact even after supporting onto the surface of ZrO₂ and post reduction, there is a strong interaction (hydrogen bonding) between terminal oxygen of TPA with the hydrogen of surface hydroxyl groups of ZrO₂. The presence and oxidation states of Pd(0) and W(VI) are confirmed by XPS. TEM, HRTEM and STEM confirm the presence of homogeneously dispersed PdNPs onto surface of ZrO₂.

Catalytic Activity

SM Coupling

(i) Aqueous medium

To evaluate the efficiency of the catalyst for SM coupling, iodobenzene (1.96 mmol) and phenylboronic acid (2.94 mmol) were selected as test substrates. Effect of different reaction parameters such as palladium concentration, time, temperature, base, solvent and solvent ratio were studied to optimize the conditions for maximum conversion.

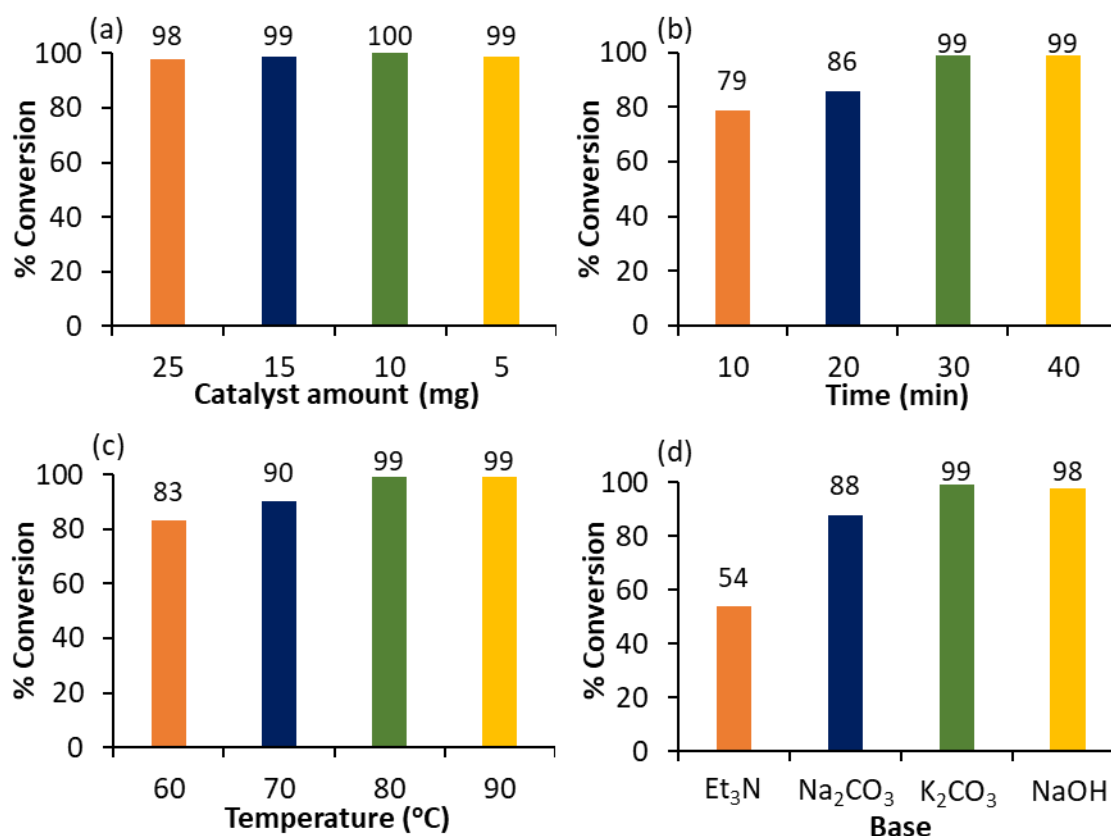


Figure 9 Optimization of parameters for SM coupling. Reaction conditions: (a) Effect of catalyst amount- K₂CO₃ (3.92 mmol), EtOH: H₂O (3:7 mL), time (30 min), temperature (80 °C); (b) Effect of time- catalyst (5 mg), K₂CO₃ (3.92 mmol), EtOH: H₂O (3:7 mL), temperature (80 °C); (c) Effect of temperature- catalyst (5 mg), K₂CO₃ (3.92 mmol), EtOH: H₂O (3:7 mL), time (30 min); (d) Effect of base- catalyst (5 mg), base (3.92 mmol), EtOH: H₂O (3:7 mL), time (30 min), temperature (80 °C).

The effect Pd(0) concentration on the reaction is shown in figure 9a. The reactions were carried out by varying the catalyst amount in the range of 25-5 mg with concentration of Pd(0) in the range of 37.4×10^{-4} mmol (0.192 mol%) to 1.88×10^{-4} mmol (0.0096 mol%), respectively. Initially, the reaction was carried out using (0.192 mol%) and conversion remain unchanged with decrease in the concentration of Pd(0) up to 0.0096 mol%. This indicates that very low concentration of Pd(0) is sufficient for the maximum % conversion.

The influence of time on catalytic conversion was screened between 10 min to 40 min as shown in figure 9b. Initially, ≈ 1.25 -fold % conversion increase from 10 to 30 min of reaction time. Further, prolonging the reaction (40 min), no significant effect on reaction conversion was observed. Hence, 30 min was optimized for the reaction.

The effect of temperature was assessed between 60 to 90 °C and obtained results are presented in figure 9c. It can be seen from the results that with increase in temperature, the % conversion also increases. 99 % conversion was obtained at 80 °C. Further, increase in temperature does not show any effect on conversion. Hence, 80 °C was considered as optimum for the maximum % conversion.

Effect of various bases was also carried out and obtained results are presented in figure 9d. The study indicates that organic base triethyl amine (Et_3N) is less favorable for coupling reaction compare to that of inorganic base. The highest conversion was found in the case of K_2CO_3 and NaOH compared to Na_2CO_3 . As K_2CO_3 is environmentally benign, easy to handle and non-hygroscopic in nature compared to NaOH , further study was carried out with K_2CO_3 .

The effect of different solvents is shown in table 1.

Table 1 Effect of solvent

Solvent	% Conversion
Toluene	5
Acetonitrile	47
Ethanol	53
H_2O	42

Reaction conditions: Catalyst (5 mg), K_2CO_3 (3.92 mmol), solvent (10 mL), time (30 min), temperature (80 °C).

From the results it is clear that in case of ethanol the highest conversion was achieved compare to acetonitrile and toluene. The results are in good

agreement with reported one [17], stating that polar solvents tend to give the best result for coupling reaction. Low conversion in case of water as solvent is may be due to the low solubility of substrates. Hence, ethanol was selected as an appropriate solvent for further study.

Finally, the effect of solvent to water (Ethanol: H₂O) ratio was studied and obtained results are presented in table 2. Obtained results show that initially, with increase in ethanol amount the % conversion increases, this may be due to the increase in solubility of substrates in ethanol. This trend was found from ratio (1:9) mL to (3:7) mL. For higher ratio (4:6) to (5:5) mL, no significant change in % conversion was observed. Maximum 99 % conversion was achieved for (3:7) mL.

Table 2 Effect of solvent ratio

Ethanol: H ₂ O	% Conversion
1:9	75
2:8	82
3:7	99
4:6	99
5:5	99

Reaction conditions: Catalyst (5 mg), K₂CO₃ (3.92 mmol), time (30 min), temperature (80 °C).

From the above study, the optimized conditions for the maximum % conversion (99) are: iodobenzene (1.96 mmol), phenylboronic acid (2.94 mmol), K₂CO₃ (3.92 mmol), conc. of Pd (1.88×10^{-4} mmol, 0.0096 mol%), substrate/catalyst ratio (10429/1), C₂H₅OH:H₂O (3:7 mL), time (30 min), temperature (80 °C). The calculated TON is 10,325 and TOF is 20,650 h⁻¹.

Further, the obtained product was purified by column chromatography on silica gel with a mixture of ethyl acetate and petroleum ether as eluent. Isolated yield (99%) was found to be the same with the conversion (99%) found by GC.

From the obtained results of solvent ratio effect (Table 2), it is interesting to note down that water has significant effect on % conversion. Hence, it was thought of interest to study all reaction parameters by taking only water as a solvent.

(ii) Neat Water

To evaluate the efficiency of the catalyst for SM coupling using water as solvent, iodobenzene (1.96 mmol) and phenylboronic acid (2.94 mmol) were selected as test substrates. Effect of different reaction parameters such as palladium concentration, time, temperature and base were studied to optimize the conditions for maximum conversion (Figure 10).

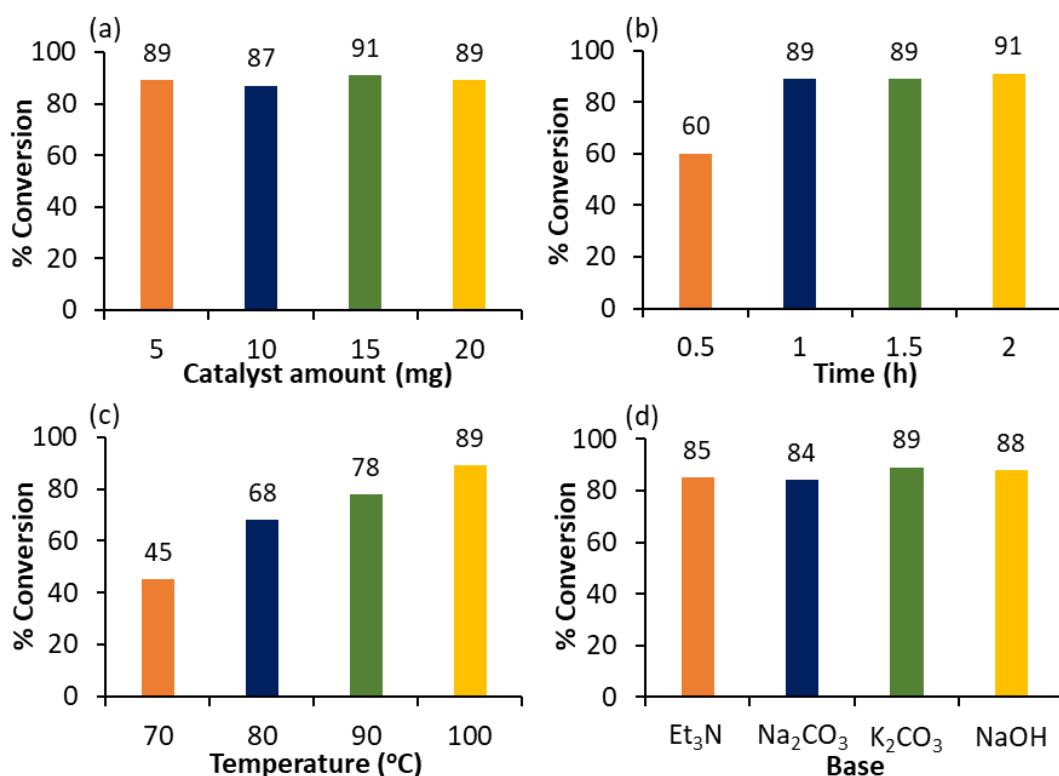


Figure 10 Optimization of parameters for SM reaction in neat water. Reaction conditions: (a) Effect of catalyst amount- K₂CO₃ (3.92 mmol), H₂O (6 mL), time (1 h), temperature (100 °C); (b) Effect of time- catalyst (5 mg), K₂CO₃ (3.92 mmol), H₂O (6 mL), temperature (100 °C); (c) Effect of temperature- catalyst (5 mg), K₂CO₃ (3.92 mmol), H₂O (6 mL), time (1 h); (d) Effect of base- base (3.92 mmol), H₂O (6 mL), time (1 h), temperature (100 °C).

The effect of Pd(0) concentration was studied by varying the amount from 5 to 15 mg with concentration of Pd(0) from 1.88×10^{-4} mmol (0.0096 mol%) to 5.61×10^{-4} mmol (0.0288 mol%), respectively as shown in figure 10a. Obtain results show that conversion remains unchanged with increase in the concentration of Pd(0). This indicates that very low concentration of Pd(0) (0.0096 mol%) is sufficient for the maximum 89 % conversion.

The effect of time was screened by varying the time from 30 min to 2 h (Figure 10b). Results indicate that initially, with increase in time (up to 1 h) % conversion also increases. Further, prolonging of reaction (up to 2 h) has no significant effect on conversion. Maximum 89 % conversion is obtained in 1 h.

Effect of temperature was studied from the range of 80-100 °C and the obtained results are summarized in figure 10c. It shows that conversion increases with increase in temperature and found to be maximum at 100 °C. Effect of various bases was also carried out and achieved results are shown in figure 10d. Similar to previous case, here also K_2CO_3 was found to be the most suitable base for the maximum % conversion.

Finally, the effect of water amount on the reaction was also studied by keeping all other parameters constant. Obtained results are presented in figure 11. From the figure it is seen that with increase in the water volume up to 6 mL, the conversion also increases. This may be due to the increase in the solubility of substrates as well as base. However, with further increase in volume of water, the conversion eventually decreases. This is because of the dilution of base [25]. Under the optimized conditions, 6 mL of water is found to be the appropriate volume for the maximum % conversion.

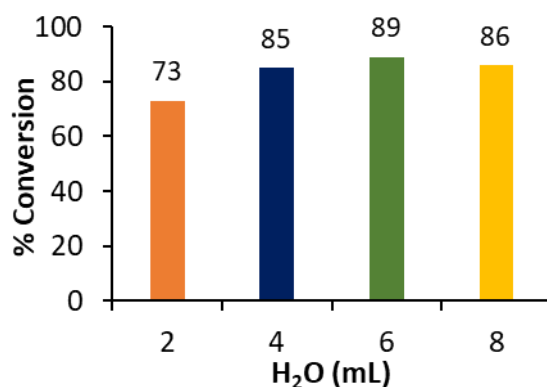


Figure 11 Effect of water: catalyst (5 mg), K₂CO₃ (3.92 mmol), time (1 h), temperature (100 °C).

From the above study, the optimized conditions for the maximum % conversion (89) are: iodobenzene (1.96 mmol), phenylboronic acid (2.94 mmol), K₂CO₃ (3.92 mmol), conc. of Pd (1.88×10^{-4} mmol, 0.0096 mol%), substrate/catalyst ratio (10,429/1), H₂O (6 mL), time (1 h), temperature (100 °C). The calculated TON is 9282 and TOF is 9282 h⁻¹.

In addition, obtained product was purified by column chromatography on silica gel with a mixture of ethyl acetate and petroleum ether as eluent. Isolated yield (89 %) was found to be the same with the conversion (89 %) found by GC.

Comparison of catalyst efficiency in terms of solvent medium

Effect of solvent medium on the reaction conversion also compared under the optimized conditions of the respective media (Table 3) and results show that catalyst is highly effective in aqueous medium compared to neat water.

Table 3 Comparison of catalyst activity in terms of solvent medium

Medium	Temp. (°C)	Time (h)	% Conversion	TON	TOF (h ⁻¹)
Aqueous	80	0.5	99	10325	20650
Neat water	100	1	89	9282	9282

Reaction conditions: Iodobenzene (1.96 mmol), phenylboronic acid (2.94 mmol), catalyst (0.02 mg Pd, 0.0096 mol% Pd), K₂CO₃ (3.92 mmol).

Aqueous medium: C₂H₅OH: H₂O (3:7 mL); Neat water: H₂O (6 mL).

This difference may be due to the presence of ethanol in aqueous medium, which helps organic substrates to solubilize easily in the reaction mixture for the productive conversion. Whereas in case of water alone, substrates require high temperature as well as prolong time for the same.

Heck coupling

To evaluate the efficiency of the catalyst for heck coupling, iodobenzene (0.98 mmol) and styrene (1.47 mmol) were selected as test substrates. Effect of different reaction parameters such as palladium concentration, time, temperature, base, solvent and solvent ratio was studied to optimize the conditions for maximum conversion. As described in SM coupling, in the present case also, all parameters were varied and results are shown in respective figures (Figure 12).

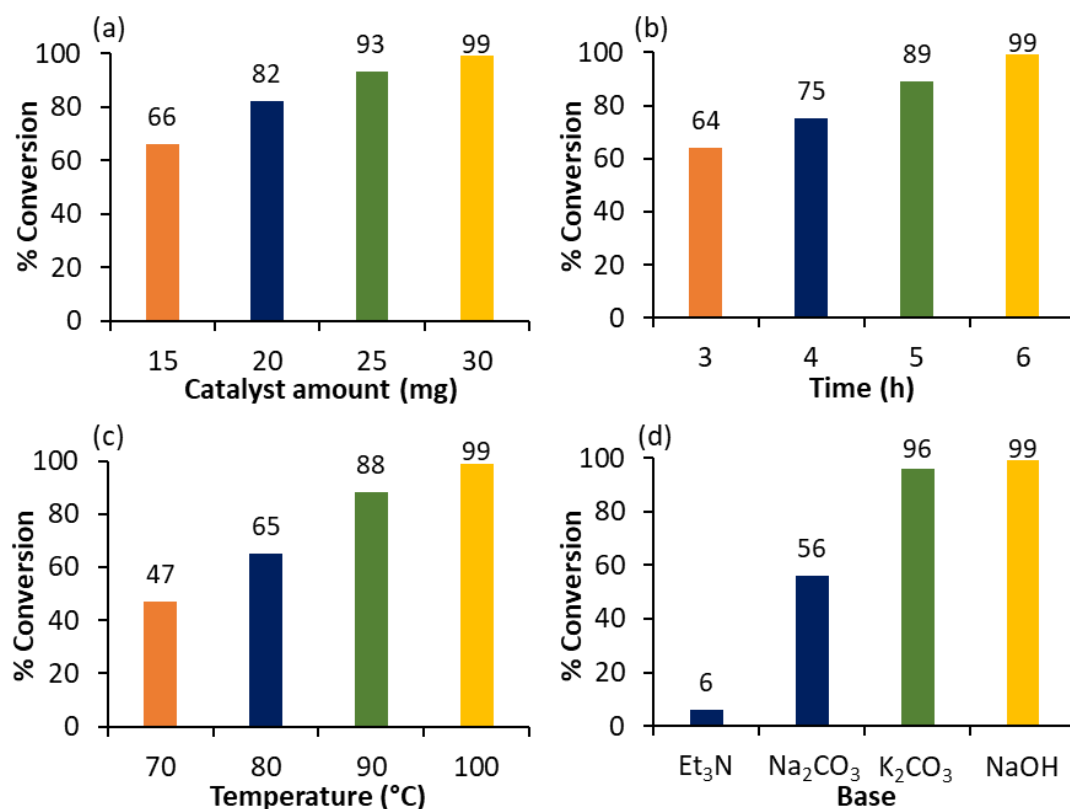


Figure 12 Optimization of Heck coupling. Reaction conditions: (a) Effect of catalyst amount- K_2CO_3 (1.96 mmol), DMF:H₂O (3:2 mL), time (6 h), temperature (100 °C); (b) Effect of time- catalyst (30 mg), K_2CO_3 (1.96 mmol), DMF:H₂O (3:2 mL), temperature (100 °C), (c) Effect of temperature- catalyst (30 mg), K_2CO_3 (1.96 mmol), DMF:H₂O (3:2 mL), time (6 h); (d) Effect of base- catalyst (30 mg), base (1.96 mmol), DMF:H₂O (3:2 mL), time (6 h), temperature (100 °C).

It should be noted that the explanation will remain the same as given in the section of SM coupling (Aqueous medium).

The effect of different solvents was also studied and obtained results are shown in table 4. Study indicates that maximum % conversion was obtained in case of DMF compare to toluene and ethanol. This is in good agreement with the reported one [26-28] , stating that polar, aprotic solvents tend to give the best results for Heck coupling. Low % conversion is observed in case of water may be due to the lower solubility of substrate. Hence, DMF was selected as an appropriate solvent for further study.

Table 4 Effect of solvent

Solvent	% Conversion
Toluene	3
Ethanol	26
DMF	51
H ₂ O	7

Reaction conditions: Catalyst (30 mg), K₂CO₃ (1.96 mmol), time (6 h), temperature (100 °C).

Finally, the effect of solvent to water (DMF: H₂O) ratio was assessed and data are tabulated in table 5.

Table 5 Effect of solvent ratio

DMF: H ₂ O	% Conversion
1:4	12
2:3	50
3:2	99
4:1	81

Reaction conditions: Catalyst (30 mg), K₂CO₃ (1.96 mmol), time (6 h), temperature (100 °C).

Obtained results show that initially, with increase in DMF amount the % conversion increases, this may be due to the increase in solubility of substrates in DMF. This trend was found from ratio (1:4) mL to (3:2) mL. For higher ratio (4:1) mL, % conversion decreases, because of incomplete solubility of base in 1 mL of water. Maximum 99 % conversion was achieved for (3:2) mL.

The optimized conditions for the maximum % conversion (99) are: iodobenzene (0.98 mmol), styrene (1.47 mmol), K₂CO₃ (1.96 mmol), conc. of Pd (1.13×10^{-3} mmol, 0.115 mol%), substrate/catalyst ratio (869/1), DMF:H₂O (3:2 mL), time (6 h), temperature (100 °C). The calculated turnover number (TON) is 860 and turnover frequency (TOF) is 143 h⁻¹.

Hydrogenation

(i) Cyclohexene hydrogenation

To evaluate the efficiency of the catalyst for hydrogenation, cyclohexene (9.87 mmol) was selected as test substrate. Effect of different reaction parameters such as palladium concentration, time, temperature, pressure and solvent were studied to optimize the conditions for maximum conversion (Figure 13).

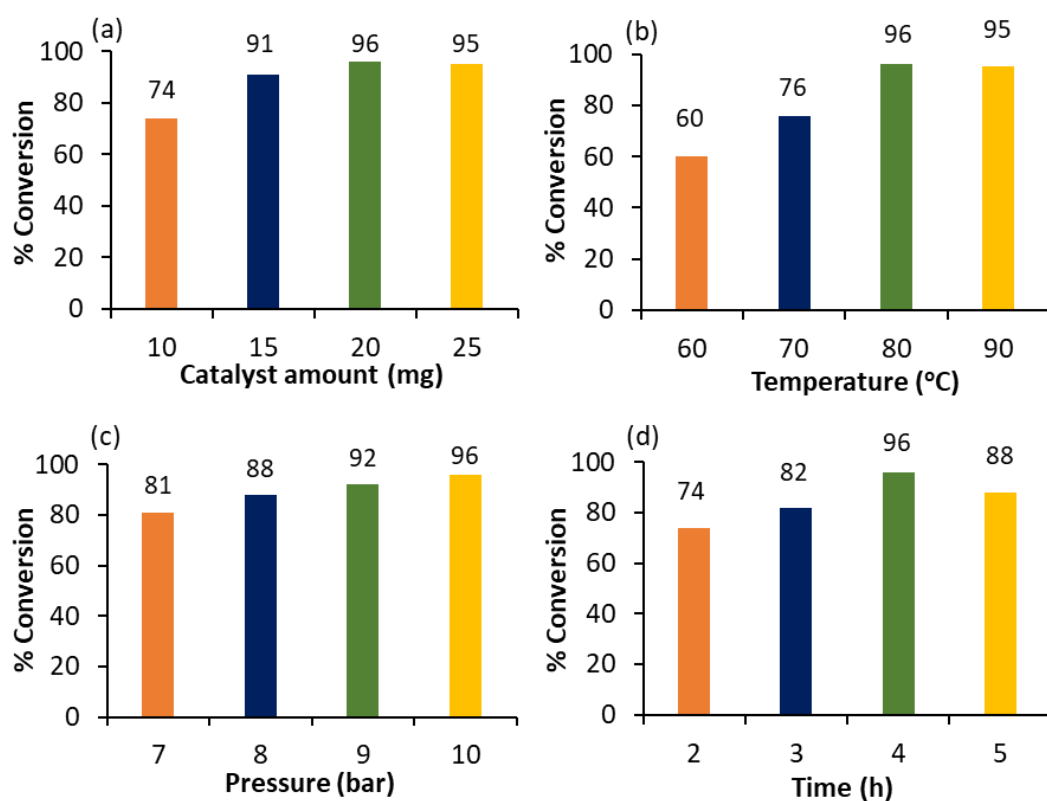


Figure 13 Optimization of cyclohexene hydrogenation. Reaction conditions: (a) Effect of catalyst amount- cyclohexene (9.87 mmol), H₂O (50 mL), time (4 h), temperature (80 °C), H₂ pressure (10 bar); (b) Effect of temperature- cyclohexene (9.87 mmol), H₂O (50 mL), catalyst (20 mg), time (4 h), H₂ pressure (10 bar); (c) Effect of pressure- cyclohexene (9.87 mmol), H₂O (50 mL), catalyst (20 mg), time (4 h), temperature (80 °C); (d) Effect of time- cyclohexene (9.87 mmol), H₂O (50 mL), catalyst (20 mg), temperature (80 °C), H₂ pressure (10 bar).

The effect of Pd concentration was evaluated by varying the catalyst amount from 10 mg to 25 mg (substrate/catalyst ratio from 26259/1 to 10504/1 respectively). Initially, with increase in concentration of Pd, % conversion also increases i.e. 10 mg to 20 mg (Figure 13a). Higher concentration of Pd would mean a higher number of active sites to tolerate the substrate and gives higher conversion. With further increasing Pd concentration, the conversion remains constant. The highest, 96 % conversion was achieved by 20 mg of catalyst.

Effect of temperature was screened from 60 to 90 °C and obtained results are presented in figure 13b. Results show that % conversion increases with increase in temperature from 50 to 80 °C as expected. Further increase in the temperature shows no effect on the % conversion. 80 °C was optimized for maximum % conversion.

Influence of hydrogen pressure was evaluated and obtained results are presented in figure 13c. Initially, with increase in pressure from 7 to 10 bar, the % conversion also increased linearly. Hence, the reaction is first order with respect to H₂ pressure. Further study for effect of high pressure was not carried out as our main focus is to establish environmentally green process. Highest 96 % conversion was obtained for 10 bar H₂ pressure.

The effect of time was investigated by varying the reaction time from 2 to 5 h (Figure 13d). obtained results show that initially with increase in time up to 4 h, the % conversion also increases, which is in good agreement with the well-known fact that as time increases, the formation of reactive intermediates from the reactant increases, and finally converted into the products. On further increasing the reaction time, the % conversion decreases. This might be due to occurrence of reversible process.

Effect of various solvents were studied and obtained results are presented in table 6. Comparatively, low % conversion was obtained in case of CH₃CN-H₂O solvent system due to its oxidizing nature which resists the reduction of

cyclohexene. Whereas, it was achieved maximum for IPA-H₂O and CH₃OH-H₂O systems and this may be due to their reducing nature. However, high % conversion was obtained under the identical reaction conditions for neat water as a solvent (i.e. 96 %). Hence, water was selected as a solvent for further study.

Table 6 Effect of solvent

Solvent (20: 30) mL	% Conversion
CH ₃ CN: H ₂ O	84
IPA: H ₂ O	93
EtOH: H ₂ O	99
H ₂ O (50 mL)	96

Reaction conditions: cyclohexene (9.87 mmol), catalyst (20 mg), time (4 h), temperature (80 °C), H₂ pressure (10 bar).

The optimized conditions for the maximum % conversion (96) are: cyclohexene (9.87 mmol), H₂O (50 mL), conc. of Pd (7.52×10^{-4} mmol, 0.0076 mol%), substrate/catalyst ratio (13130/1), time (4 h), temperature (80 °C) and H₂ pressure (10 bar). The calculated TON is 12,604 and TOF is 3151 h⁻¹.

The obtained products from all the reactions were purified by column chromatography on silica gel with a mixture of ethyl acetate and petroleum ether as eluent. Isolated yields were found to be identical with the conversion found by GC. The isolated products were identified by ¹H & ¹³C NMR (Figure 14, Biphenyl; Figure 15, Stilbene; Figure 16, Cyclohexane).

In similar way, for all the catalytic systems, products isolation and identification were carried out.

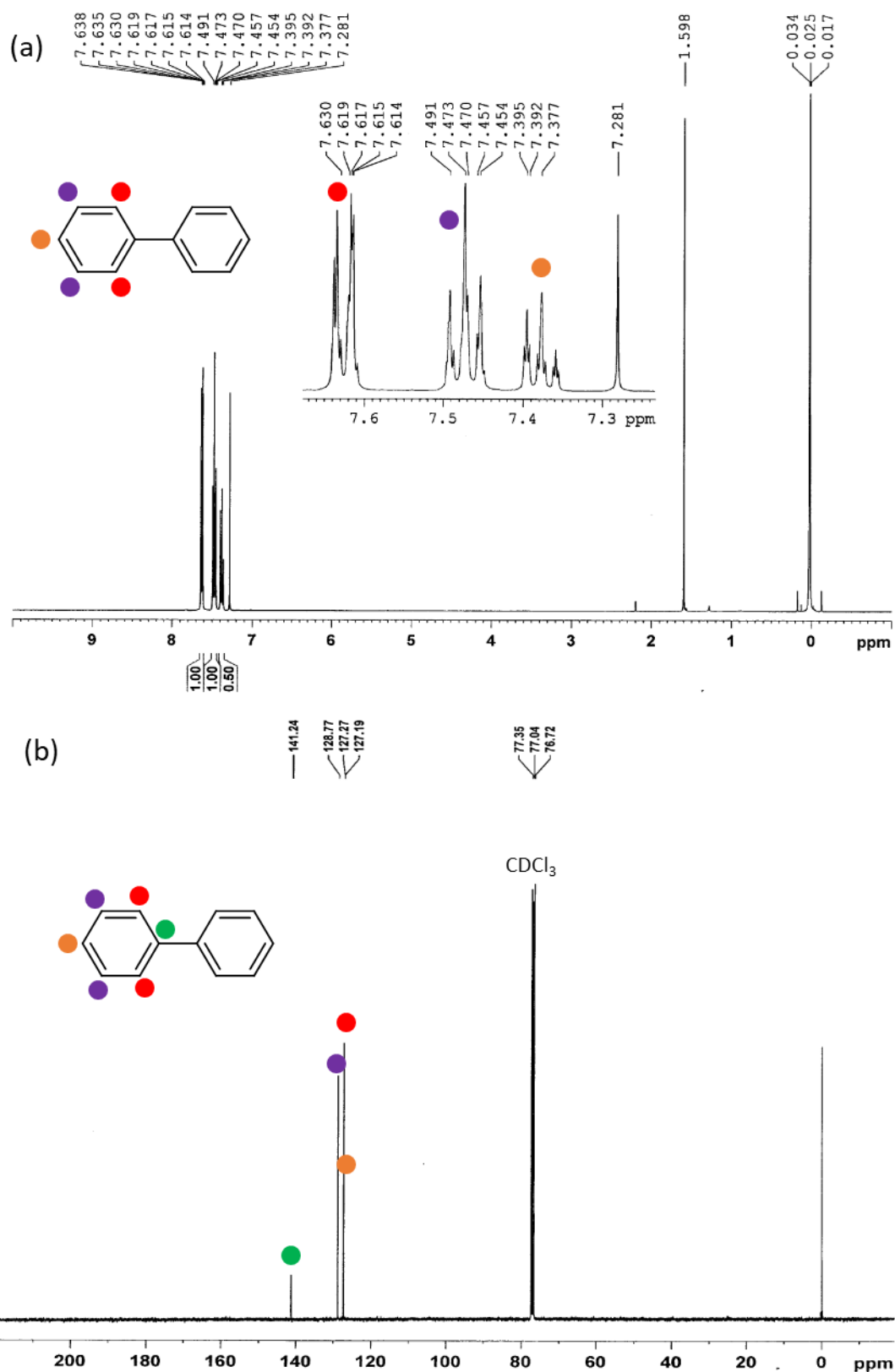


Figure 14 (a) ^1H and (b) ^{13}C NMR spectra of isolated product biphenyl.

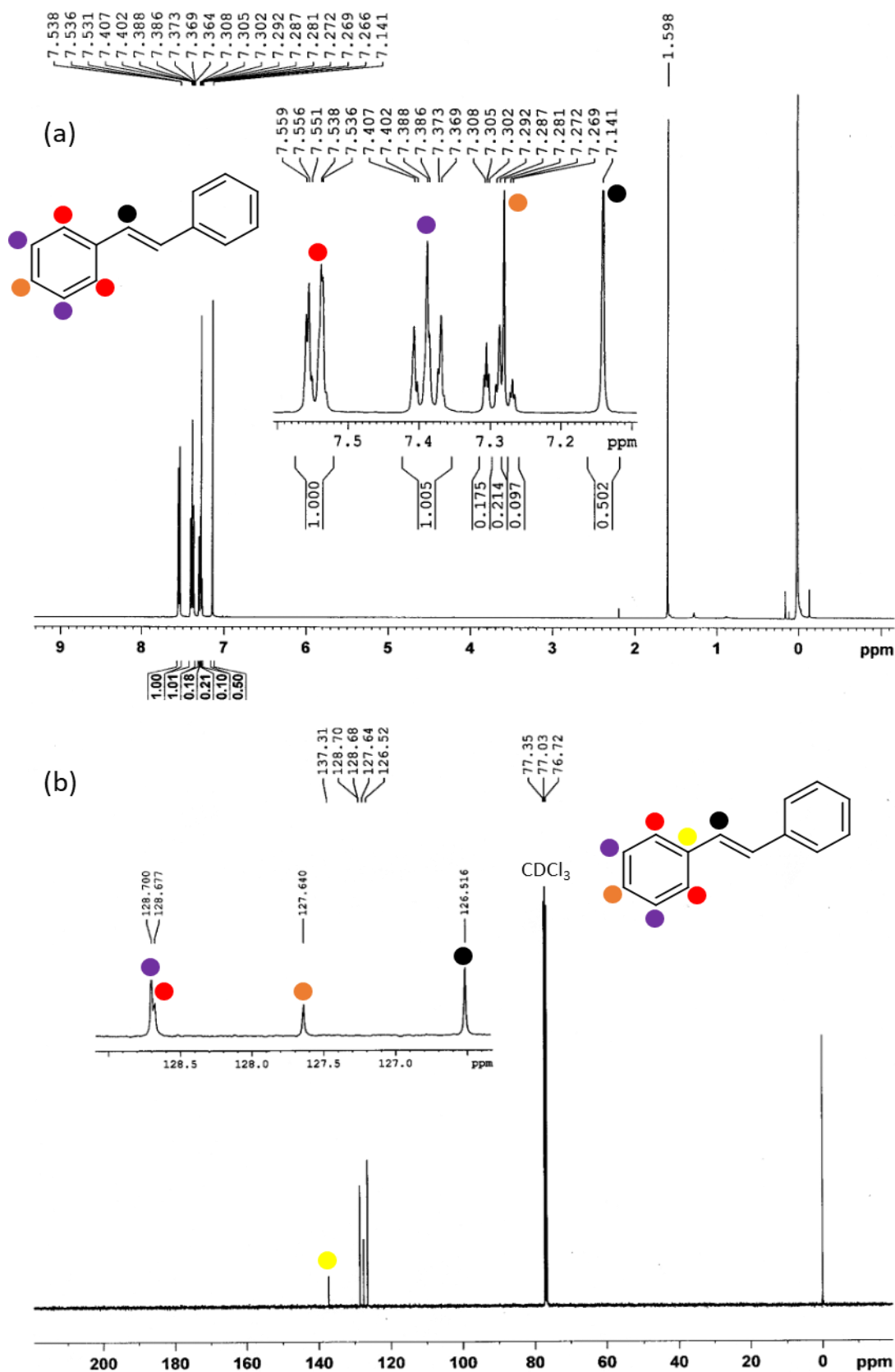


Figure 15 (a) ¹H and (b) ¹³C NMR spectra of isolated product stilbene.

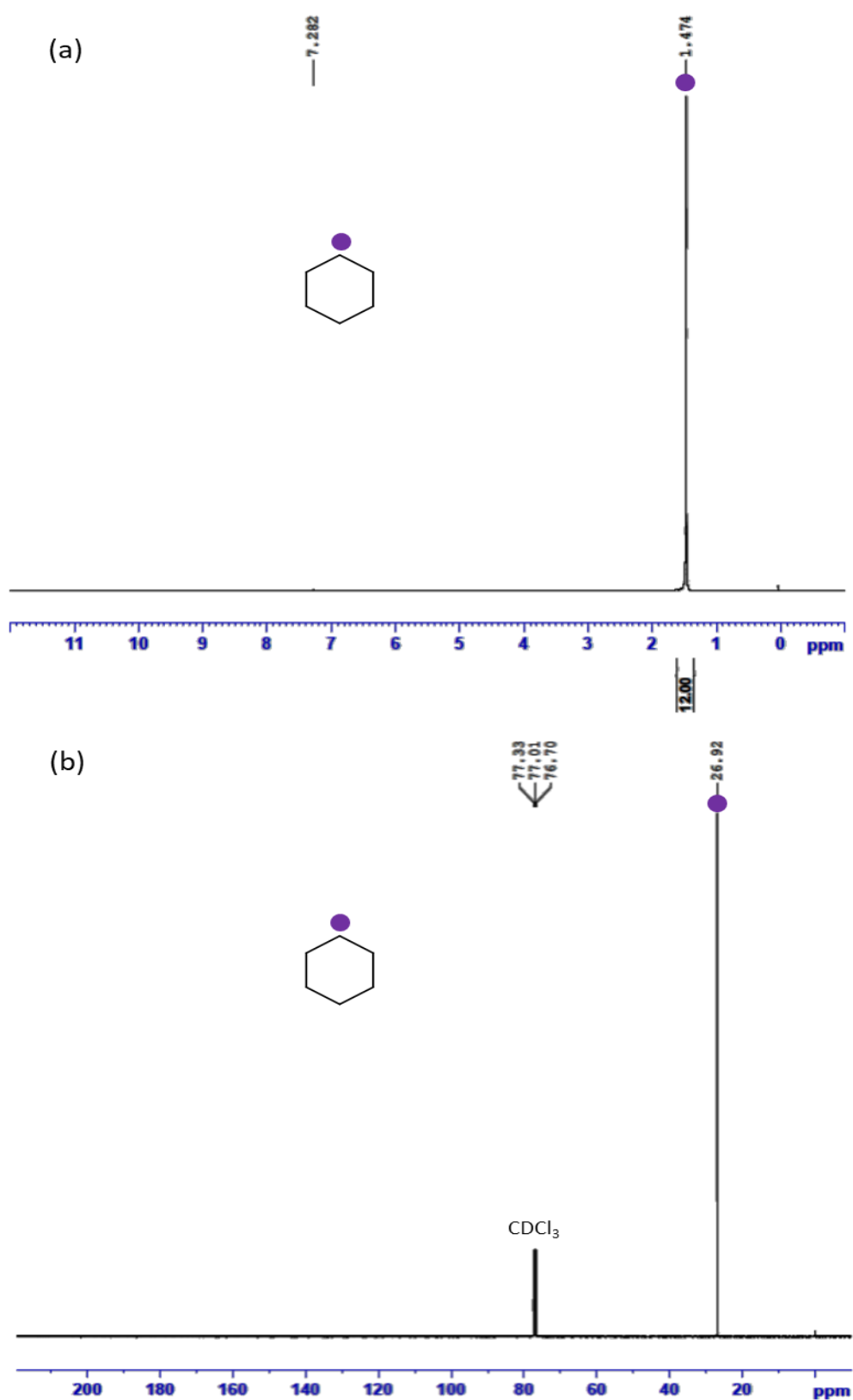


Figure 16 (a) ^1H and (b) ^{13}C NMR spectra of isolated product cyclohexane.

(ii) Crotonaldehyde hydrogenation

From the above obtained excellent results of cyclohexene hydrogenation, it was thought to investigate the efficiency of the catalyst towards selective hydrogenation using another industrially important substrate.

Selective C=C hydrogenation of crotonaldehyde can yield n-butyraldehyde, an industrially important chemical intermediate for n-butyl alcohol, 2-ethylhexanol, trimethylolpropane (TMP), polyvinyl butyral (PVB), pharmaceuticals, pesticides, antioxidants, flavors, synthetic perfumes, vulcanization accelerators, crop protecting agent and many more. Considering this, we have selected crotonaldehyde as the test substrate to evaluate the efficiency of the catalyst towards selective C=C hydrogenation. In detail, effect of different reaction parameters such as palladium concentration, time, temperature, pressure and solvent were studied to optimize the conditions for maximum conversion.

As described in above section of cyclohexene hydrogenation, in the present case also, all parameters were varied and obtained results are shown in respective figures (Figure 17).

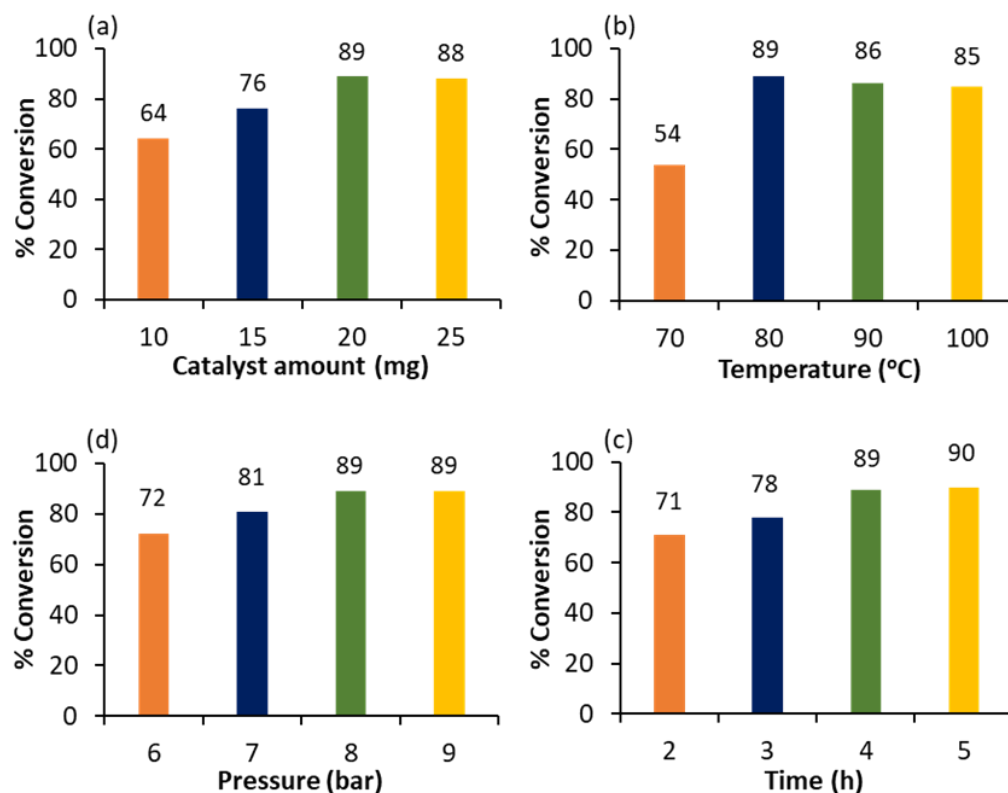


Figure 17 Optimization of crotonaldehyde hydrogenation. Reaction conditions: (a) Effect of catalyst amount- crotonaldehyde (9.87 mmol), H₂O (50 mL), time (4 h), temperature (80 °C), H₂ pressure (8 bar); (b) Effect of temperature- crotonaldehyde (9.87 mmol), H₂O (50 mL), catalyst (20 mg), time (4 h), H₂ pressure (8 bar); (c) Effect of pressure- crotonaldehyde (9.87 mmol), H₂O (50 mL), catalyst (20 mg), time (4 h), temperature (80 °C); (d) Effect of time- crotonaldehyde (9.87 mmol), H₂O (50 mL), catalyst (20 mg), temperature (80 °C), H₂ pressure (8 bar).

It should be noted that the explanation is remain same as given in the section of cyclohexene hydrogenation. Here, in all the cases, butyraldehyde was obtained with 100% selectively. Whereas in case of EtOH: H₂O (20:30) mL solvent system (table 7), we achieved 91% conversion with 60% butyraldehyde and 40% crotyl alcohol selectively. An explanation for the same is provided in mechanism section (afterward).

Table 7 Effect of solvent

Solvent	% Conversion	% Selectivity	
		Butyraldehyde	Crotyl alcohol
IPA	100	100	0
H ₂ O	89	100	0
EtOH: H ₂ O (20:30) mL	91	60	40

Reaction conditions: crotonaldehyde (9.87 mmol), solvent (50 mL), catalyst (20 mg), time (4 h), temperature (80 °C), H₂ pressure (8 bar).

The optimized conditions for the maximum % conversion (89) are: crotonaldehyde (9.87 mmol), H₂O (50 mL), conc. of Pd(0) (7.52×10^{-4} mmol, 0.0076 mol%), substrate/catalyst ratio (13130/1), temperature (80 °C), H₂ pressure (8 bar) and time (4 h). The calculated TON is 11744 while the TOF is 2936 h⁻¹.

Control Experiments

In all the reactions, control experiments were carried out with TPA, ZrO₂, TPA/ZrO₂, PdCl₂, Pd/ZrO₂ and Pd-TPA/ZrO₂ under optimized conditions in order to understand the role of each component, and results are shown in table 8. It is seen from the table that TPA, ZrO₂ and TPA/ZrO₂ were inactive toward the reactions. Almost same conversion was found in the case of PdCl₂, Pd/ZrO₂ and Pd-TPA/ZrO₂ in all reactions. This indicates that Pd is real active

species responsible for the reactions. In order to confirm the formation of homocoupling products, control experiments were carried out with iodobenzene as well as phenylboronic acid also, and no conversion confirmed that there was no formation of homocoupling products in both the C-C coupling reactions. The same was also confirmed by substrate study also.

Table 8 Control experiment

Catalyst	SM	Heck	Hydrogenation
	% Conversion ^{a/b}	% Conversion ^c	% Conversion ^{d/e}
TPA (^{a,b} 1.15, ^c 6.92, ^{d,e} 4.62 mg)	N. R.	N. R.	N. R.
ZrO ₂ (^{a,b} 3.85, ^c 23.08, ^{d,e} 15.38 mg)	N. R.	N. R.	N. R.
TPA/ZrO ₂ (^{a,b} 5, ^c 30, ^{d,e} 20 mg)	N. R.	N. R.	N. R.
PdCl ₂	99/84	96	94/88
Pd/ZrO ₂	95/84	96	92/86
Pd-TPA/ZrO ₂	99/89	99	96/89

Reaction conditions: *SM coupling* (a) Aqueous medium- iodobenzene (1.96 mmol), phenylboronic acid (2.94 mmol), catalyst (0.02 mg Pd, 0.0096 mol% Pd), K₂CO₃ (3.92 mmol), C₂H₅OH: H₂O (3:7 mL), time (30 min), temperature (80 °C); (b) Neat water- iodobenzene (1.96 mmol), phenylboronic acid (2.94 mmol), catalyst (0.02 mg Pd, 0.0096 mol% Pd), K₂CO₃ (3.92 mmol), H₂O (6 mL), time (1 h), temperature (100 °C). *Heck coupling* (c) iodobenzene (0.98 mmol), styrene (1.47 mmol), catalyst (0.12 mg Pd, 0.115 mol% Pd), K₂CO₃ (1.96 mmol), DMF: H₂O (3:2 mL), time (6 h), temperature (100 °C). *Hydrogenation* (d) cyclohexene (9.87 mmol), catalyst (0.08 mg Pd, 0.0076 mol% Pd), H₂O (50 mL), time (4 h), temperature (80 °C), H₂ pressure (10 bar); (e) crotonaldehyde (9.87 mmol), catalyst (0.08 mg Pd, 0.0076 mol% Pd), H₂O (50 mL), time (4 h), temperature (80 °C), H₂ pressure (8 bar). N.R.- No reaction.

Leaching and Heterogeneity test

Before exchanging Pd with available protons of TPA/ZrO₂, the leaching of TPA from ZrO₂ was investigated after completion of the reactions, by treating the aqueous layer with 10 % ascorbic acid solution and absence of blue colour indicated no leaching of TPA. The leaching of PdNPs from support was investigated for Pd/ZrO₂ as well as Pd-TPA/ZrO₂ in all reactions by centrifuging the catalyst in between the reactions under optimized conditions (Figure 18). In case of SM coupling, reaction was carried out for 10 min and 20 min in aqueous and water media respectively, centrifuged and then filtrate was allowed to react up to 30 min and 60 min in respective medium. Similarly, in case of Heck coupling, reaction was carried out for 3 h, centrifuged and then filtrate was allowed to react up to 6 h. Whereas, in case of hydrogenation, reaction was carried out for 2 h, centrifuged and then filtrate was allowed to react up to 4 h. After that obtained reaction mixtures were extracted by dichloromethane and analyzed by Gas chromatogram. In case of Pd/ZrO₂, in all reactions, obtained results show that there is significant change in % conversion of the reaction after removal of the catalyst, indicates the presence of active species in the reaction mixture which proves that there was leaching of PdNPs during the reactions. Whereas, in case of Pd-TPA/ZrO₂, in all reactions, obtained results show that there is no significant change in % conversion of the reaction after removal of the catalyst, indicates the absence of active species in the reaction mixture which proves that there was no leaching of PdNPs during the reactions. However, minor change in % conversion may be due to the instrument error ($\pm 1-1.5$ %). In addition, product mixture was also analyzed by AAS, and obtained results were below its detection limit indicating no emission of Pd into the reaction mixture. The leaching of palladium from the catalyst was also confirmed by carrying out EDX analysis of the used catalyst. The analysis of the recycled PdTPA/ZrO₂ catalyst did not show appreciable loss in the Pd content (0.39 wt%) as compared to the fresh catalyst (0.4 wt%). In the mixture whereas in case of Pd/ZrO₂, recycled catalyst

showed appreciable loss in the Pd content (3.69 wt%) as compared to the fresh catalyst (6.05 wt%). This study indicates the stabilization of PdNPs by TPA and does not allow to leach it into the reaction mixture, making it a true heterogeneous catalyst to recycle and reuse. Here, withholding of active species onto support during the reaction show that present catalyst is of category C [29] and truly heterogeneous in nature.

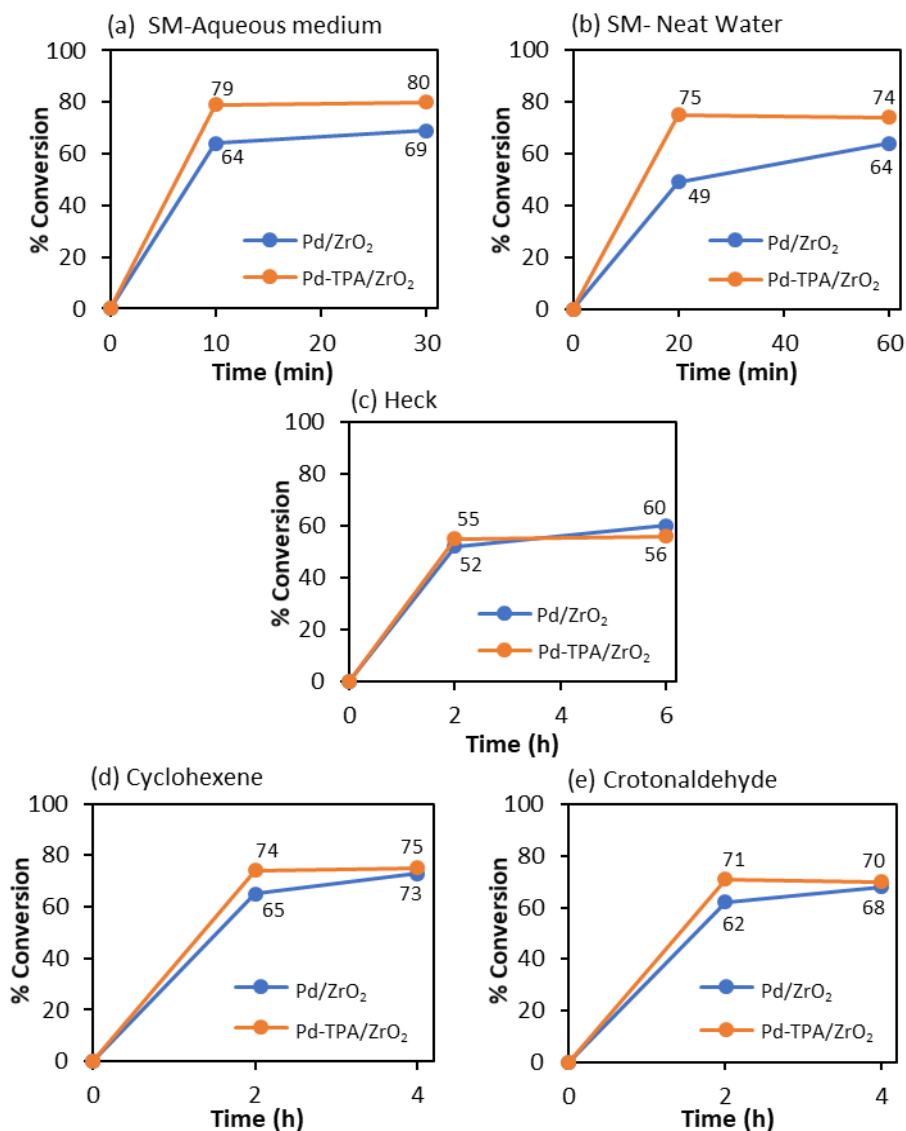


Figure 18 Leaching test. Reaction conditions: *SM coupling* (a) Aqueous medium-iodobenzene (1.96 mmol), phenylboronic acid (2.94 mmol), catalyst (0.02 mg Pd, 0.0096 mol% Pd), K₂CO₃ (3.92 mmol), C₂H₅OH: H₂O (3:7 mL), temperature (80 °C); (b) Neat water-iodobenzene (1.96 mmol), phenylboronic acid (2.94 mmol), catalyst (0.02 mg Pd, 0.0096 mol% Pd), K₂CO₃ (3.92 mmol), H₂O (6 mL), temperature (100 °C). *Heck coupling* (c) iodobenzene (0.98 mmol), styrene (1.47 mmol), catalyst (0.12 mg Pd, 0.115 mol% Pd), K₂CO₃ (1.96 mmol), DMF: H₂O (3:2 mL), temperature (100 °C). *Hydrogenation* (d) cyclohexene (9.87 mmol), catalyst (0.08 mg Pd, 0.0076 mol% Pd), H₂O (50 mL), temperature (80 °C), H₂ pressure (10 bar); (e) crotonaldehyde (9.87 mmol), catalyst (0.08 mg Pd, 0.0076 mol% Pd), H₂O (50 mL), temperature (80 °C), H₂ pressure (8 bar).

Recyclability and sustainability of the catalyst

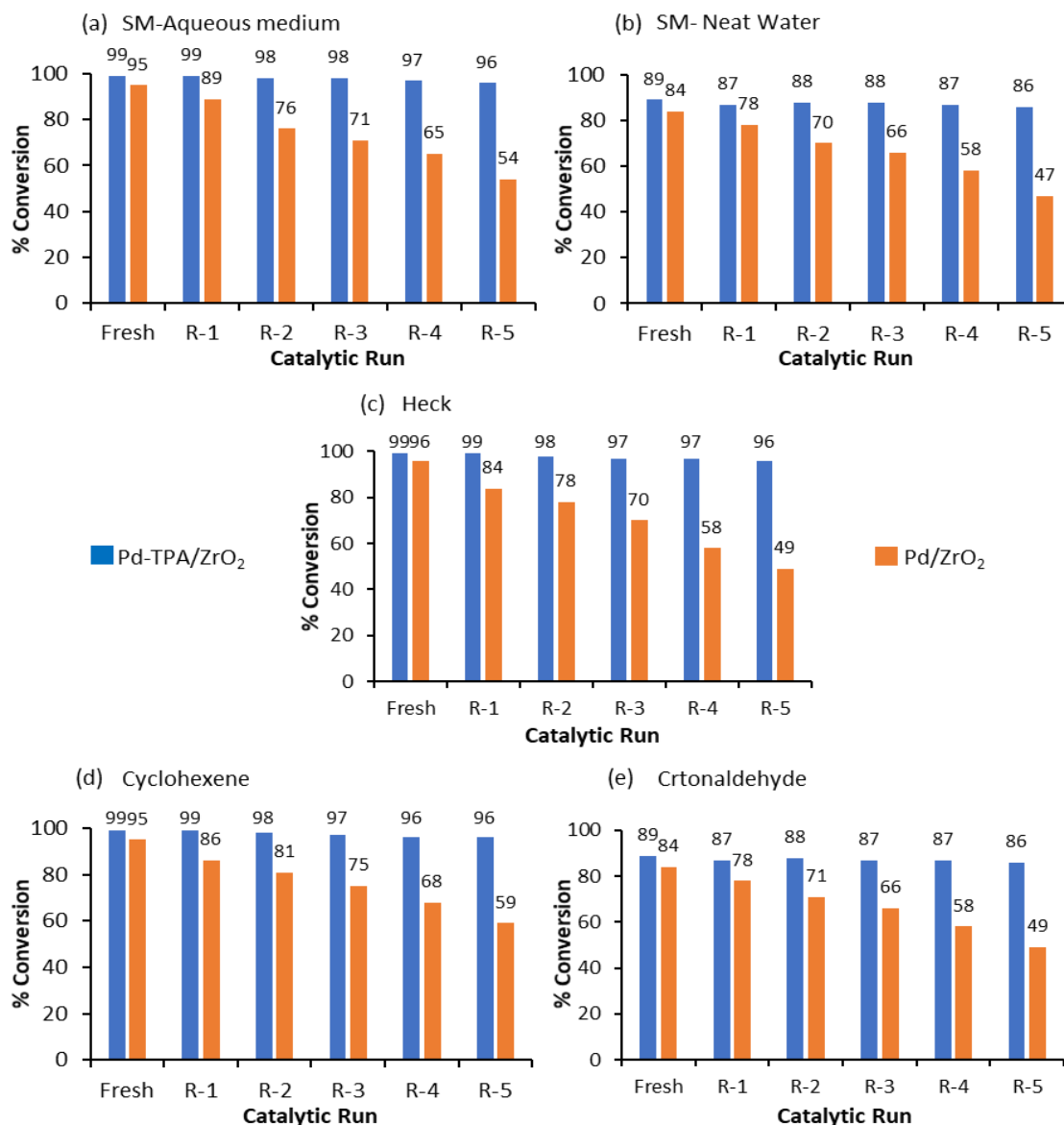


Figure 19 Recycling test. Reaction conditions: *SM coupling* (a) Aqueous medium- iodobenzene (1.96 mmol), phenylboronic acid (2.94 mmol), catalyst (0.02 mg Pd, 0.0096 mol% Pd), K₂CO₃ (3.92 mmol), C₂H₅OH: H₂O (3:7 mL), time (30 min), temperature (80 °C); (b) Neat water - iodobenzene (1.96 mmol), phenylboronic acid (2.94 mmol), catalyst (0.02 mg Pd, 0.0096 mol% Pd), K₂CO₃ (3.92 mmol), H₂O (6 mL), time (1 h), temperature (100 °C). *Heck coupling* (c) iodobenzene (0.98 mmol), styrene (1.47 mmol), catalyst (0.12 mg Pd, 0.115 mol% Pd), K₂CO₃ (1.96 mmol), DMF: H₂O (3:2 mL), time (6 h), temperature (100 °C). *Hydrogenation* (d) cyclohexene (9.87 mmol), catalyst (0.08 mg Pd, 0.0076 mol% Pd), H₂O (50 mL), time (4 h), temperature (80 °C), H₂ pressure (10 bar); (e) crotonaldehyde (9.87 mmol), catalyst (0.08 mg Pd, 0.0076 mol% Pd), H₂O (50 mL), time (4 h), temperature (80 °C), H₂ pressure (8 bar).

Sustainability of the catalyst is the key challenge for any process, and for the same recycling test was studied for Pd/ZrO₂ and Pd-TPA/ZrO₂ (Figure 19). In order to regenerate the catalysts, after reaction completion, the catalysts were centrifuged, washed with dichloromethane followed by consequent washes with distilled water and finally dried at 100 °C for an hour to reuse it for next catalytic run. Obtained results show the gradual decrease in the % conversion in case of Pd/ZrO₂ during all the reactions, confirming the leaching of active species PdNPs from the support. In contrast, Pd-TPA/ZrO₂ did not show any appreciable change in the % conversion up to five cycles for all reactions, indicating that the catalyst was stable, heterogeneous, can be regenerated and reused for further catalytic runs also. Here, TPA plays an important role by stabilizing PdNPs and makes the system sustainable.

Characterization of regenerated catalyst

In order to check the stability, the regenerated catalyst was characterized by EDS, XRD, BET and XPS.

EDX values of Pd (0.46 wt%) and W (16.90 wt%) of regenerated Pd-TPA/ZrO₂ is in good agreement with values of fresh catalyst (16.87 wt% of W, 0.47 wt% of Pd) confirming no emission of Pd as well as TPA from ZrO₂. This indicates that TPA plays an important role as a stabilizer to keep the Pd(0) active and also prevent it to leach from the support. EDX mapping of the regenerated catalyst is shown in figure 20.

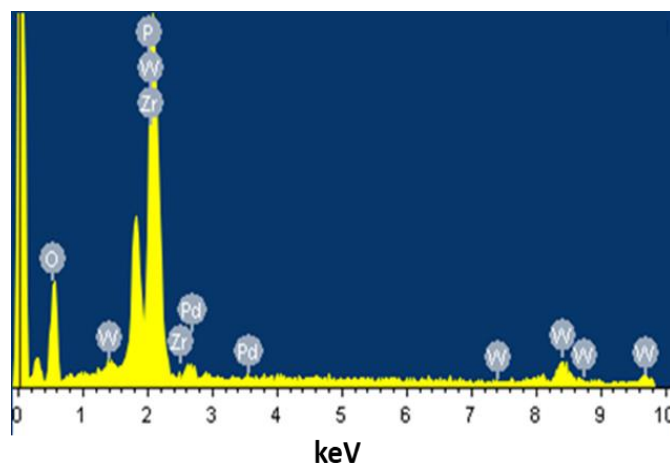


Figure 20 EDX mapping of regenerated Pd-TPA/ZrO₂.

XRD patterns of fresh and regenerated catalysts are shown in figure 21. Obtained results revealed the retention of highly dispersed nature of the catalyst. Absence of any characteristic peaks regarding Pd aggregates as well as TPA clearly indicates the sustainability of the catalyst during the reaction.

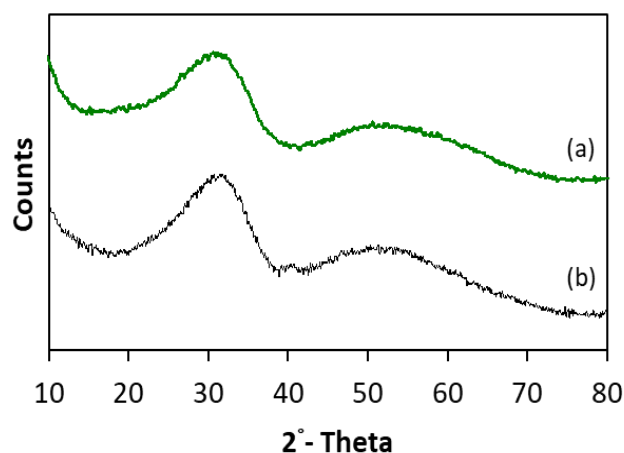


Figure 21 XRD patterns of (a) Pd-TPA/ZrO₂ and (b) Regenerated Pd-TPA/ZrO₂.

The drastic decrease in BET surface area of regenerated catalyst (104 m²/g) is as compare to that of fresh catalyst (204 m²/g) indicates that during the reaction Pd(0) nanoparticles undergo aggregate formation. This is an expected and known fact [30]. However, no change in nitrogen adsorption desorption isotherm (Figure 22) as compare to that of fresh catalyst indicates that surface phenomena remains intact even after the completion of the reaction.

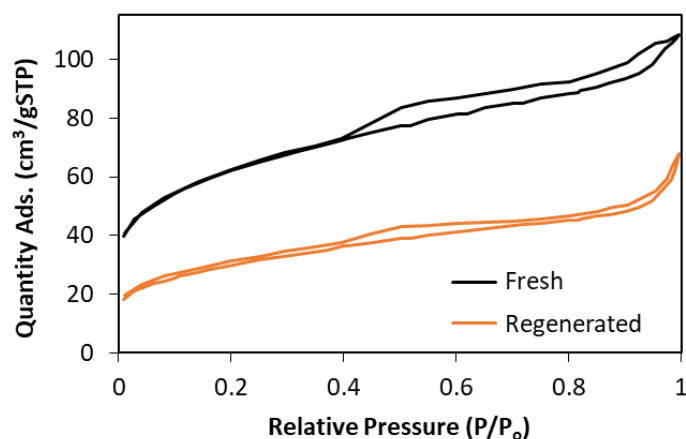


Figure 22 N₂ sorption isotherms of fresh and regenerated catalysts.

XPS spectra of regenerated Pd-TPA/ZrO₂ is displayed in figure 23. The spectrum of regenerated catalyst is found to be identical with fresh one (Figure 4), confirms the retention of Pd(0) active species as well as W(VI), which did not undergo reduction during the reaction, indicating the sustainability of the catalyst.

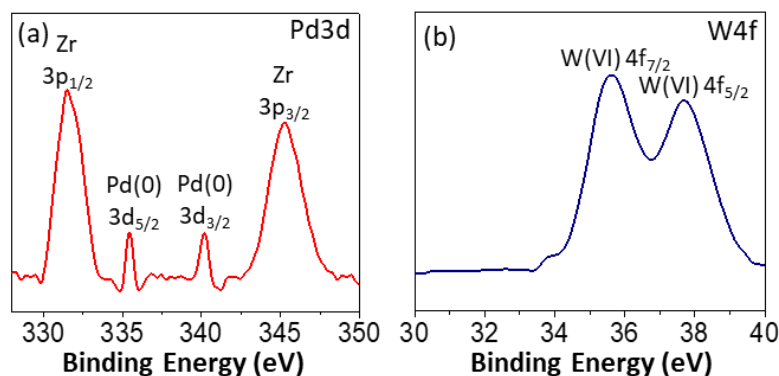
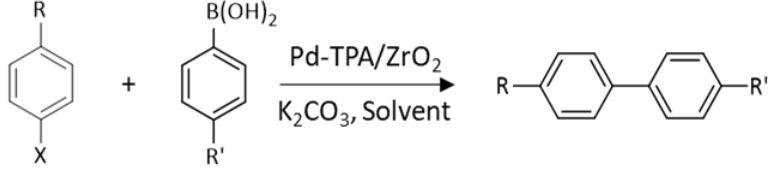
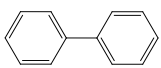
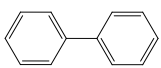
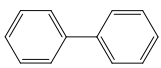
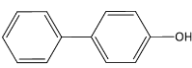
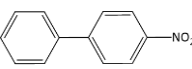
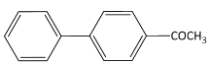


Figure 23 XPS spectra of regenerated catalyst.

Viability of the catalyst

Under the optimized condition, the scope and limitations of substrates were investigated by using different halobenzenes (Table 9).

Table 9 Substrate study for SM coupling

							
R	X	R'	Product	%		TON (a/b)	TOF (h ⁻¹) (a/b)
				Conversion (a)	(b)		
H	I	H		99	89	10325/9282	20650/9282
H	Br	H		8 98*	10	834/1043 10221*	1668/1043 1022*
H	Cl	H		1 86*	7	104/730 8969*	208/730 897*
OH	Br	H		100	98	10429/10221	20858/10221
NO ₂	Br	H		99	4	10325/417	20650/417
COCH ₃	Br	H		94	48	9803/5006	19606/5006

Reaction conditions: Halobenzene (1.96 mmol), phenylboronic acid (2.94 mmol), K₂CO₃ (3.92 mmol), conc. of Pd (0.0096 mol%), substrate/catalyst ratio (10429/1).

(a) Aqueous medium: C₂H₅OH: H₂O (3:7) mL, 30 min, 80 °C. (b) Neat water: H₂O (6 mL), time (1 h), 100 °C. †Isolated yield. *Time (10 h).

Coupling of iodobenzene with phenylboronic acid gives higher conversion compared to bromobenzene and chlorobenzene as expected, because iodide is a good leaving group due to its low electronegativity as well as big radius compared to bromide and chloride groups, making the reaction more feasible compared to bromide and chloride groups. The found reactivity order was Ph-I > Ph-Br > Ph-Cl. Presence of strongly electron donating group like -OH is less favorable for coupling reaction, though in case of p-bromophenol, high conversion was obtained in both the media. This may be due to the complete solubility of the substrate in reaction medium at optimized temperature which facilitates the reaction. Substituted bromobenzene with strongly electron withdrawing group such as -NO₂ facilitates the reaction, and hence p-bromonitrobenzene gives the 99 % conversion in aqueous medium but almost negligible in neat water because of its low solubility. Similarly, p-bromoacetophenone gives the high conversion in aqueous medium due to the presence of moderate electron withdrawing group -COCH₃ but shows moderate conversion in neat water may be due to its low solubility in water.

Similarly, under optimized conditions, scope and limitations of substrates for Heck coupling were also investigated by using different halobenzenes and styrene derivatives (Table 10). Coupling of iodobenzene with styrene gives higher conversion compare to bromobenzene and chlorobenzene as expected. The found reactivity order was Ph-I > Ph-Br > Ph-Cl. However, in case of bromobenzene and chlorobenzene higher % conversion was achieved by prolonging the reaction time. Coupling of iodobenzene with α -methyl styrene (74 %) is lower compared to the coupling of iodobenzene with styrene (99 %). This may be due to crowding effect of the methyl group. This study also confirms that there was no formation of homocoupling products in both the C-C coupling reactions.

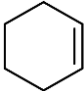
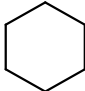
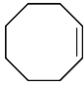
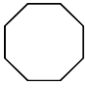
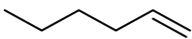
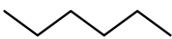
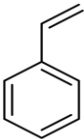
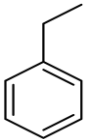
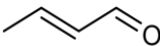

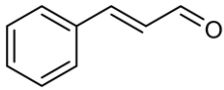
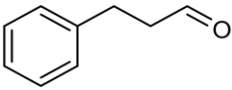
Table 10 Substrate study for Heck coupling

X	R	Product	% Conversion	TON/TOF (h ⁻¹)
I	H		99	860/143
Br	H		72	626/104
			97*	843*/141*
Cl	H		12	104/17
			49*	426*/71*
I	CH ₃		74	643/107
			89*	773*/129*

Reaction conditions: Halobenzene (0.98 mmol), styrene (1.49 mmol), K₂CO₃ (1.96 mmol), Conc. of Pd (0.115 mol%), substrate/catalyst ratio (869/1), DMF: H₂O (3:2 mL), time (6 h), temperature (100 °C). *Time (10 h).

For hydrogenation, the efficiency of the catalyst was evaluated towards different aliphatic and aromatic alkenes and obtained results are presented in (Table 11). Ring size effect was observed for the activity of the catalyst. Moreover, the catalyst was found to be active for selective hydrogenation of the C=C bond without tolerating the C=O bond when simultaneously present in the substrates.

Table 11 Substrate study for hydrogenation

Substrate	Product	% Conversion/Selectivity	TON/TOF (h ⁻¹)
		^a 96	12604/3151
		^a 72	9453/2363
		^a 86	11292/2823
		^a 79	10372/2593
		^b 89/100	11685/2921
		^b 76/100	9978/2495

Reaction conditions: Substrate (9.87 mmol), Conc. of Pd (0.0076 mol%), substrate/catalyst ratio (13130/1), H₂O (50 mL), temperature (80 °C), H₂ pressure (^a10 bar and ^b8 bar), time (4 h).

Comparison with reported catalyst

Catalytic activity of the present catalyst is compared with reported catalysts for SM coupling in aqueous medium (Table 12) as well as in neat water (Table 13) in terms of iodobenzene as one of the substrate. Li et al. [31], Hong et al. [32] and Bai and co-worker [33] reported the reaction in aqueous medium with high conversion but the catalyst amount was very high compared to the present work. Gholinejad and co-workers [34], Veisi and co-workers [35] and Azadi and co-workers [36] have reported the reaction in aqueous medium with high conversion but they required higher concentration of palladium.

Table 12 Comparison of catalytic activity for SM coupling with reported catalyst in organic-water solvent mixture with respect to iodobenzene

Catalyst	Pd (mol %)	Solvent	Temp. (°C)/Time (h)	% Conversion /TON/TOF (h ⁻¹)
PdCl ₂ (py) ₂ @SHS [31]	0.0188	C ₂ H ₅ OH: H ₂ O (3:2) mL	60/0.17	96/5211/30,650
Pd-ScBTC NMOFs [32]	0.5	C ₂ H ₅ OH: H ₂ O (1:1) mL	40/0.5	99/194/388
Pd/C [51]	0.37	C ₂ H ₅ OH: H ₂ O (1:1) mL	40/0.5	99/268/535
Oximepalladacycle catalyst [34]	0.3	C ₂ H ₅ OH: H ₂ O (1:1) mL	RT/0.3	95/317/1057
Fe ₃ O ₄ /Ethyl-CN/Pd [35]	0.2	C ₂ H ₅ OH: H ₂ O (1:1) mL	RT/0.2	98/49/245
G-BI-Pd [36]	0.45	C ₂ H ₅ OH: H ₂ O (1:1) mL	80/0.084	98/219/2613
Pd-TPA/ZrO₂ (Present catalyst)	0.0096	C₂H₅OH: H₂O (3:7) mL	80/0.5	99/10325/20650

Karimi et al. [37], Dutta and group [38], Siril and co-workers [39], Yang et al. [40] and Dyson et al. [41] have reported the reaction in neat water (Table 13) with high conversion but required more time comparatively for the completion of the reaction. Sabounchei et al. [42] reported the reaction with high conversion and fewer time but used high concentration of Pd. Overall, the present catalytic system is superior to all the reported system in terms of concentration of Pd(0), 0.0096 mol%, TON as well as TOF.

Table 13 Comparison of catalytic activity with reported catalyst in neat water with respect to iodobenzene

Catalyst	Pd (mol %)	Temp(°C) /Time (h)	% Conversion	TON/TOF (h ⁻¹)
Mag-IL-Pd [37]	0.025	60/6	95	3798/633
Pd0-Mont. [38]	0.07	60/1	90	341/341
Pd-PANI [39]	0.01	90/4	86	8600/2150
Pd/PdO [40]	0.1	90/4	99	992/248
Pd-NP-PIL [41]	1.7	100/4	98	56/14
{[Ph ₂ PCH ₂ PPh ₂ - CH=C(O)(C ₁₀ H ₇)]PdCl ₂ } [42]	0.134	80/0.34	93	712/2093
Pd(0)-TPA/ZrO₂ (Present catalyst)	0.0096	100/1	89	9383/9383

In case of Heck coupling (Table 14) also, activity of the present catalyst is compared with reported catalysts in terms of iodobenzene as one of the substrates. Shabbani and his co-worker [43] reported the reaction using universal green solvent water with moderate reaction conversion and low TON/TOF compare to the present report. Guo et al. [44], Patil et al. [45], Sajiki et al. [46] and Zekri et al. [47] have reported the reaction using organic solvent only with consumption of high mol% of Pd as active species as well as comparatively lower % conversion. Here, the uniqueness of the present catalyst lies in terms of the used reaction medium, water-organic solvent mixture (DMF: H₂O), lower mol% of Pd, high % conversion as well as high TON/TOF.

Table 14 Comparison of catalytic activity for Heck reaction with reported catalyst with respect to iodobenzene

Catalyst	Pd (mol %)	Solvent	Temp. (°C)/Time (h)	% Conversion/TON /TOF (h ⁻¹)
PdTSPc@KP-GO [43]	0.792	H ₂ O (10 mL)	reflux/9	89/111.2/12.36
Pd/CNCs [44]	1.412	DMF (10 mL)	40/5	93/65.1/13
NO ₂ -NHC-Pd@Fe ₃ O ₄ [45]	1.0	CH ₃ CN (5 mL)	80/5	96/96/19.2
5% Pd/CM [46]	0.2	DMA	80/24	61/3050/127
PFG-Pd [47]	1.7	DMF (3 mL)	120/6	95/56/9
Pd-TPA/ZrO₂ (Present catalyst)	0.115	DMF: H₂O (3:2 mL)	100/6	99/860/143

In case of cyclohexene hydrogenation (Table 15), Liu et al. [48] reported very high conversion at lower temperature with very small amount of catalyst but they had utilized very high H₂ pressure (20 bar) for the reaction compared to present work. Zhang et al. [49] reported the same reaction at 35 °C with very low conversion, moreover use of catalyst amount is too high. Leng et al. [50] achieved high conversion using formic acid as a solvent with very high amount of the catalyst compared to the present catalytic system. Panpranot et al. [51] achieved excellent conversion using supercritical CO₂ as a solvent at 60 bar pressure (extremely high condition). Enumerated data of table 15 indicates that the present catalytic system is best one of all reported one in terms of activity under mild reaction conditions.

Table 15 Comparison with the reported catalyst with respect to cyclohexene hydrogenation

Catalyst	Pd (mole%)	Solvent	Temp. (°C)	Pressure (bar)	% Conversion/TON/TOF
SH-IL-1.0wt%Pd [48]	0.02	Auto-clave	60	20	99/5000/5000
Pd/MSS@ZIF-8 [49]	0.1738	Ethyl acetate	35	1	5.6/560/93
Pd@CN [50]	2.208	Formic acid	90	(Proton transfer)	96/44/3.67
Pd/SiO ₂ [51]	0.091	CO ₂ (60 bar)	25	10	96/1097/6582
Pd-TPA/ZrO ₂ (Present catalyst)	0.0076	Water	80	10	96/12604/3151

In case of crotonaldehyde hydrogenation (Table 16), Iwasa et al. [52] reported 100 % conversion at 200 °C temperature with very high amount of catalyst, moreover selectivity of the desired product butyraldehyde was only 31 %. Here, reason for the low selectivity was weaker adsorption of formed product butyraldehyde onto surface of the catalyst, which easily gets disorb and hydrogenated to form another products. Zhao et al. [53] achieved 100 % conversion at 50 °C with very low amount of Pd, but they have used super critical CO₂ as solvent under 80 bar pressure (very harsh condition with 40 bar H₂ pressure). Here, the use of CO₂ favours to obtain 100 % selectivity of butyraldehyde.

Table 16 Comparison with reported catalyst with respect to crotonaldehyde hydrogenation

Catalyst	Pd (mol%)	Solvent	Temp. (°C)	% Conversion/% Selectivity of butyraldehyde	TON/TOF (h ⁻¹)
Pd/CeO ₂ [52]	10	Fix bed reactor	200	100/31	-
10 % Pd/C [53]	0.026	CO ₂ (80 bar)	50	100/100	3789/7578
Pd/PEG [54]	0.5	Ethanol	RT	100/100	1277/851
Pd-TPA/ZrO ₂ (Present catalyst)	0.0076	Water	80	89/100	11685/2921

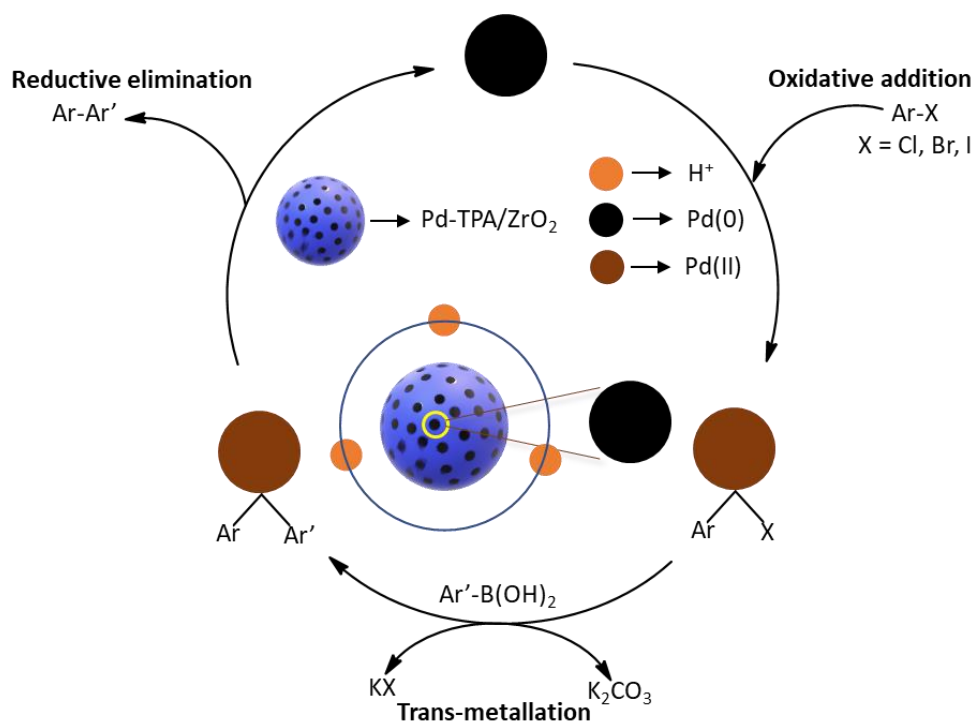
It is interesting to note down that no report was found in which the same catalyst has been applied for both the C-C coupling as well hydrogenation reactions with respect to iodobenzene and cyclohexene as one of the substrates, respectively. The present catalyst is superior in terms of used concentration of Pd, reaction time as well as TON in all reactions. Here, high activity of the

present catalyst compared to reported catalytic systems, may be due to the high efficiency of the PdNPs.

Plausible mechanism

C-C coupling

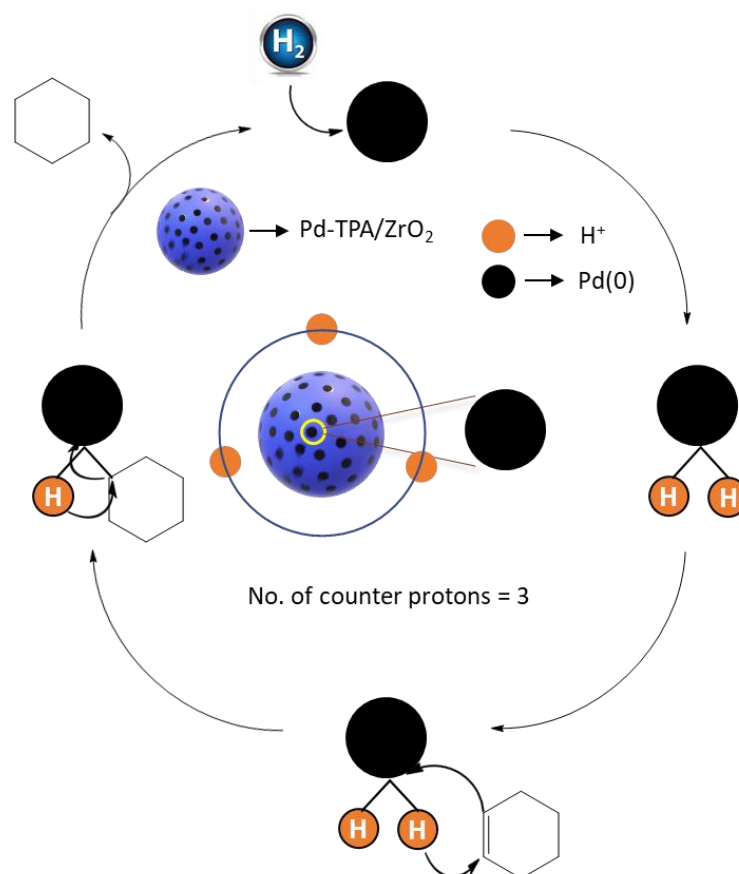
In the present work, we are expecting the well-known mechanism, which involves oxidative addition, transmetallation and reductive elimination [55]. During the oxidative addition and transmetallation steps, we could not isolate the Pd(II) species due to the high rate of the reaction. The steric and electronic characteristics of TPA are important for catalysis. In general, the oxidative addition is governed by electronic factors, whereas the transmetallation and reductive elimination processes are controlled by a mixture of both electronic and steric effect [56]. Thus, TPA would achieve a suitable balance between these two factors. The plausible mechanism for the C-C coupling is shown in scheme 4.



Scheme 4 Plausible mechanism for C-C coupling.

Hydrogenation

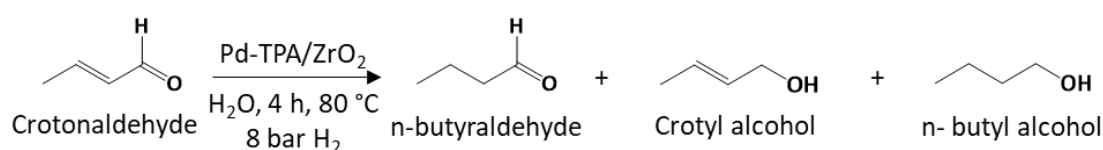
It is well known that in case of Pd catalyzed hydrogenation, mechanism is governed by palladium hydride (Pd-H) formation. In present system, we are also expecting the same mechanism in which molecular hydrogen initially gets adsorbed onto Pd surface to form Pd-H. This formed species subsequently transfer the hydrogen to unsaturated bond of prely adsorbed substrate over the surface to form product. The plausible mechanism for cyclohexene hydrogenation is shown in scheme 5.



Scheme 5 Plausible hydrogenation mechanism.

 Crotonaldehyde hydrogenation

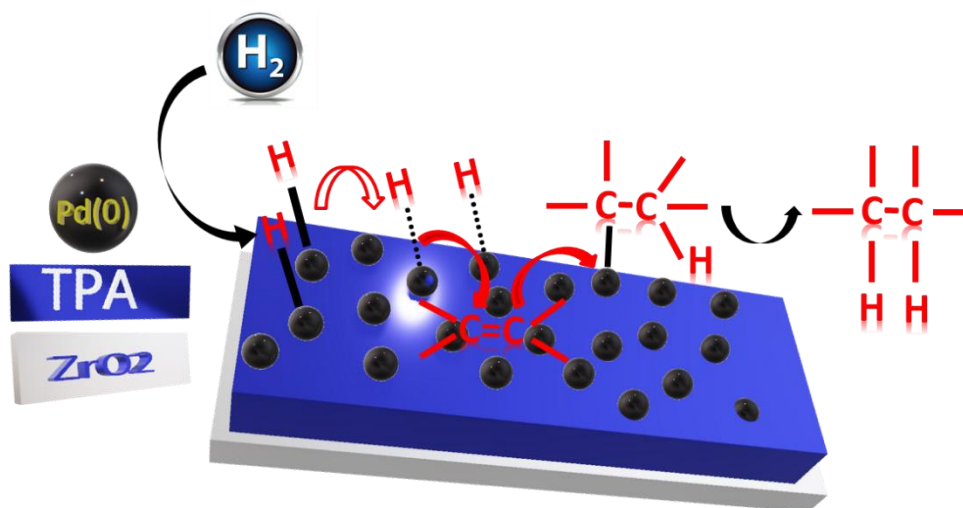
Mechanistic investigation has been carried out for crotonaldehyde hydrogenation. Generally, crotonaldehyde on hydrogenation gives three products (Scheme 6) (i) butyraldehyde (ii) crotyl alcohol and (iii) n-butanol. It is well known that thermodynamic parameters favor the hydrogenation of C=C over the C=O bond [57] due to high activation energy of C=O tolerance to yield selectively butyraldehyde. However, C=O selectively can be reduced by either designing the suitable bimetallic catalyst in which one of the metals having oxidic species (acidic sites) would attract the lone pair of the carbonyl group, or using the alcohols as preferred solvents which can easily activate the C=O bond. However, use of alcohols can arise the undesirable secondary effect such as formation of acetals and hemiacetals [58].



Scheme 6 Crotonaldehyde hydrogenation.

In the present work, we achieved single selective product that is butyraldehyde instead of product mixture. There might be two reasons for the selective reduction of C=C bond. (i) The presence of only water as a solvent instead of any organic solvent as discussed above. Here, the absence of organic solvent would not activate C=O bond and selectively produce butyraldehyde only. To check the same, we have carried out the same reaction under optimized condition using EtOH: H₂O (20:30) mL as a solvent. Obtained results showed 91 % conversion with 60 % butyraldehyde and 40 % crotyl alcohol selectivity, indicating the activation of C=O bond for hydrogenation due to the presence of EtOH as solvent. (ii) The high adsorption capacity of the catalyst towards the substrates and initially formed products [59-65]. In the present case, initially

formed product butyraldehyde get adsorbed on the surface of the catalyst, and did not allow it to desorb for further hydrogenation to generate other product butanol. Hence, we are expecting the well-known mechanism for both the reactions. The proposed mechanism for both the reactions is shown in scheme 7.



Scheme 7 Plausible mechanism for crotonaldehyde hydrogenation.

For all the catalytic systems, we are expecting the same mechanism for both the reactions and hence not included in the proceeding chapters.

Conclusion

- Designing of PdNPs stabilized by Zirconia supported TPA (Pd-TPA/ ZrO_2) was carry out. FT-IR, XRD and BET reveal the retention of Keggin structure, XPS confirms the oxidation states of Pd(0) and W(VI) whereas TEM, HRTEM and STEM confirm the presence of homogeneously dispersed PdNPs onto surface of ZrO_2
- The catalyst exhibits outstanding activity for C-C coupling (SM and Heck) and hydrogenation (cyclohexene and crotonaldehyde) under mild reaction conditions (> 89 % conversion)
- Leaching and heterogeneity test confirm the true heterogeneous nature of the catalyst. The catalyst is regenerated and reused up to five cycles (and can be used for more) without loss in activity. EDX, FT-IR, XRD, BET and XPS of regenerated catalyst confirm the stability of the catalyst
- Substrate study shows the viability of the catalyst towards different functionality of the substrates as well as superiority of the present catalyst with those of reported systems

References

- [1] K. Mori, K. Furubayashi, S. Okada and H. Yamashita, *RSC Adv.*, 2, 1047-1054, (2012).
- [2] Y. Zhang, H. Wang, Q. Yao, F. Yan, C. Cui, M. Sun and H. Zhang, *RSC Adv.*, 6, 39618-39626, (2016).
- [3] J. Hu, X. Wu, Q. Zhang, M. Gao, H. Qiu, K. Huang, S. Feng, Y. Yang, Z. Liu and B. Zhao, *Electrochem. Commun.*, 83, 56-60, (2017).
- [4] X. Kong, Y. Wang, Q. Zhang, T. Zhang, Q. Teng, L. Wang, H. Wang and Y. Zhang, *J. Colloid Interface Sci.*, 505, 615-621, (2017).
- [5] Y. Leng, C. Zhang, B. Liu, M. Liu, P. Jiang and S. Dai, *ChemSusChem*, 11, 3396-3401, (2018).
- [6] L. Wang, T. Meng, J. Sun, S. Wu, M. Zhang, H. Wang and Y. Zhang, *Anal. Chim. Acta*, 1047, 28-35, (2019).
- [7] S. Patel, N. Purohit and A. Patel, *J. Mol. Catal. A: Chem.*, 192, 195-202, (2003).
- [8] N. Bhatt, C. Shah and A. Patel, *Catal. Lett.*, 117, 146-152, (2007).
- [9] P. Sharma Dr and A. Patel, *Bull. Mater. Sci.*, 29, 439-447, (2006).
- [10] N. Bhatt, P. Sharma, A. Patel and P. Selvam, *Catal. Commun.*, 9, 1545-1550, (2008).
- [11] N. Bhatt and A. Patel, *J. Taiwan Inst. Chem. Eng.*, 42, 356-362, (2011).
- [12] P. A. Shringarpure and A. Patel, *Reaction Kinetics, React. Kinet. Mech. Catal.*, 103, 165-180, (2011).
- [13] A. Patel and S. Singh, *Ind. Eng. Chem. Res.*, 52, 10896-10904, (2013).
- [14] A. Patel and S. Singh, *Fuel*, 118, 358-364, (2014).
- [15] S. Singh and A. Patel, *Catal. Lett.*, 144, 1557-1567, (2014).
- [16] S. Singh and A. Patel, *J. Taiwan Inst. Chem. Eng.*, 52, 120-126, (2015).
- [17] S. Pathan and A. Patel, *RSC Adv.*, 2, 116-120, (2012).
- [18] G. D. Yadav and V. V. Bokade, *Appl. Catal., A*, 147, 299-323, (1996).
- [19] A. I. Vogel and G. H. Jeffery, *Vogel's textbook of quantitative chemical analysis*, Longman Scientific & Technical, (1989).

-
- [20] A. V. Matveev, V. V. Kaichev, A. A. Saraev, V. V. Gorodetskii, A. Knop-Gericke, V. I. Bukhtiyarov and B. E. Nieuwenhuys, *Catal. Today*, **244**, 29-35, (2015).
- [21] R. Villanneau, A. Roucoux, P. Beaunier, D. Brouri and A. Proust, *RSC Adv.*, **4**, 26491-26498, (2014).
- [22] L. D'Souza, M. Noeske, R. M. Richards and U. Kortz, *Appl. Catal., A*, **453**, 262-271, (2013).
- [23] Y. Zhu, W. D. Wang, X. Sun, M. Fan, X. Hu and Z. Dong, *ACS Appl. Mater. Interfaces*, **12**, 7285-7294, (2020).
- [24] S. Rana and K. M. Parida, *Catal. Sci. Technol.*, **2**, 979-986, (2012).
- [25] C. Röhlich, A. S. Wirth and K. Köhler, *Chem. Eur. J.*, **18**, 15485-15494, (2012).
- [26] F. Zhao, K. Murakami, M. Shirai and M. Arai, *J. Catal.*, **194**, 479-483, (2000).
- [27] J. P. Stambuli, S. R. Stauffer, K. H. Shaughnessy and J. F. Hartwig, *J. Am. Chem. Soc.*, **123**, 2677-2678, (2001).
- [28] P. W. Böhm Volker and A. Herrmann Wolfgang, *Chem. Eur. J.*, **7**, 4191-4197, (2001).
- [29] R. A. Sheldon, M. Wallau, I. W. C. E. Arends and U. Schuchardt, *Acc. Chem. Res.*, **31**, 485-493, (1998).
- [30] M. De bruyn and R. Neumann, *Adv. Synth. Catal.*, **349**, 1624-1628, (2007).
- [31] Z. Guan, J. Hu, Y. Gu, H. Zhang, G. Li and T. Li, *Green Chem.*, **14**, 1964-1970, (2012).
- [32] L. Zhang, Z. Su, F. Jiang, Y. Zhou, W. Xu and M. Hong, *Tetrahedron*, **69**, 9237-9244, (2013).
- [33] Z. Shi and X. F. Bai, *Open Mater. Sci. J.* **9**, 173-177, (2015).
- [34] M. Gholinejad, M. Razeghi and C. Najera, *RSC Adv.*, **5**, 49568-49576, (2015).
-

-
- [35] B. Abbas Khakiani, K. Pourshamsian and H. Veisi, *Appl. Organomet. Chem.*, 29, 259-265, (2015).
- [36] M. Sarvestani and R. Azadi, *Appl. Organomet. Chem.*, 31, e3667, (2016).
- [37] B. Karimi, F. Mansouri and H. Vali, *Green Chem.*, 16, 2587-2596, (2014).
- [38] B. J. Borah, S. J. Borah, K. Saikia and D. K. Dutta, *Appl. Catal., A*, 469, 350-356, (2014).
- [39] S. Dutt, R. Kumar and P. F. Siril, *RSC Adv.*, 5, 33786-33791, (2015).
- [40] F. Yang, C. Chi, S. Dong, C. Wang, X. Jia, L. Ren, Y. Zhang, L. Zhang and Y. Li, *Catal. Today*, 256, 186-192, (2015).
- [41] S. Ghazali-Esfahani, E. Păunescu, M. Bagherzadeh, Z. Fei, G. Laurenczy and P. J. Dyson, *Sci. China Chem.*, 59, 482-486, (2016).
- [42] S. J. Sabounchei, M. Hosseinzadeh, M. Panahimehr, D. Nematollahi, H. R. Khavasi and S. Khazalpour, *Transition Met. Chem.*, 40, 657-663, (2015).
- [43] Z. Hezarkhani and A. Shaabani, *RSC Adv.*, 6, 98956-98967, (2016).
- [44] X.-W. Guo, C.-H. Hao, C.-Y. Wang, S. Sarina, X.-N. Guo and X.-Y. Guo, *Catal. Sci. Technol.*, 6, 7738-7743, (2016).
- [45] V. Kandathil, B. D. Fahlman, B. S. Sasidhar, S. A. Patil and S. A. Patil, *New J. Chem.*, 41, 9531-9545, (2017).
- [46] Y. Monguchi, F. Wakayama, S. Ueda, R. Ito, H. Takada, H. Inoue, A. Nakamura, Y. Sawama and H. Sajiki, *RSC Adv.*, 7, 1833-1840, (2017).
- [47] R. Fareghi-Alamdari, M. G. Haqiqi and N. Zekri, *New J. Chem.*, 40, 1287-1296, (2016).
- [48] R. Tao, S. Miao, Z. Liu, Y. Xie, B. Han, G. An and K. Ding, *Green Chem.*, 11, 96-101, (2009).
- [49] T. Zhang, B. Li, X. Zhang, J. Qiu, W. Han and K. L. Yeung, *Microporous Mesoporous Mater.*, 197, 324-330, (2014).
- [50] C. Zhang, Y. Leng, P. Jiang, J. Li and S. Du, *ChemistrySelect*, 2, 5469-5474, (2017).
-

- [51] J. Panpranot, K. Phandinthong, P. Prasertthdam, M. Hasegawa, S.-i. Fujita and M. Arai, *J. Mol. Catal. A: Chem.*, 253, 20-24, (2006).
- [52] N. Iwasa, M. Takizawa and M. Arai, *Appl. Catal., A*, 283, 255-263, (2005).
- [53] F. Zhao, Y. Ikushima, M. Chatterjee, M. Shirai and M. Arai, *Green Chem.*, 5, 76-79, (2003).
- [54] F. A. Harraz, S. E. El-Hout, H. M. Killa and I. A. Ibrahim, *J. Mol. Catal. A: Chem.*, 370, 182-188, (2013).
- [55] N. Miyaura and A. Suzuki, *Chem. Rev.*, 95, 2457-2483, (1995).
- [56] P. Das and W. Linert, *Coord. Chem. Rev.*, 311, 1-23, (2016).
- [57] J. Ruiz-Martínez, Y. Fukui, T. Komatsu and A. Sepúlveda-Escribano, *J. Catal.*, 260, 150-156, (2008).
- [58] B. C. Campo, M. A. Volpe and C. E. Gigola, *Ind. Eng. Chem. Res.*, 48, 10234-10239, (2009).
- [59] P. Gallezot and D. Richard, *Catal. Rev. Sci. Eng.*, 40, 81-126, (1998).
- [60] M. A. Vannice and B. Sen, *J. Catal.*, 115, 65-78, (1989).
- [61] M. Abid, G. Ehret and R. Touroude, *Appl. Catal., A*, 217, 219-229, (2001).
- [62] R. Hubaut, M. Daage and J. P. Bonnelle, *Appl. Catal. A*, 22, 231-241, (1986).
- [63] R. L. Augustine, *Catal. Rev. Sci. Eng.*, 13, 285-316, (1976).
- [64] R. Touroude, *J. Catal.*, 65, 110-120, (1980).
- [65] M. Shirai, T. Tanaka and M. Arai, *J. Mol. Catal. A: Chem.*, 168, 99-103, (2001).

CHAPTER 2

PdNPs Stabilized by Zirconia
Supported LTPA: Synthesis,
Characterization and
Applications to C-C coupling
and Hydrogenation

The outstanding activity of Pd-TPA/ZrO₂ in both C-C coupling and hydrogenation, encourage us to design another catalyst for the same applications as well as to investigate the effect of addenda atom on the reactions (i.e. mono lacunary tungstophosphoric acid, PW₁₁, later LTPA).

In literature, we found only one art on Pd nanoparticles stabilized by supported LTPA. In 2002, Neumann et al. derived palladium nanoparticles from a palladium substituted mono lacunary tungstophosphoric acid supported on γ -Al₂O₃ by impregnation method [K₅[PdPW₁₁O₃₉].12H₂O/ γ -Al₂O₃] and utilized for base and solvent free SM coupling of chlorobenzene to obtain 99 % yield of biphenyl at 130 °C in 16 h [1].

In this context, present chapter describes the synthesis of Pd nanoparticles (PdNPs) stabilized by Zirconia supported mono lacunary tungstophosphoric acid (Pd-LTPA/ZrO₂) by exchange method. The synthesized material was characterized by elemental analysis EDX, TGA, FT-IR, BET, XRD, XPS, TEM, HRTEM and STEM. The efficiency of the catalyst was evaluated as a sustainable heterogeneous catalyst for C-C coupling (SM and Heck) and hydrogenation. Influence of various parameters such as catalyst amount, temperature, pressure, time, base, solvent, solvent ratio was studied for respective reactions to obtain maximum conversion. The catalyst was regenerated, reused and the regenerated catalyst was characterized by EDX, FT-IR, XRD, XPS and HRTEM to confirm the stability of the catalyst. Scope and limitation of synthesized catalyst was investigated towards different substrates. Activity of the catalyst for the said reactions was compared with the reported systems. Further, in order to understand the role of addenda atom, the catalytic activity was compared with Pd-TPA/ZrO₂ (Pd-TPA/ZrO₂) and explained on the bases of acidity and available protons (generated on removal of one “WO” unit from PW₁₂).

EXPERIMENTAL

Materials

All chemicals used were of A. R. grade. Anhydrous disodium hydrogen phosphate, sodium tungstate dihydrate, acetone, nitric acid, hydrochloric acid, zirconium oxychloride, 25 % (w/w) ammonia, palladium chloride, iodobenzene, phenylboronic acid, styrene, dimethyl formamide, potassium carbonate, cyclohexene, styrene, crotonaldehyde, petroleum ether, ethyl acetate and dichloromethane were obtained from Merck and used as received.

Catalyst Synthesis

Palladium nanoparticles stabilized by zirconia supported mono lacunary tungstophosphoric acid (Pd-LTPA/ZrO₂) was synthesized in three steps.

Step-1: Synthesis of ZrO₂

Zirconia was synthesized as discussed in chapter-1.

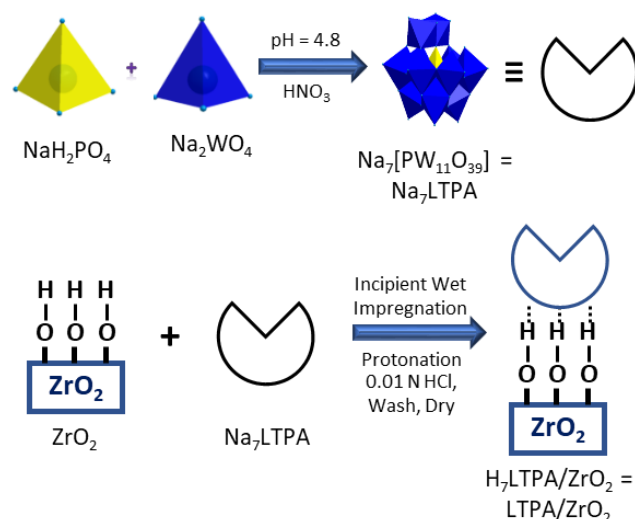
Step-2: Synthesis of supported mono lacunary tungstophosphoric acid (LTPA/ZrO₂) by incipient wet impregnation method

Sodium salt of mono lacunary tungstophosphoric acid [2] (Na₇PW₁₁O₃₉, later Na₇LTPA) and LTPA/ZrO₂ [3] were synthesized following the methods reported by Brevard et al. and our group, respectively, as shown in scheme 1.

Sodium tungstate dihydrate (0.022 mol, 7.2 g) and anhydrous disodium hydrogen phosphate (0.002 mol, 0.284 g) were dissolved in 15-20 mL of distilled water and heated at 80 °C followed by the addition of diluted nitric acid to adjust the pH to 4.8. The volume was then reduced to half by evaporation and the heteropoly anion was separated by liquid-liquid extraction with 80-100 mL of acetone. The extraction was repeated until the acetone extract showed the

absence of NO_3^- ions (ferrous sulfate test). The extracted sodium salt was dried in air. The resulting material was designated as Na_7LTPA .

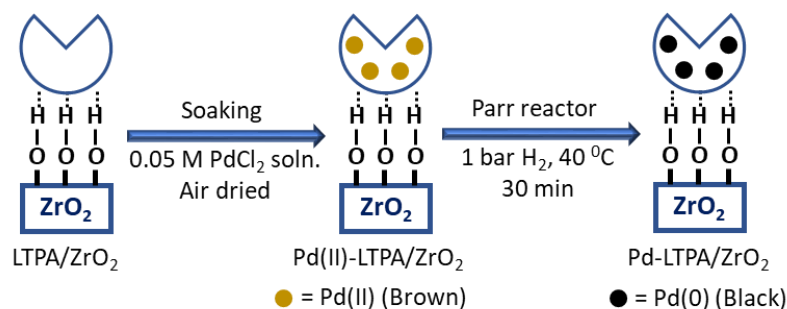
LTPA/ZrO_2 was synthesized by wet impregnation method. 1 g of ZrO_2 was impregnated with an aqueous solution of Na_7LTPA ($0.3/30 \text{ g mL}^{-1}$ of double distilled water) at 100°C followed by drying at same temperature in oven for 10 h. The obtained material ($\text{Na}_7\text{LTPA}/\text{ZrO}_2$) was protonated with 0.01 N HCl, filtered, washed with double distilled water and dried at 100°C . The obtained material was designated as LTPA/ZrO_2 .



Scheme 1 Synthesis of LTPA/ZrO_2 .

Step-3: Synthesis of Pd-LTPA/ ZrO_2 by soaking and post reduction method.

Palladium was deposited on LTPA/ZrO_2 via exchanging the available protons of LTPA. 1 g of LTPA/ZrO_2 was soaked with 25 mL of 0.05 M aqueous solution of PdCl_2 for 24 h with stirring. The solution was filtered, washed with distilled water in order to remove the excess of PdCl_2 and dried in air at room temperature. The resulting (brown colored) material was designated as $\text{Pd(II)-LTPA}/\text{ZrO}_2$. Finally, the synthesized material was charged into the Parr reactor under 1 bar H_2 pressure, at 40°C for 30 min to reduce Pd(II) to Pd(0) . The obtained (black colored) material was designated as $\text{Pd-LTPA}/\text{ZrO}_2$. The synthetic scheme is presented in scheme 2. The same procedure was followed for the synthesis of Pd/ZrO_2 .



Scheme 2 Synthesis of Pd-LTPA/ ZrO_2 .

Catalytic Evaluation

The C-C coupling and hydrogenation reactions were carried out following the same procedure as mentioned in chapter 1.

RESULTS AND DISCUSSION

Catalyst Characterization

The gravimetric analysis of standard solution and filtrate showed 6.05 wt% and 0.72 wt% of Pd in Pd/ ZrO_2 and Pd(II)-LTPA/ ZrO_2 , respectively [4]. For Pd-LTPA/ ZrO_2 , EDX values of W (15.57 wt%) and Pd (0.76 wt%) are in good agreement with analytical one (15.19 wt% of W, 0.72 wt% of Pd). EDX elemental mapping of Pd-LTPA/ ZrO_2 is shown in figure 1.

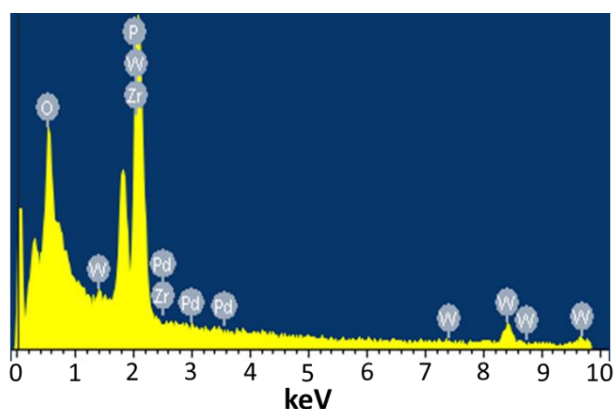


Figure 1 EDX mapping of Pd-LTPA/ ZrO_2 .

Thermal stability of Pd-LTPA/ZrO₂ was evaluated by TGA and the obtained curve is plotted in figure 2. Curve indicates 8.13 % weight loss in the temperature range of 50 to 110 °C due adsorbed water molecule. Alongside, there was no significant weight loss observed up to 500 °C indicating the high thermal stability of the material.

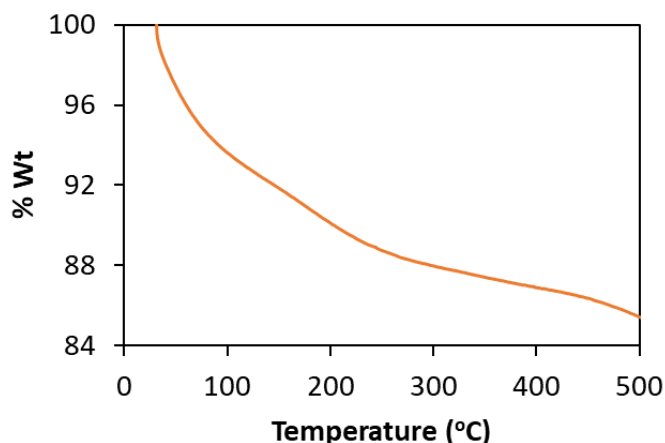


Figure 2 TGA curve of Pd-LTPA/ZrO₂.

The FT-IR spectra of ZrO₂, LTPA, LTPA/ZrO₂, Pd-LTPA/ZrO₂ are shown in figure 3. ZrO₂ shows broad bands in the region of 1600, 1370, and 600 cm⁻¹ attributed to H-O-H and O-H-O bending and Zr-OH bending, respectively. FT-IR spectrum of LTPA exhibits bands at 1088, 1042, 964, 903 and 810 cm⁻¹ corresponding to P-O, W=O and W-O-W stretching, respectively. Here, the splitting of P-O bond is due to the lowering of symmetry around central hetero atom phosphorus, indicates the formation of lacunary spices. Similarly, LTPA/ZrO₂ exhibits bands at 1090, 1047, 964 and 812 cm⁻¹ corresponding to P-O, W=O, and W-O-W stretching vibration frequencies, respectively. No significant change in the bands indicate the retention of the Keggin unit in the synthesized material. The spectrum of Pd-LTPA/ZrO₂ shows bands at 1092, 1049, 960 and 806 cm⁻¹ corresponding to P-O, W=O and W-O-W, respectively. The slight shift in the bands may be due to the change in environment by Pd.

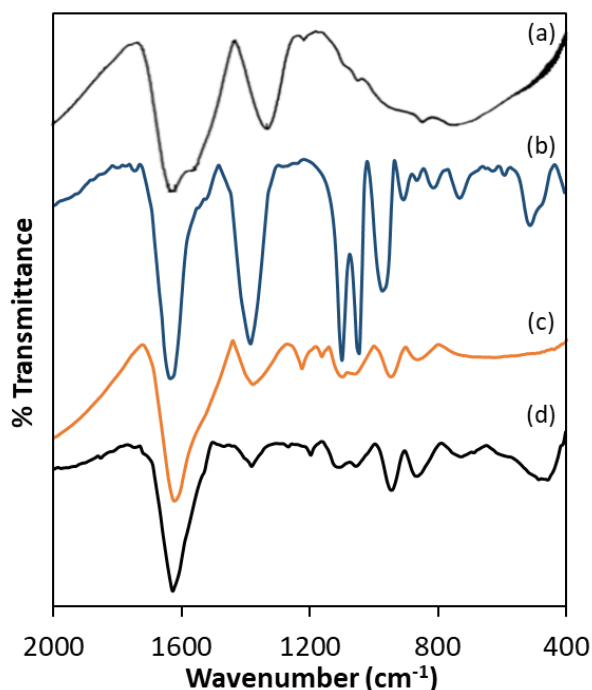


Figure 3 FT-IR spectra of (a) ZrO_2 , (b) LTPA, (c) LTPA/ ZrO_2 and (d) Pd-LTPA/ ZrO_2 .

The surface area of LTPA/ ZrO_2 ($224 \text{ m}^2/\text{g}$) is found to be higher than support ZrO_2 ($170 \text{ m}^2/\text{g}$), because of bulky anionic nature of LTPA [3]. The decrease in surface area of Pd(II)-LTPA/ ZrO_2 ($199 \text{ m}^2/\text{g}$) compared to LTPA/ ZrO_2 indicates the strong interaction of Pd with the loaded material. The drastic rise in surface area of Pd-LTPA/ ZrO_2 ($213 \text{ m}^2/\text{g}$) compared to Pd(II)-LTPA/ ZrO_2 is the first evidence for the presence of Pd(0) nanoparticles (PdNPs), due to the downsizing of Pd during the reduction of Pd(II) to Pd(0). In spite of having different surface area, the unaltered nature of the N_2 sorption isotherms of LTPA/ ZrO_2 and Pd-LTPA/ ZrO_2 (Figure 4) indicate the identical basic structure, the same is also reflected by FT-IR analysis.

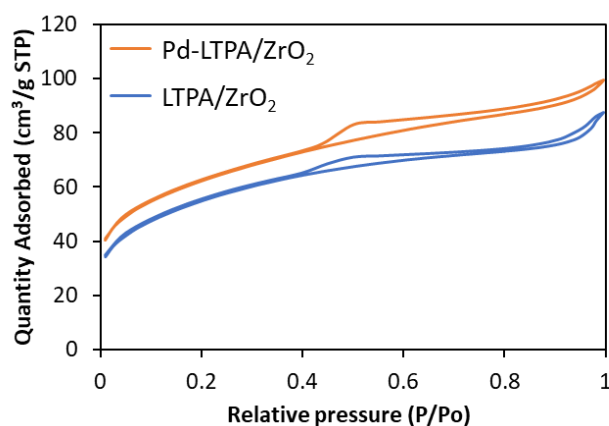


Figure 4 N₂ sorption isotherms.

XRD patterns of LTPA, ZrO₂, LTPA/ZrO₂ and Pd-LTPA/ZrO₂ were recorded (Figure 5). XRD patterns of LTPA shows the characteristic peaks between 2 θ range of 20 to 35 degree. Whereas, the absence of all patterns corresponds to LTPA in LTPA/ZrO₂ indicates the uniform dispersion onto surface of the support. XRD patterns of Pd-LTPA/ZrO₂ did not reflect any diffraction corresponds to LTPA as well as Pd, indicates the high degree of dispersion onto surface as well as no sintering of Pd during the synthesis of the catalyst.

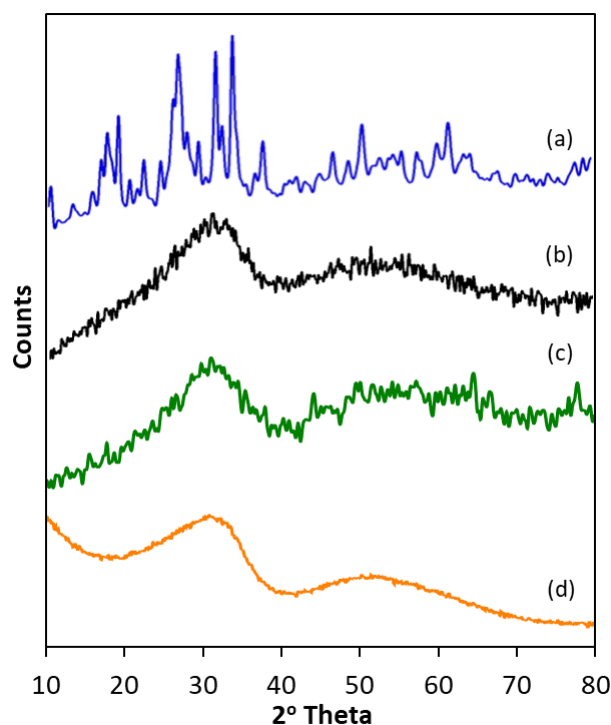


Figure 5 XRD patterns of (a) LTPA, (b) ZrO₂, (c) LTPA/ZrO₂ and (d) Pd-LTPA/ZrO₂.

To confirm the electronic state of the Pd, W and O high resolution XPS spectra of LTPA/ZrO₂ and Pd-LTPA/ZrO₂ were recorded (Figure 6). LTPA/ZrO₂ shows (Figure 6a) a very intense peak at binding energy 532 eV corresponds to O1s as it contains number of O atoms of LTPA and ZrO₂ support, whereas Pd-LTPA/ZrO₂ shows (Figure 6d) the direct overlap peak between Pd3p_{3/2} and O1s peaks at binding energy 532 eV, which is in good agreement with the reported one [5], and cannot be assigned to confirm the presence of Pd(0). Hence, we have presented instrument generated full spectra (Figure 6a & 6d) images, supporting the presence of Pd(0). This is further confirmed by recording the high resolution Pd3d spectrum which (Figure 6e) shows a low intense spin orbit doublet peak at binding energy 335.9 eV and 340.5 eV correspond to Pd3d_{5/2} and Pd3d_{3/2}, confirming the presence of Pd(0) [6-8]. Two additional high intense peaks at binding energy 331 eV and 345 eV attributed to Zr3p_{3/2} and Zr3p_{1/2}, respectively [9].

LTPA/ZrO₂ shows (Figure 6c) a well resolved spin-orbit doublet of W4f_{7/2} and W4f_{5/2} at binding energy 35.6 and 37.6 eV (spin-orbit splitting, 2.0 eV), characteristic of W(VI), confirming the presence of W(VI). Pd-LTPA/ZrO₂ also shows (Figure 6f) a single spin-orbit pair at binding energy 35.6 and 37.5 eV (spin-orbit splitting, 1.9 eV) confirming no reduction of W(VI) during the synthesis [7, 10].

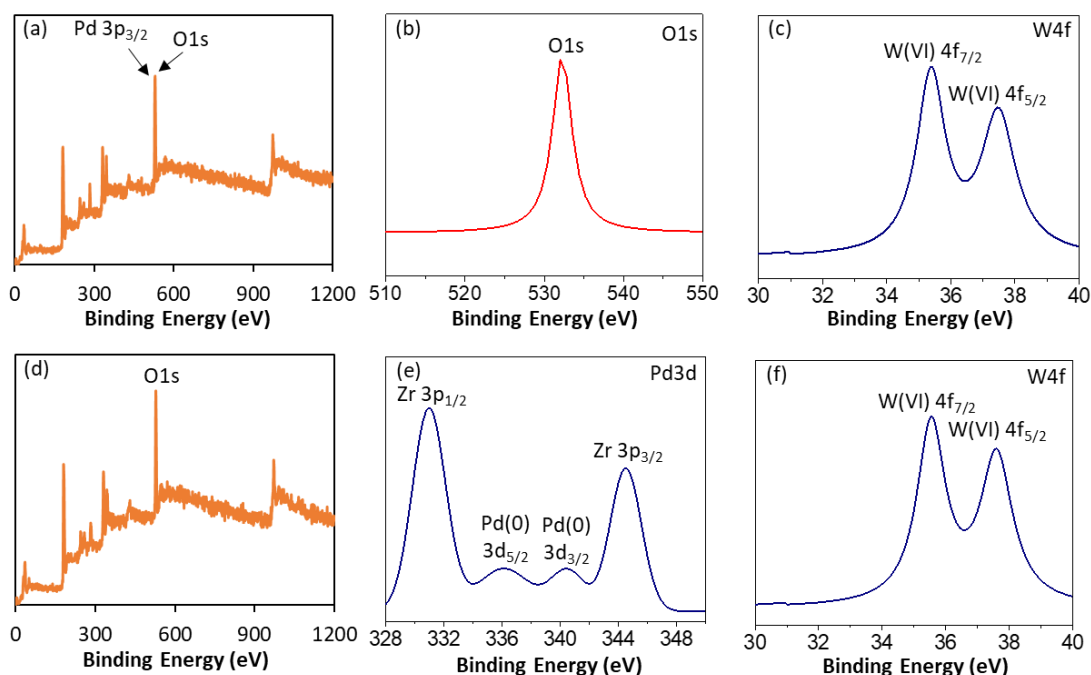


Figure 6 XPS spectra of LTPA/ZrO₂ (a-c) and Pd-LTPA/ZrO₂ (d-f).

TEM micrographs of LTPA/ZrO₂ (Figure 7a-b) and Pd-LTPA/ZrO₂ (Figure 7c-d) were recorded at various resolution. TEM micrographs of LTPA/ZrO₂ show the homogeneous dispersion of LTPA onto surface of the ZrO₂. Whereas, figure 7(c-d) show the high degree of homogeneously dispersed very small isolated PdNPs onto surface of support. SAED image of Pd-LTPA/ZrO₂ shows the non-crystalline nature of highly dispersed PdNPs in the synthesized material (Figure 7e). To further confirm, HRTEM micrographs were also recorded as shown in figure 7(f-g), which clearly display the uniform dispersion of PdNPs (particle size, ~2 nm) throughout the morphology, without aggregates formation, confirming the stabilization of PdNPs by LTPA.

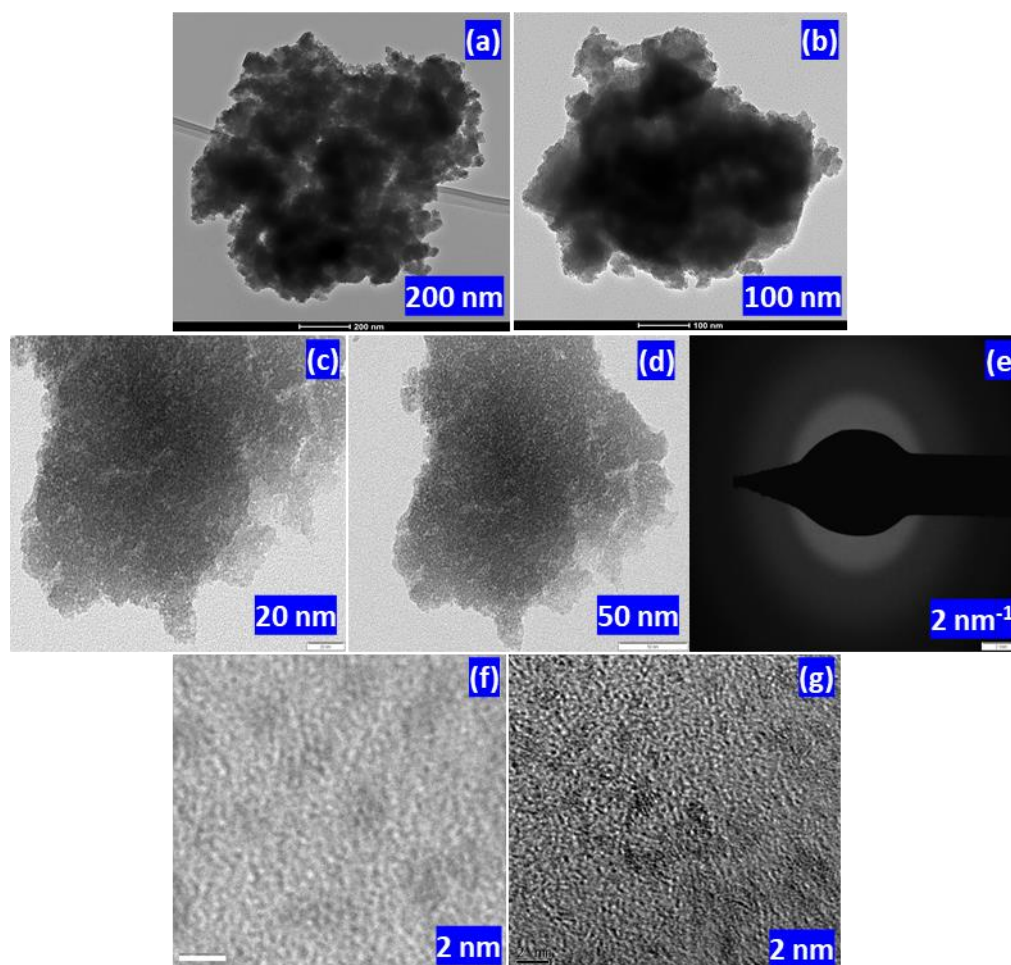


Figure 7 TEM micrographs of LTPA/ZrO₂ (a,b) and Pd-LTPA/ZrO₂ (c,d), SAED image of Pd-LTPA/ZrO₂ (e), HRTEM micrographs of Pd-LTPA/ZrO₂ (c, d).

For more insight of PdNPs, an advance technique, STEM was utilized to probe the behavior of PdNPs. Bright/dark field STEM (BF/DF-STEM) images (Figure 8a-b, respectively) show the highly dispersed PdNPs in the synthesized material. Whereas, overlapping image (Figure 8c) as well as elemental image of Pd (Figure 8d) clearly indicates the presence of isolated PdNPs homogeneously dispersed without any cross talks between them. The absence Pd of aggregates conclude that LTPA/ZrO₂ is very much capable to decrease the high surface free energy of PdNPs, by providing combinedly the facility of high surface area for dispersion as well as stabilizing nature. Whereas images (8d-h) show the presence of all the possible elements in the synthesized catalyst.

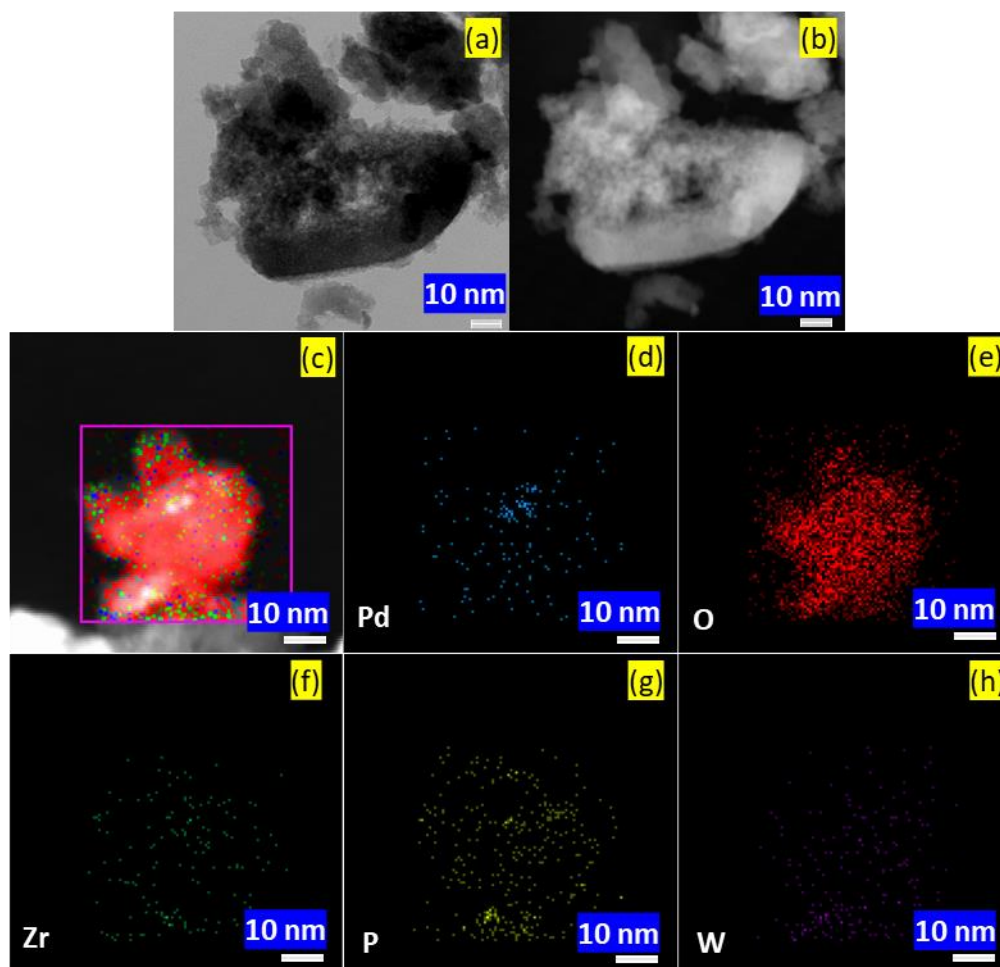


Figure 8 (a) Bright field, (b) dark field STEM images of Pd-LTPA/ZrO₂. (c) Overlapping, (d-h) elemental images of Pd-LTPA/ZrO₂.

In summary, FT-IR shows the retention of Keggin structure even after impregnation, soaking and post-reduction of the catalyst. The presence and oxidation states of Pd(0) and W(VI) are confirmed by XPS while the presence of homogeneously dispersed PdNPs onto surface of ZrO₂ was confirmed by TEM, HRTEM and STEM.

Catalytic activity

SM Coupling

To evaluate the efficiency of the catalyst for SM coupling, iodobenzene (1.96 mmol) and phenylboronic acid (2.94 mmol) were selected as test substrates. Effect of different reaction parameters such as palladium concentration, time, temperature, base, solvent and solvent ratio were studied to optimize the conditions for maximum conversion (Figure 9).

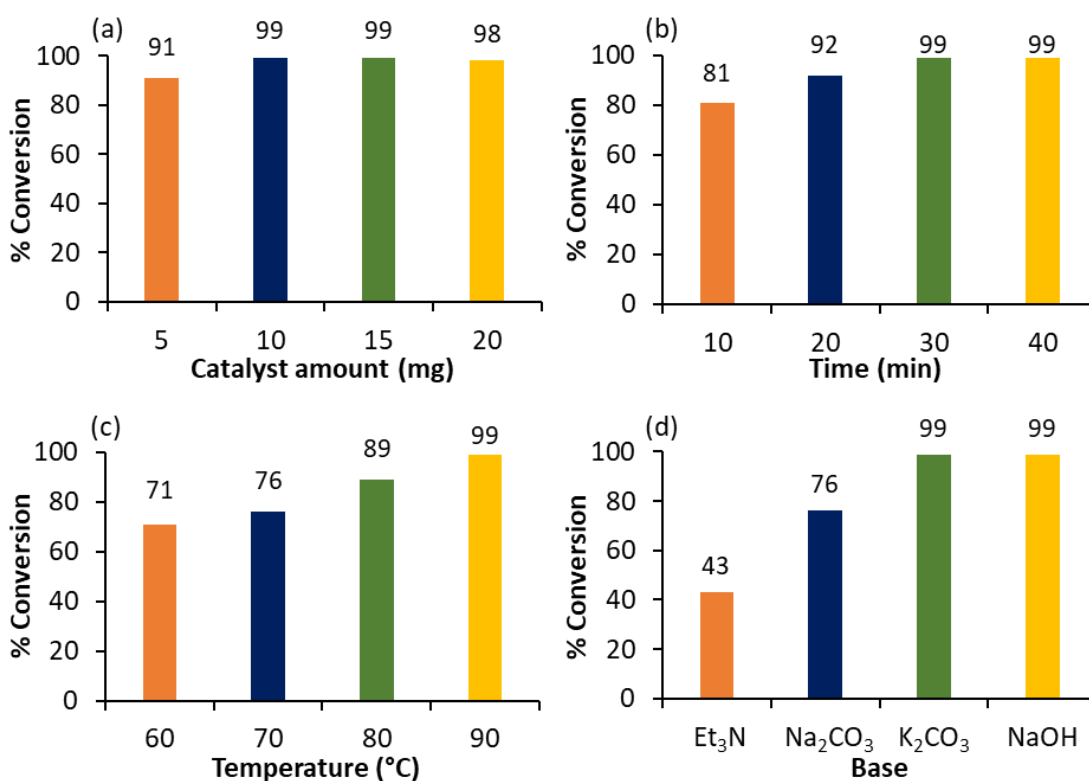


Figure 9 Optimization of parameters for SM coupling. Reaction conditions: (a) Effect of catalyst amount- K₂CO₃ (3.92 mmol), EtOH: H₂O (3:7 mL), time (30 min), temperature (90 °C); (b) Effect of time- catalyst (10 mg), K₂CO₃ (3.92 mmol), EtOH: H₂O (3:7 mL), temperature (90 °C); (c) Effect of temperature: catalyst (10 mg), K₂CO₃ (3.92 mmol), EtOH: H₂O (3:7 mL), time (30 min); (d) Effect of base- catalyst (10 mg), base (3.92 mmol), EtOH: H₂O (3:7 mL), time (30 min), temperature (90 °C).

The effect of catalyst amount is screened between 5-20 mg with concentration of Pd(0) in the range of 3.38×10^{-4} mmol (0.0173 mol%) to 1.35×10^{-3} mmol (0.069 mol%), respectively, and obtained results are shown in figure 9a. Initially, ≈ 1.09 -fold % conversion increase was observed from 5 to 10 mg of catalyst. With further increase in the catalyst amount, conversion remains unchanged. Maximum, 99 % conversion was achieved with 10 mg of catalyst.

The effect of time was studied between 10 to 40 min range as shown in figure 9b. Initially, ≈ 1.22 -fold % conversion increase was observed from 10 to 30 min of reaction time. Further, prolonging the reaction (40 min), no significant effect on reaction conversion was observed. Hence, 30 min was optimized for the reaction.

The effect of temperature was evaluated between 60 to 90 °C and obtained results are displayed in figure 9c. It can be seen from the results that with increase in temperature, the % conversion also increases. 99 % conversion was obtained at 90 °C. Further, increase in temperature has no significant effect on conversion. Hence, 90 °C was considered as optimum for the maximum % conversion.

Influence of various bases was also examined using various organic and inorganic bases. Obtained results (Figure 9d) indicate that organic base triethyl amine (Et_3N) is less favorable for coupling reaction compare to that of inorganic base. The highest conversion was found in the case of K_2CO_3 and NaOH compared to Na_2CO_3 . As K_2CO_3 is environmentally benign, easy to handle and non-hygroscopic in nature compared to NaOH , further study was carried out with K_2CO_3 .

The effect of different solvents on reaction conversion is shown in table 1. From the results it is clear that in case of ethanol the highest conversion was achieved compare to acetonitrile and toluene. Low conversion in case of water as solvent is may be due to the low solubility of substrates. The results are in good agreement with reported one [11], stating that polar solvents tend to give the best result for coupling reaction. Hence, ethanol was selected as an appropriate solvent for further study.

Table 1 Effect of solvent

Solvent	% Conversion
Toluene	12
Acetonitrile	20
Ethanol	71
H ₂ O	28

Reaction conditions: Catalyst (10 mg), K₂CO₃ (3.92 mmol), solvent (10 mL), time (30 min), temperature (90 °C).

Finally, the effect of solvent to water (Ethanol: H₂O) ratio was evaluated and obtained results are presented in table 2.

Table 2 Effect of solvent ratio

Ethanol: H ₂ O	% Conversion
1:9	94
2:8	96
3:7	99
4:6	99
5:5	99

Reaction conditions: Catalyst (10 mg), K₂CO₃ (3.92 mmol), time (30 min), temperature (90 °C).

Obtained results show that initially, with increase in ethanol amount the % conversion increases, this may be due to the increase in solubility of substrates in ethanol. This trend was found from ratio (1:9) mL to (3:7) mL ratios. For higher ratio (4:6) to (5:5) mL, no significant change in % conversion was observed. Maximum 99 % conversion was achieved for (3:7) mL.

From the above study, the optimized conditions for the maximum % conversion (99) are: iodobenzene (1.96 mmol), phenylboronic acid (2.94 mmol), K_2CO_3 (3.92 mmol), conc. of Pd (6.77×10^{-4} mmol, 0.035 mol%), substrate/catalyst ratio (2897/1), $C_2H_5OH:H_2O$ (3:7 mL), time (30 min), temperature (90 °C). The calculated TON is 2868 and TOF is 5736 h^{-1} .

Further, the obtained product was purified by column chromatography on silica gel with a mixture of ethyl acetate and petroleum ether as eluent. Isolated yield (99%) was found to be the same with the conversion (99%) found by GC.

As discussed in chapter-1, in the present case also, optimization of SM coupling was carried out using water as solvent by varying various reaction parameters. Obtain results showed low % conversion at high temperature with prolong reaction time compared to aqueous medium. This may be due to the low solubility of the organic substrate in water. Hence, aqueous medium was optimized for SM coupling.

Heck coupling

To evaluate the efficiency of the catalyst for heck coupling, iodobenzene (0.98 mmol) and styrene (1.47 mmol) were selected as test substrates. Effect of different reaction parameters such as palladium concentration, time, temperature, base, solvent and solvent ratio was studied to optimize the conditions for maximum conversion. As described in SM coupling, in the present case also, all parameters were varied and results are shown in respective figures (Figure 10). It should be noted that the explanation will remain the same as given in the section of SM coupling.

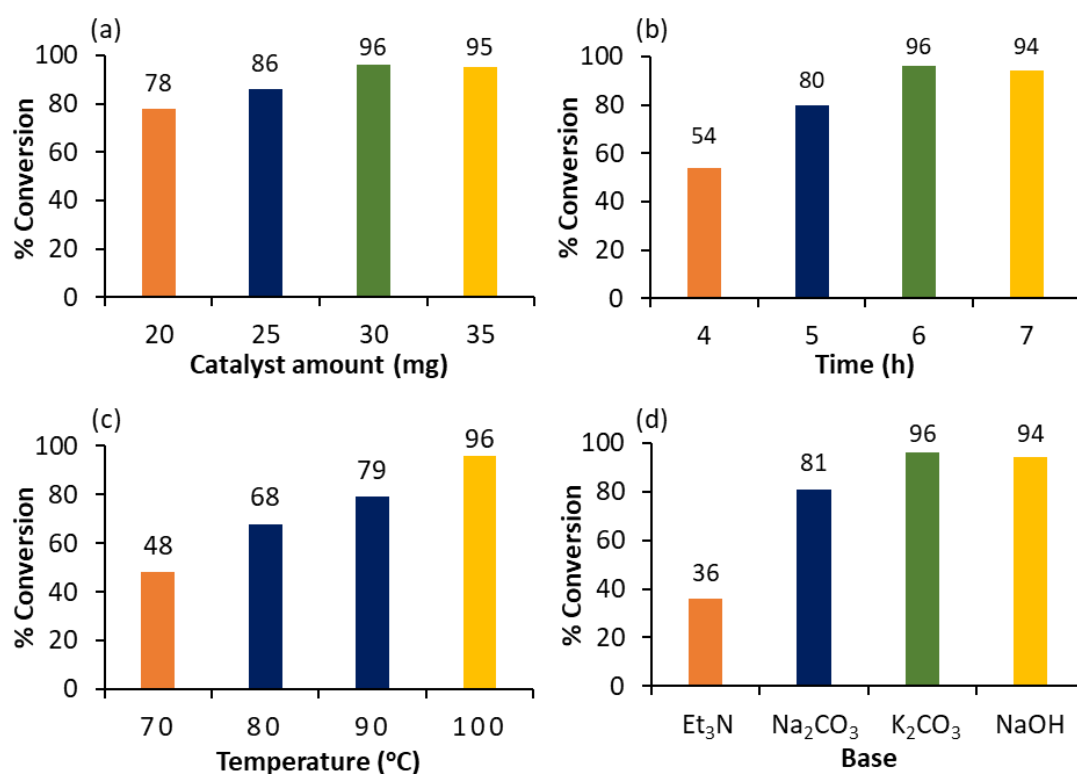


Figure 10 Optimization of Heck coupling. Reaction conditions: (a) Effect of catalyst amount- K₂CO₃ (1.96 mmol), DMF:H₂O (3:2 mL), time (6 h), temperature (100 °C); (b) Effect of time- catalyst (30 mg), K₂CO₃ (1.96 mmol), DMF:H₂O (3:2 mL), temperature (100 °C), (c) Effect of temperature- catalyst (30 mg), K₂CO₃ (1.96 mmol), DMF:H₂O (3:2 mL), time (6 h); (d) Effect of base- catalyst (30 mg), base (1.96 mmol), DMF:H₂O (3:2 mL), time (6 h), temperature (100 °C).

The effect of different solvents was studied and obtained results are shown in table 3. Results indicate that maximum 72 % conversion was attained in case of DMF compare to toluene and ethanol. This is in good agreement with the reported one [12-14], stating that polar, aprotic solvents tend to give the best results for Heck coupling. Low % conversion is observed in case of water may be due to the lower solubility of substrate. Hence, DMF was selected as an appropriate solvent for further study.

Table 3 Effect of solvent

Solvent	% Conversion
Toluene	3
Ethanol	21
DMF	72
H ₂ O	1

Reaction conditions: Catalyst (30 mg), K₂CO₃ (1.96 mmol), time (6 h), temperature (100 °C).

Finally, the effect of solvent to water (DMF: H₂O) ratio was evaluated and data are presented in table 4.

Table 4 Effect of solvent ratio

DMF: H ₂ O	% Conversion
1:4	14
2:3	31
3:2	96
4:1	81

Reaction conditions: Catalyst (30 mg), K₂CO₃ (1.96 mmol), time (6 h), temperature (100 °C).

Obtained results show that initially, with increase in DMF amount the % conversion increases, this may be due to the increase in solubility of substrates

in DMF. This trend was found from ratio (1:4) mL to (3:2) mL. For higher ratio (4:1) mL, % conversion decreases, because of incomplete solubility of base in 1 mL of water. Maximum 96 % conversion was achieved for (3:2) mL.

The optimized conditions for the maximum % conversion (96) are: iodobenzene (0.98 mmol), styrene (1.47 mmol), K_2CO_3 (1.96 mmol), conc. of Pd (2.03×10^{-3} mmol, 0.207 mol%), substrate/catalyst ratio (483/1), DMF:H₂O (3:2 mL), time (6 h), temperature (100 °C). The calculated turnover number (TON) is 464 and turnover frequency (TOF) is 77 h⁻¹.

Hydrogenation

To evaluate the efficiency of the catalyst for hydrogenation, cyclohexene (9.87 mmol) was selected as test substrate. Effect of different reaction parameters such as palladium concentration, time, temperature, pressure and solvent were studied to optimize the conditions for maximum conversion (Figure 11).

The effect of substrate to catalyst ratio was evaluated by varying the catalyst amount from 5 to 20 mg. Obtained results (Figure 11a) show that with increasing the catalyst amount from 5 to 20 mg there was no effect on the reaction conversion. Here, very small amount of catalyst i.e. 5 mg (0.0034 mol% of Pd) has sufficient active sites and capable to tolerate very high amount of substrate (substrate to catalyst ratio, 29177/1), clearly indicates the high efficiency of PdNPs.

The influence of time was assessed between 1 to 4 h (Figure 11b). Initially, up to 2 h, with increasing time, ≈ 1.14 -fold % conversion also increases. Hence, 2 h is the sufficient time for the maximum productive collision of the substrates to yield cyclohexane. Further, increase in time (up to 4 h) has no influence on the % conversion, Maximum 96 % conversion was achieved in 2 h.

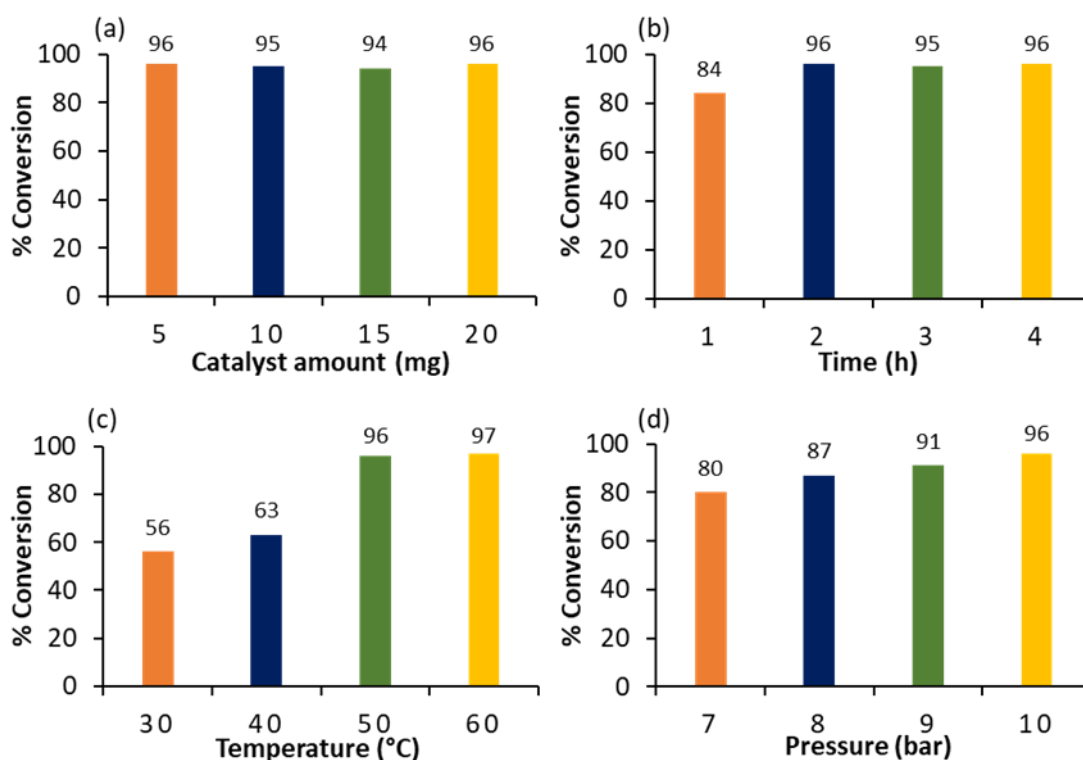


Figure 11 Optimization of cyclohexene hydrogenation. Reaction conditions: (a) Effect of catalyst amount- cyclohexene (9.87 mmol), H₂O (50 mL), time (4 h), temperature (80 °C), H₂ pressure (10 bar); (b) Effect of time- cyclohexene (9.87 mmol), H₂O (50 mL), catalyst (5 mg), temperature (80 °C), H₂ pressure (10 bar); (c) Effect of temperature- cyclohexene (9.87 mmol), H₂O (50 mL), catalyst (5 mg), time (2 h), H₂ pressure (10 bar); (d) Effect of pressure- cyclohexene (9.87 mmol), H₂O (50 mL), catalyst (5 mg), time (2 h), temperature (50 °C).

The effect of temperature on reaction was screened in the region of 30-60 °C (Figure 11c). Obtained results show ≈ 1.71 -fold increase in % conversion with increasing temperature from 30 to 50 °C. Further, rise in temperature shows no appreciable increase in % conversion. At higher temperature there are two facts which resist the reaction conversion: (i) desorption of cyclohexene from the surface of the catalyst and; (ii) lower adsorption rate of hydrogen onto surface of catalyst [15, 16]. Hence, required activation energy was obtained in just 50 °C for 96 % conversion.

The effect of H₂ pressure was studied in the region of 7 to 10 bar (Figure 11d). Obtained results show that % conversion increases from 80 to 96 % linearly.

Hence, the reaction is first order with respect to H₂ pressure, which is in good agreement with the reported one [17] stating that hydrogenation is always first order with respect to H₂ pressure. Further study for effect of high pressure was not carried out as our main focus is to establish environmentally green process. Highest 96 % conversion was obtained by applying 10 bar H₂ pressure.

Effect of various solvents were studied and obtained results are presented in table 5.

Table 5 Effect of solvent

Solvent (20: 30) mL	% Conversion
CH ₃ CN: H ₂ O	63
IPA: H ₂ O	95
EtOH: H ₂ O	97
H ₂ O (50 mL)	96

Reaction conditions: cyclohexene (9.87 mmol), catalyst (5 mg), time (2 h), temperature (50 °C), H₂ pressure (10 bar).

Comparatively, low % conversion was obtained in case of CH₃CN-H₂O solvent system due to its oxidizing nature which resists the reduction of cyclohexene. Whereas, it was achieved maximum for IPA-H₂O and CH₃OH-H₂O systems and this may be due to their reducing nature. However, it was miracle that higher % conversion was obtained under the identical reaction conditions for neat water as a solvent (i.e. 96 %). Hence, water was selected as a solvent for further study.

The optimized conditions for the maximum % conversion (96) are: cyclohexene (9.87 mmol), H₂O (50 mL), conc. of Pd (3.38×10^{-4} mmol, 0.0034 mol%), substrate/catalyst ratio (29177/1), time (2 h), temperature (50 °C) and H₂ pressure (10 bar). The calculated TON is 28010 and TOF is 14005 h⁻¹.

Control Experiments

In all the reactions, control experiments were carried out with LTPA, ZrO₂, LTPA/ZrO₂, PdCl₂, Pd/ZrO₂ and Pd-LTPA/ZrO₂ under optimized conditions in order to understand the role of each component, and results are shown in table 6. It is seen from the table that LTPA, ZrO₂ and LTPA/ZrO₂ were inactive toward the reactions. Almost same conversion was found in the case of PdCl₂, Pd/ZrO₂ and Pd-LTPA/ZrO₂ in all reactions. This indicates that Pd is real active species responsible for the reactions.

Table 6 Control experiment

Catalyst	SM	Heck	Hydrogenation
	% Conversion ^a	% Conversion ^b	% Conversion ^c
LTPA (^a 2.31, ^b 6.92, ^c 1.15 mg)	N. R.	N. R.	N. R.
ZrO ₂ (^a 7.69, ^b 23.08, ^c 3.85 mg)	N. R.	N. R.	N. R.
LTPA/ZrO ₂ (^a 10, ^b 30, ^c 5 mg)	N. R.	N. R.	N. R.
PdCl ₂	98	97	91
Pd/ZrO ₂	97	94	95
Pd-LTPA/ZrO ₂	99	96	96

Reaction conditions. (a) *SM coupling*: iodobenzene (1.96 mmol), phenylboronic acid (2.94 mmol), catalyst (0.076 mg Pd, 0.035 mol% Pd), K₂CO₃ (3.92 mmol), C₂H₅OH: H₂O (3:7 mL), time (30 min), temperature (90 °C); (b) *Heck coupling*: iodobenzene (0.98 mmol), styrene (1.47 mmol), catalyst (0.216 mg Pd, 0.207 mol% Pd), K₂CO₃ (1.96 mmol), DMF: H₂O (3:2 mL), time (6 h), temperature (100 °C). (c) *Hydrogenation*: cyclohexene (9.87 mmol), catalyst (0.036 mg Pd, 0.0034 mol% Pd), H₂O (50 mL), time (2 h), temperature (50 °C), H₂ pressure (10 bar). N. R. – No reaction.

Leaching and Heterogeneity test

The leaching of LTPA from ZrO_2 (before exchanging Pd with available protons) as well as leaching of PdNPs from support was checked for Pd/ ZrO_2 and Pd-LTPA/ ZrO_2 in all the reactions following the same method as discussed in chapter-1 (Please refer, Page No. 94-96) and found no leaching of either Pd or LTPA from ZrO_2 . Whereas, in case of Pd/ ZrO_2 , leaching of Pd was found, recycled catalyst showed appreciable loss in the Pd content (3.53 wt%) as compared to the fresh catalyst (6.05 wt%). The minor change in % conversion (Figure 12) may be due to the instrument error ($\pm 1-1.5$ %).

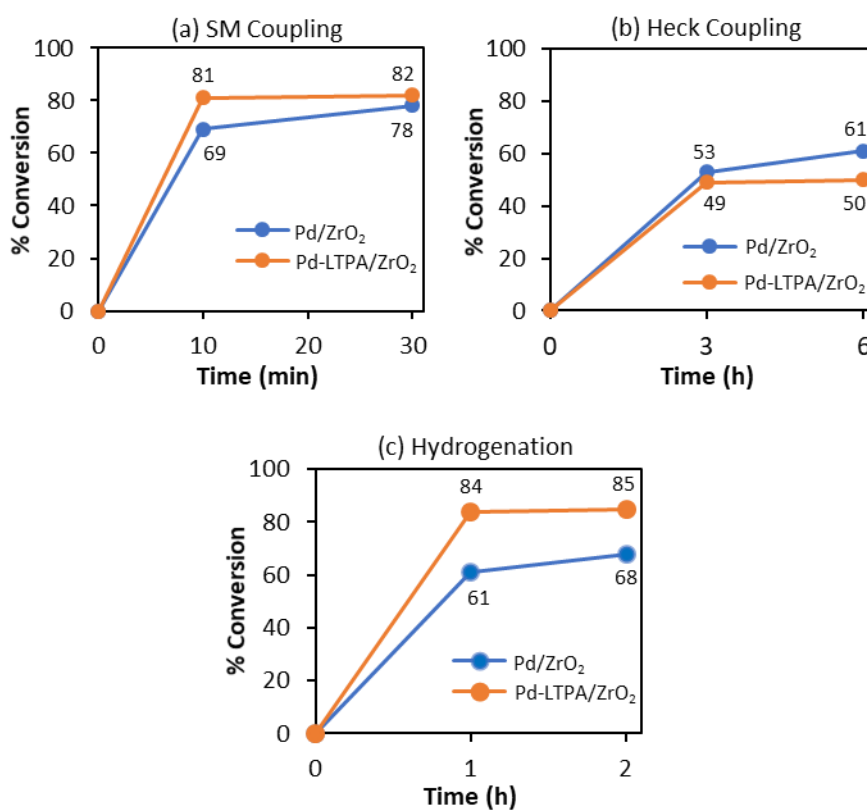


Figure 12 Leaching test. Reaction conditions: (a) *SM coupling*- iodobenzene (1.96 mmol), phenylboronic acid (2.94 mmol), catalyst (0.076 mg Pd, 0.035 mol% Pd), K_2CO_3 (3.92 mmol), $\text{C}_2\text{H}_5\text{OH}$: H_2O (3:7 mL), temperature (90 °C); (b) *Heck coupling*- iodobenzene (0.98 mmol), styrene (1.47 mmol), catalyst (0.216 mg Pd, 0.207 mol% Pd), K_2CO_3 (1.96 mmol), DMF: H_2O (3:2 mL), temperature (100 °C); (c) *Hydrogenation*- cyclohexene (9.87 mmol), catalyst (0.036 mg Pd, 0.0034 mol% Pd), H_2O (50 mL), temperature (50 °C), H_2 pressure (10 bar).

Like in case of Pd-TPA/ ZrO_2 (Chapter-1), in the present case, it was also found that LTPA stabilizes PdNPs and does not allow to leach it into the reaction mixture, making it a true heterogeneous catalyst falling in category C [18].

Recyclability and sustainability of the catalyst

Recyclability and sustainability for Pd/ ZrO_2 and Pd-LTPA/ ZrO_2 were studied as described in chapter-1 (Please refer, Page No. 97-98) and the results are described in figure 13.

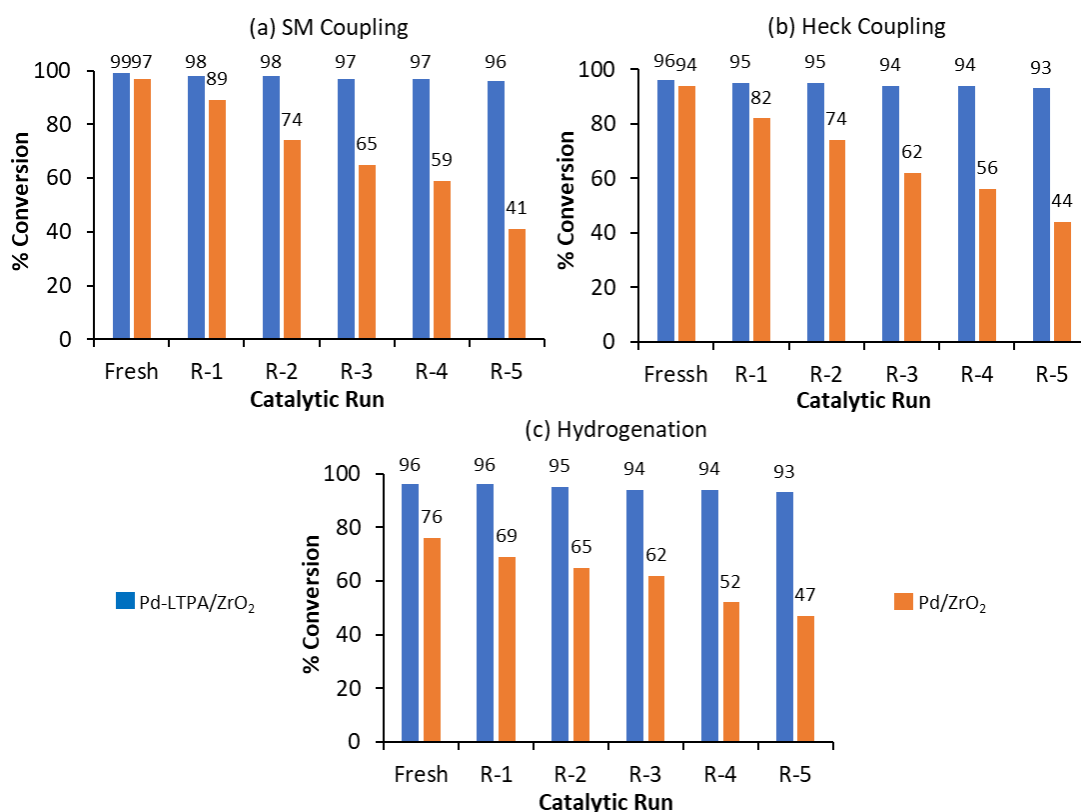


Figure 13 Recycling test. Reaction conditions: (a) *SM coupling*- iodobenzene (1.96 mmol), phenylboronic acid (2.94 mmol), catalyst (0.076 mg Pd, 0.035 mol% Pd), K_2CO_3 (3.92 mmol), $\text{C}_2\text{H}_5\text{OH}$: H_2O (3:7 mL), time (30 min), temperature (90 °C); (b) *Heck coupling*- iodobenzene (0.98 mmol), styrene (1.47 mmol), catalyst (0.216 mg Pd, 0.207 mol% Pd), K_2CO_3 (1.96 mmol), DMF: H_2O (3:2 mL), time (6 h), temperature (100 °C); (c) *Hydrogenation*- cyclohexene (9.87 mmol), catalyst (0.036 mg Pd, 0.0034 mol% Pd), H_2O (50 mL), time (2 h), temperature (90 °C), H_2 pressure (10 bar).

Obtained results show that, while Pd/ZrO₂ exhibited gradual decrease in % conversion due to leaching of PdNPs, Pd-LTPA/ZrO₂ displayed constant % conversion up to five cycles for all reactions, as in case of Pd-TPA/ZrO₂ thereby confirming the important role played by the support.

Characterization of regenerated catalyst

The stability of the regenerated catalyst was studied by its characterization also, such as EDX, FT-IR, XRD, XPS and HRTEM.

For regenerated Pd-LTPA/ZrO₂, the EDX values of Pd (0.71 %wt) and W (15.08 %wt) are in good agreement with the fresh one (0.72 wt% Pd and 15.19 wt% W), confirming no emission of Pd as well as W from the catalyst during the reaction. This indicates that LTPA plays an important role as a stabilizer to keep the Pd(0) active and also prevent it to leach from the support. Elemental mapping is shown in figure 14.

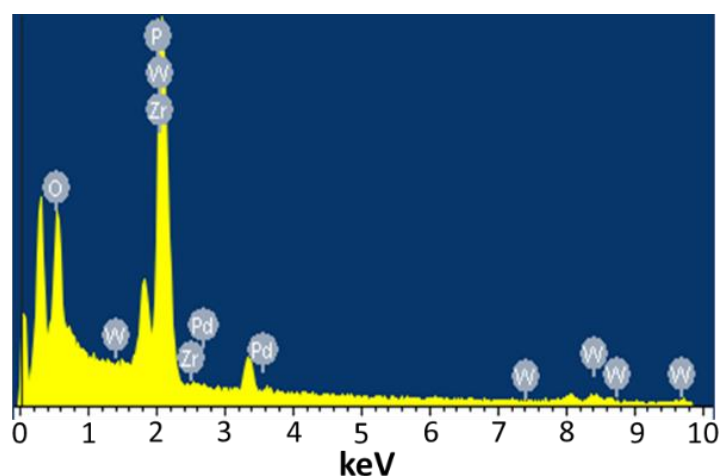


Figure 14 EDX mapping of regenerated Pd-LTPA/ZrO₂.

FT-IR spectra of fresh and regenerated catalysts are displayed in figure 15. The spectrum of regenerated catalyst was found to be almost identical to fresh one, without any significant shift in the bands. However, the bands intensity for regenerated catalyst was slightly low compared to fresh one, may be due to the sticking of the substrates, which had no effect on the efficiency of the catalyst.

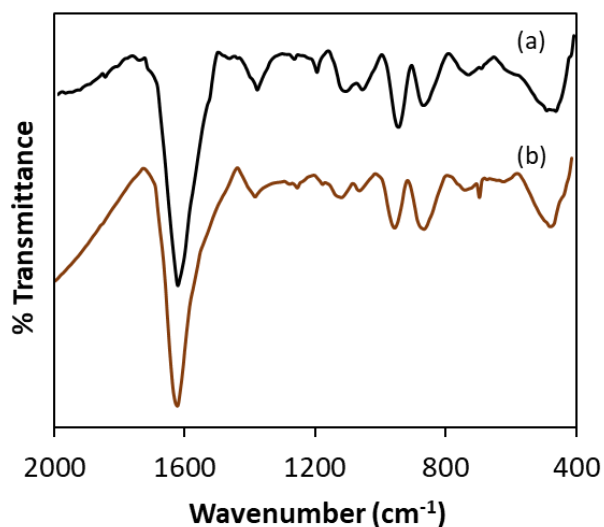


Figure 15 FT-IR spectra of (a) fresh and (b) regenerated Pd-LTPA/ZrO₂.

XRD patterns of fresh and regenerated catalyst are shown in figure 16. Obtained results reveal the retention of highly dispersed nature of the catalyst. Absence of any characteristic peaks regarding Pd aggregates as well as LTPA clearly indicates the sustainability of the catalyst during the reaction.

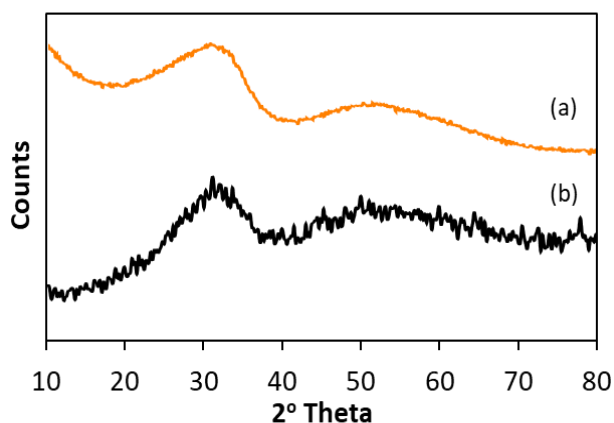


Figure 16 XRD patterns of (a) Pd-LTPA/ZrO₂ and (b) Regenerated Pd-LTPA/ZrO₂.

XPS spectra of regenerated Pd-LTPA/ZrO₂ is displayed in figure 17. The spectrum of regenerated catalyst is found to be identical with fresh one (Figure 6), confirms the retention of Pd(0) active species as well as W(VI), which did not

undergo reduction during the reaction, indicating the sustainability of the catalyst.

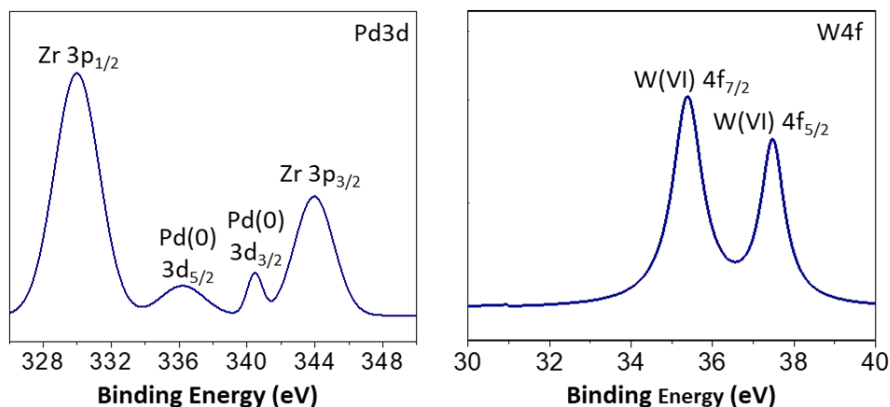
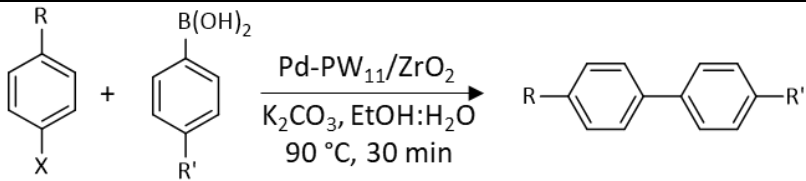
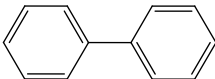
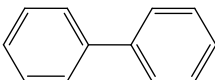
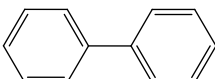
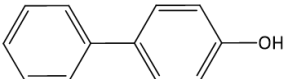
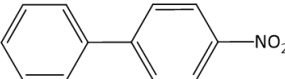
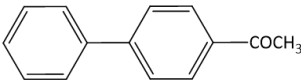


Figure 17 XPS spectra of regenerated Pd-LTPA/ZrO₂.

Viability of the catalyst

Under the optimized condition, the scope and limitations of substrates were investigated by using different halobenzenes (Table 7). Coupling of iodobenzene with phenylboronic acid gives higher conversion compared to bromobenzene and chlorobenzene as expected, because iodide is a good leaving group due to its low electronegativity as well as big radius compared to bromide and chloride groups. The found reactivity order was Ph-I > Ph-Br > Ph-Cl. Presence of strongly electron donating group like -OH is less favorable for coupling reaction, though in case of p-bromophenol, high conversion was obtained. This may be due to the complete solubility of the substrate in reaction medium at optimized temperature which facilitates the reaction. Substituted bromobenzene with strongly electron withdrawing group such as -NO₂ facilitates the reaction, and hence p-bromonitrobenzene gives the 94 % conversion. Similarly, p-bromoacetophenone gives the high conversion due to the presence of moderate electron withdrawing group -COCH₃.

Table 7 Substrate study for SM coupling

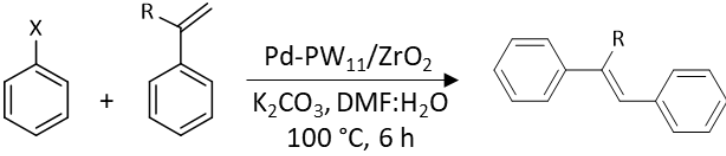
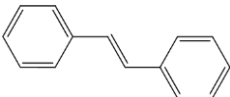
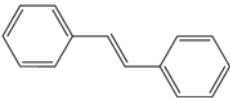
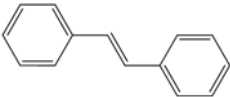
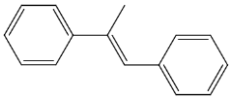
					
R	X	R'	Product	% Conversion	TON/TOF (h ⁻¹)
H	I	H		99	2868/5736
H	Br	H		56	1537/3074
				88 (5 h)	2549/510
				9	261/522
H	Cl	H		82 (10 h)	2376/238
OH	Br	H		92	2665/5330
NO ₂	Br	H		94	2723/5446
COCH ₃	Br	H		86	2491/4982

Reaction conditions: Halobenzene (1.96 mmol), phenylboronic acid (2.94 mmol), K₂CO₃ (3.92 mmol), conc. of Pd (0.035 mol%), substrate/catalyst ratio (2897/1), C₂H₅OH: H₂O (3:7) mL, 30 min, 90 °C.

Similarly, under optimized conditions, scope and limitations of substrates for Heck coupling were also investigated by using different halobenzenes and styrene derivatives (Table 8). Coupling of iodobenzene with styrene gives higher conversion compare to bromobenzene and chlorobenzene as expected. The found reactivity order was Ph-I > Ph-Br > Ph-Cl. However, in case of bromobenzene and chlorobenzene higher % conversion was achieved by prolonging the reaction time. Coupling of iodobenzene with α-methyl styrene

(79 %) is lower compared to the coupling of iodobenzene with styrene (99 %). This may be due to crowding effect of the methyl group.

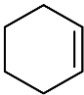
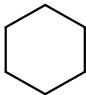
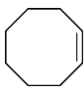
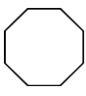
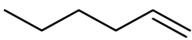
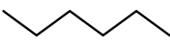
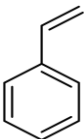
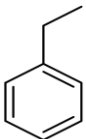
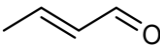
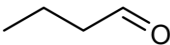
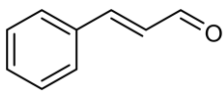
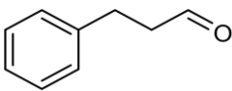
Table 8 Substrate study for Heck coupling

				
X	R	Product	% Conversion	TON/TOF (h ⁻¹)
I	H		96	464/77
Br	H		76 92*	367/61 444*/44*
Cl	H		10 52*	48/8 251*/25*
I	CH ₃		79 88*	381/64 423*/42*

Reaction conditions: Halobenzene (0.98 mmol), styrene (1.47 mmol), K₂CO₃ (1.96 mmol), conc. of Pd (0.207 mol%), substrate/catalyst ratio (483/1), DMF: H₂O (3:2 mL), time (6 h), temperature (100 °C). *Time (10 h).

The scope for hydrogenation of different substrates was also evaluated and the obtained results are enumerated in table 9. From the results it is clear that the catalyst is dominantly viable for the selective hydrogenation of C=C including aliphatic and aromatic compounds.

Table 9 Substrate study for hydrogenation

Substrate	Product	% Conversion/Selectivity	TON/TOF (h ⁻¹)
		96	28010/14005
		62	18090/9045
		74	21591/10780
		99	28885/14443
		92/100	26843/13422
		71/100	20716/10358

Reaction conditions: Substrate (9.87 mmol), Pd (0.0034 mol%), substrate/catalyst ratio (29177/1), H₂O (50 mL), temperature (50 °C), H₂ pressure (10 bar), time (2 h).

Comparison with reported catalyst

Catalytic activity of the present catalyst is also compared with reported catalysts for C-C coupling reactions (Table 10 & 11) in terms of iodobenzene and hydrogenation reaction (Table 12) in terms of cyclohexene as one of the substrates.

It is seen for SM coupling (Table 10), that present catalyst is superior in terms of mol% of Pd, TON as well as TOF compared to all reported catalytic systems.

Table 10 Comparison of catalytic activity for SM coupling with reported catalyst in organic-water solvent mixture with respect to iodobenzene

Catalyst	Pd (mol %)	Solvent	Temp. (°C)/Time (h)	% Conversion/TON /TOF (h ⁻¹)
Pd-ScBTC NMOFs [19]	0.5	C ₂ H ₅ OH: H ₂ O (1:1 mL)	40/0.5	99/194/388
Pd/C [20]	0.37	C ₂ H ₅ OH: H ₂ O (1:1 mL)	40/0.5	99/268/535
Oximepalladacycle catalyst [21]	0.3	C ₂ H ₅ OH: H ₂ O (1:1 mL)	RT/0.3	95/317/1057
Fe ₃ O ₄ /Ethyl-CN/Pd [22]	0.2	C ₂ H ₅ OH: H ₂ O (1:1 mL)	RT/0.2	98/49/245
G-BI-Pd [23]	0.45	C ₂ H ₅ OH: H ₂ O (1:1 mL)	80/0.084	98/219/2613
Pd-LTPA/ZrO₂ (Present catalyst)	0.035	C₂H₅OH: H₂O (3:7 mL)	90/0.5	99/2868/5736

In case of Heck coupling (Table 11) also, present catalyst is found superior in terms of the used solvent medium, mol% of Pd, % conversion as well as high TON/TOF.

Table 11 Comparison of catalytic activity for Heck reaction with reported catalysts with respect to iodobenzene

Catalyst	Pd (mol %)	Solvent	Temp. (°C)/Time (h)	% Conversion/TON/ TOF (h ⁻¹)
PdTSPc@KP-GO [24]	0.792	H ₂ O (10 mL)	reflux/9	89/111/12
Pd/CNCs [25]	1.412	DMF (10 mL)	40/5	93/65/13
NO ₂ -NHC- Pd@Fe ₃ O ₄ [26]	1.0	CH ₃ CN (5 mL)	80/5	96/96/19
5% Pd/CM [27]	0.2	DMA	80/24	61/3050/127
PFG-Pd [28]	1.7	DMF (3 mL)	120/6	95/56/9
Pd-LTPA/ZrO₂ (Present catalyst)	0.207	DMF: H₂O (3:2 mL)	100/6	96/464/77

The efficiency of the catalyst with reported systems is enumerated in table 12 with respect to cyclohexene hydrogenation in terms of % conversion, TON as well as TOF. Liu et al. [29] achieved 99 % conversion at moderate temperature and very high H₂ pressure (20 bar) compared to present system. Zhang et al. [30] performed the reaction at low temperature with very poor yield and with high catalyst concentration. Leng et al. [31] reported the use of formic acid as proton transferring agent to achieve 96 % conversion using high temperature and catalyst amount compared to the present system. Panpranot et al. [32] obtained 96 % conversion utilizing supercritical CO₂ as a solvent at 60 bar pressure (harsh conditions). Obtain data shows that the present catalyst is best one amongst all reported systems to till date in terms of used catalyst amount, TON as well as TOF under mild reaction conditions.

Table 12 Comparison with the reported catalyst with respect to cyclohexene hydrogenation

Catalyst	Pd (mole%)	Solvent	Temp. (°C)	Pressure (bar)	% Conversion/TON/TOF
SH-IL-1.0wt%Pd [29]	0.02	Auto- clave	60	20	99/5000/5000
Pd/MSS@ZIF-8 [30]	0.1738	Ethyl acetate	35	1	5.6/560/93
Pd@CN [31]	2.208	Formic acid	90	(Proton transfer)	96/44/3.67
Pd/SiO ₂ [32]	0.091	CO ₂ (60 bar)	25	10	96/1097/6582
Pd-LTPA/ZrO₂ (Present catalyst)	0.0034	Water	50	10	96/28010/14005

Comparison study of Pd-TPA/ZrO₂ and Pd-LTPA/ZrO₂

In order to compare the activity of the catalysts, both coupling and hydrogenation reactions were carried out under identical experimental conditions. Obtained results (Table 13) are compared in terms of % conversion, TON/TOF.

In case of C-C coupling, the results show that Pd-TPA/ZrO₂ is more active compared to Pd-LTPA/ZrO₂. This can be explained on the basis of total acidic sites. The high activity of Pd-TPA/ZrO₂ is attributed to its lower acidity compared to Pd-LTPA/ZrO₂. As base K₂CO₃ was used in the reaction, which is necessary for the transmetallation step for the formation of product, gets neutralized with acidity of the catalyst and lowers the rate of the reaction. As a result, Pd-TPA/ZrO₂ is more active than Pd-LTPA/ZrO₂.

Table 13 Effect of addenda atom on % conversion, TON/TOF

Catalyst	Total acidity (mequi./g)	No. of counter protons	SM coupling		Heck coupling		Hydrogenation	
			% Conv.	TON/TOF(h ⁻¹)	% Conv.	TON/TOF(h ⁻¹)	% Conv.	TON/TOF (h ⁻¹)
Pd-TPA/ZrO ₂	4.2	3	99	10325/ 20650	99	860/ 143	15	4377/ 2188
Pd-LTPA/ZrO ₂	5.1	7	62	6466/ 12932	70	608/ 101	96	28010/ 14005

Reaction conditions: *SM coupling*- iodobenzene (1.96 mmol), phenylboronic acid (2.94 mmol), K₂CO₃ (3.92 mmol), conc. of Pd (0.0096 mol%), substrate/catalyst ratio (10429/1), C₂H₅OH: H₂O (3:7 mL), time (30 min), temperature (80 °C); *Heck coupling*- iodobenzene (1.96 mmol), phenylboronic acid (2.94 mmol), K₂CO₃ (3.92 mmol), conc. of Pd (0.115 mol%), substrate/catalyst ratio (869/1), DMF: H₂O (3:2 mL), time (6 h), temperature (100 °C); *Hydrogenation*- Cyclohexene (9.87 mmol), conc. of Pd (0.0034 mol%), substrate/catalyst ratio (29177/1), H₂O (50 mL), time (2 h), temperature (50 °C), H₂ pressure (10 bar).

In case of C-C coupling, the results show that Pd-TPA/ZrO₂ is more active compared to Pd-LTPA/ZrO₂. This can be explained on the basis of total acidic

sites. The high activity of Pd-TPA/ZrO₂ is attributed to its lower acidity compared to Pd-LTPA/ZrO₂. As base K₂CO₃ was used in the reaction, which is necessary for the transmetallation step for the formation of product, gets neutralized with acidity of the catalyst and lowers the rate of the reaction. As a result, Pd-TPA/ZrO₂ is more active than Pd-LTPA/ZrO₂.

In the case of hydrogenation, obtained results (Table 13) show that Pd-LTPA/ZrO₂ is more active than Pd-TPA/ZrO₂. This can be explained on the basis of number of counter protons. It is well known that for surface phenomenon type catalytic hydrogenation, the formation of Pd-H is necessary, higher the formation of Pd-H more the substrates collision for fruitful % conversion. As Pd-LTPA/ZrO₂ consists seven hydrogen (in the form of counter protons), which accelerate the formation of Pd-H to enhance the hydrogenation rate, whereas Pd-TPA/ZrO₂ has only three counter protons and as a result it activates the reaction moderately.

Activity order of the catalysts is:

C-C Coupling: Pd-TPA/ZrO₂ >> Pd-LTPA/ZrO₂

Hydrogenation: Pd-LTPA/ZrO₂ >> Pd-TPA/ZrO₂

Conclusion

- Synthesis of PdNPs stabilized by zirconia supported LTPA (Pd-LTPA/ZrO₂) is carry out successfully by ion exchange method. FT-IR, XRD and BET reveal the retention of Keggin structure, XPS confirms the oxidation states of Pd(0) and W(VI) whereas TEM, HRTEM and STEM confirm the presence of homogeneously dispersed PdNPs onto surface of ZrO₂
- The overall catalytic evaluation including catalytic activity for C-C coupling (SM and Heck) and hydrogenation under mild reaction conditions (> 95 % conversion), leaching and heterogeneity as well as activity and characterization of regenerated catalyst, showcase its superiority in terms of performance and sustainability
- Viability towards different substrates displays efficient activity of the catalyst as well as its broad scope of catalysis for all the three reactions. Comparison study proves the high strength of the present catalyst compare to the reported systems for the said reactions
- Pd-TPA/ZrO₂ presents superior catalytic activity towards C-C coupling whereas Pd-LTPA/ZrO₂ shows towards hydrogenation compared to each other. This is attributed to the removal of addenda atom, which increases the total acidity (number of protons) and leads to the difference in the catalytic activity

References

- [1] V. Kogan, Z. Aizenshtat, R. Popovitz-Biro and R. Neumann, *Org. Lett.*, 4, 3529-3532, (2002).
- [2] C. Brevard, R. Schimpf, G. Tourne and C. M. Tourne, *J. Am. Chem. Soc.*, 105, 7059-7063, (1983).
- [3] S. Singh and A. Patel, *Catal. Lett.*, 144, 1557-1567, (2014).
- [4] A. I. Vogel and G. H. Jeffery, *Vogel's textbook of quantitative chemical analysis*, Longman Scientific & Technical, (1989).
- [5] A. V. Matveev, V. V. Kaichev, A. A. Saraev, V. V. Gorodetskii, A. Knop-Gericke, V. I. Bukhtiyarov and B. E. Nieuwenhuys, *Catal. Today*, 244, 29-35, (2015).
- [6] Y. Leng, C. Zhang, B. Liu, M. Liu, P. Jiang and S. Dai, *ChemSusChem*, 11, 3396-3401, (2018).
- [7] R. Villanneau, A. Roucoux, P. Beaunier, D. Brouri and A. Proust, *RSC Adv.*, 4, 26491-26498, (2014).
- [8] L. D'Souza, M. Noeske, R. M. Richards and U. Kortz, *Appl. Catal., A*, 453, 262-271, (2013).
- [9] Y. Zhu, W. D. Wang, X. Sun, M. Fan, X. Hu and Z. Dong, *ACS Appl. Mater. Interface*, 12, 7285-7294, (2020).
- [10] S. Rana and K. M. Parida, *Catal. Sci. Technol.*, 2, 979-986, (2012).
- [11] S. Pathan and A. Patel, *RSC Adv.*, 2, 116-120, (2012).
- [12] F. Zhao, K. Murakami, M. Shirai and M. Arai, *J. Catal.*, 194, 479-483, (2000).
- [13] J. P. Stambuli, S. R. Stauffer, K. H. Shaughnessy and J. F. Hartwig, *J. Am. Chem. Soc.*, 123, 2677-2678, (2001).
- [14] P. W. Böhm Volker and A. Herrmann Wolfgang, *Chem. Eur. J.*, 7, 4191-4197, (2001).
- [15] J. Struijk, M. d'Angremond, W. J. M. L.-d. Regt and J. J. F. Scholten, *Appl. Catal., A*, 83, 263-295, (1992).

-
- [16] J. Wang, Y. Wang, S. Xie, M. Qiao, H. Li and K. Fan, *Appl. Catal., A*, 272, 29-36, (2004).
- [17] C. U. I. Odenbrand and S. T. Lundin, *J. Chem. Technol. Biotechnol.*, 31, 660-669, (1981).
- [18] R. A. Sheldon, M. Wallau, I. W. C. E. Arends and U. Schuchardt, *Acc. Chem. Res.*, 31, 485-493, (1998).
- [19] L. Zhang, Z. Su, F. Jiang, Y. Zhou, W. Xu and M. Hong, *Tetrahedron*, 69, 9237-9244, (2013).
- [20] Z. Shi and X.F. Bai, *Open Mater. Sci. J.* 9, 173-177, (2015).
- [21] M. Gholinejad, M. Razeghi and C. Najera, *RSC Adv.*, 5, 49568-49576, (2015).
- [22] B. Abbas Khakiani, K. Pourshamsian and H. Veisi, *Appl. Organomet. Chem.*, 29, 259-265, (2015).
- [23] M. Sarvestani and R. Azadi, *Appl. Organomet. Chem.*, 31, e3667, (2016).
- [24] Z. Hezarkhani and A. Shaabani, *RSC Adv.*, 6, 98956-98967, (2016).
- [25] X. W. Guo, C. H. Hao, C. Y. Wang, S. Sarina, X. N. Guo and X. Y. Guo, *Catal. Sci. Technol.*, 6, 7738-7743, (2016).
- [26] V. Kandathil, B. D. Fahlman, B. S. Sasidhar, S. A. Patil and S. A. Patil, *New J. Chem.*, 41, 9531-9545, (2017).
- [27] Y. Monguchi, F. Wakayama, S. Ueda, R. Ito, H. Takada, H. Inoue, A. Nakamura, Y. Sawama and H. Sajiki, *RSC Adv.*, 7, 1833-1840, (2017).
- [28] R. Fareghi-Alamdari, M. G. Haqiqi and N. Zekri, *New J. Chem.*, 40, 1287-1296, (2016).
- [29] R. Tao, S. Miao, Z. Liu, Y. Xie, B. Han, G. An and K. Ding, *Green. Chem.*, 11, 96-101, (2009).
- [30] T. Zhang, B. Li, X. Zhang, J. Qiu, W. Han and K. L. Yeung, *Microporous Mesoporous Mater.*, 197, 324-330, (2014).
- [31] C. Zhang, Y. Leng, P. Jiang, J. Li and S. Du, *ChemistrySelect*, 2, 5469-5474, (2017).
- [32] J. Panpranot, K. Phandinthong, P. Praserttham, M. Hasegawa, S.-i. Fujita and M. Arai, *J. Mol. Catal. A: Chem.*, 253, 20-24, (2006).
-

